UNIVERSITY OF NAPLES FEDERICO II

PHD IN CHEMICAL SCIENCES

XXVIII CYCLE

ROLE OF THE BACTERIAL CELL WALL GLYCO-CONJUGATES IN ELICITATION OR SUPPRESSION OF EUKARYOTIC INNATE IMMUNITY

Antonia De Felice

TUTOR
Prof. Alba Silipo

SUPERVISOR
Dr. Andrea Carpentieri

Index

Paper related to PhD project:

1. Structural and conformational study of the O-polysaccharide produced by the metabolically versatile photosynthetic bacterium *Rhodopseudomonas palustris* strain BisA53 (*Carbohydr. Polym.* **2014**, 114,384-91)

2. Structural and conformational study of the O-antigenic portion of the lipopolysaccharide isolated from *Burkholderia gladioli pv. cocovenenans* (*Eur. J. Org. Chem.*, **2016**, *4*, 748–755)

3. The LPS *O*-antigen in photosynthetic *Bradyrhizobium* strains is dispensable for a successful symbiosis with *Aeschynomene* legumes (*PLoS* One 2016 Feb 5; 11(2):e 0148884)

4. The structure of the LPS O-antigen from the gram negative *Pantoea ananatis* M408 involved in maize infection (submitted to *Carbohydr. Res.*)

5. Structural glycobiology of lipopolysaccharides covalently bound to hopanoids: key molecules that favour the life of *Bradyrhizobia* in stressful environments (manuscript in preparation)

Paper not related to PhD project:

6. Serotype O:8 isolates in the *Yersinia pseudotuberculosis complex* have different O-antigen gene clusters and produce various forms of rough LPS (*Innate Immunity*, **2016**, *22*, 205-217)

7. Structure, genetics and function of an exopolysaccharide produced by a bacterium living within fungal hyphae (*Chembiochem.*, **2015**, 16(3), 387-92)

Chapter I

Gram-negative bacteria

1.1 The bacterial cell

Bacteria are prokaryotic unicellular microorganisms having a very simple cellular organization. Generally, they are organized in multicellular forms with distinctive morphologies (coccus, bacillus, spirillum and filamentous) which constitute the colonies. Bacterial cell display a general architecture formed by the following components:

Nucleoid: a region of the bacterial cell where is localized the nucleic material; all processes of transcription and replication of DNA take place in the cytoplasm.

Cytoplasmatic membrane: is formed by a phospholipid bilayer, where are immersed transport proteins and enzymes involved in the biosynthesis of phospholipids. Its structure is not static, but in continuous moving to allow the permeability of membrane for the afflux of diverse molecules.

Cell wall: indispensable structure surrounding the cytoplasmatic membrane. It protects bacterial cells from external stresses as pressure, temperature and salt concentration. Cell wall composition is variable according to the bacterial strains.

Capsule: homo/hetero-polysaccharides, possessing many biological functions. Frist of all, capsule mediates the bacterial adhesion and colonization to the host cell and can be considered a virulence factor because it is able to trigger innate immunity response.

Flagella: organs designated to bacteria locomotion. The bacterial flagellum is mainly composed by the flagellin protein, a strong elicitor of innate immunity in both mammalian and plant organisms.

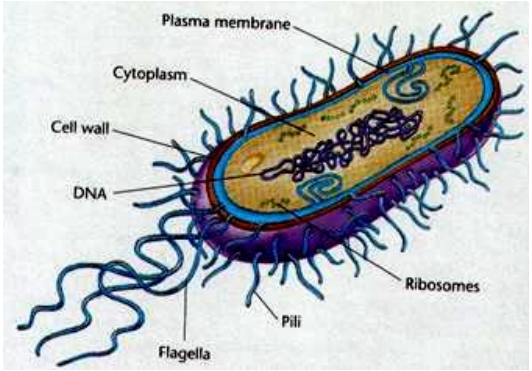

Figure 1.1: Gram-negative bacteria structure

The prokaryotes are divided into two family: *Archaebacteria* and *Eubacteria* structurally, functionally and genetically different.[1] The first group mainly involves extremophiles able to live in extreme conditions of pH, temperature, pressure and show characteristics similar to the eukaryotic system. *Eubacteria* are in turn divided into Gram-positive and Gram-negative, based upon the cell

[1] Madigan M., Artinko M.A., Parker J., *Biology of microorganism,* **2003**, (Ed.: T. Brock) Pearson education international, New York.

reaction to the Gram staining protocol. Gram-positive bacteria show thick and nearly uniformly dense cell wall. Conversely, cell envelope of Gram-negative bacteria are more complex, and include a cwll wall and a second outer membrane.[2]

1.2 Bacterial cell wall

The main component of bacterial cell wall is peptidoglycan (PGN). PGN is composed of carbohydrate chains of β-(1-4)-linked N-acetyl glucosamine and N-acetyl muramic acid cross linked by a peptide stem of L and D amino acids.[3].[4]

Gram-negative bacteria display a thin PGN layer, about 5-10% of cell wall and *meso*-diaminopimelic acid, *m*-DAP, is a component of the peptide chain. Conversely, Gram-positive bacteria exhibit a thick PGN layer, composing around 95% of bacteria cell wall, and containing lysine as third amino acid residue.

In Gram-negative bacteria, the absence of a thick PGN layer is compensated by the presence of a second membrane, called outer membrane, containing lipopolysaccharides and phospholipids. The chemical structure of these macromolecules is strain dependent.

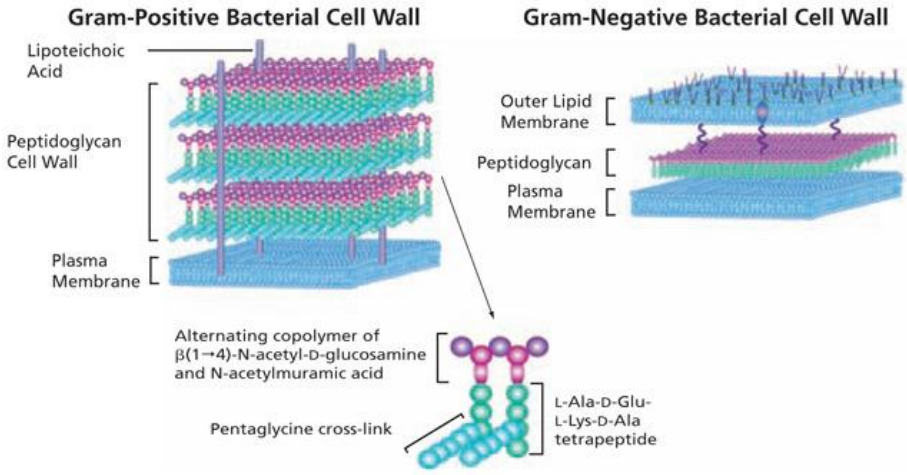

Figure 1.2: Structure and differences between bacteria's cell wall membrane.

[2] Staley J.T., Gunsalus R. P., Lory S., Perry J.J., *Microbial Life,* **2007**, second edition , chapter **4**.
[3]Dziarski R., *CMLS,* **2003**, *60*, 1793-1804.
[4] Guan R., Mariuzza A.R., *TRENDS in Microbiology,* **2007**, *15*, 126-134.

1.3 Lipopolysaccharides

The lipopolysaccharides, LPSs, are glyco-conjugates composing the outer membrane of gram-negative bacteria, having a pivotal role in the structural and mechanical support of outer membrane. LPSs cover around 75% of the bacterial surface[5] and, due to its location, mediate host-bacteria interactions like adhesion, recognition, pathogenesis, symbiosis.[6] LPSs are also crucial in triggering the innate immune system in the hosts[7]

LPS are characterized by a common structural motif consisting of three different domains:

Lipid A is the hydrophobic portion of the LPS that is capable to anchor the macromolecule to the bacterial outer membrane and represents the endotoxic principle of LPS.[8]

Core oligosaccharide is a saccharide portion covalently linked to the lipid A; is oftendivided into two regions: the inner core, and the outer core.

O-antigen is the hydrophilic domain of LPS and is composed by a polysaccharide.[6]

In order to understand the molecular basis of bacterium– host interaction, it is important to elucidate the full structure of LPS and to know how bacterium modifies its LPS structure to reply the continuous environmental changes. It has been already demonstrated that a complete structure of LPS is required to establish a disease (pathogens) or to produce a beneficial outcome (symbiont) in host-microbe interaction.[5]

[5] Lerouge I., Vanderleyden J., *FEMS microbiology reviews*, **2001**, *26*, 17-47.
[6] Konig H., Herald C., Varma A., *Prokaryotic cell wall*, chapter **4**, 133-154.
[7] Alexander C., Rietschel E.T., *J.endoxin Res*., **2001**, *7*, 167-202.
[8] Wollenweber H.W., Schlecht S., Luderiz O., Rietschel E.T., *Eur. J. Biochem*, **1983**, *130*, 167-171.

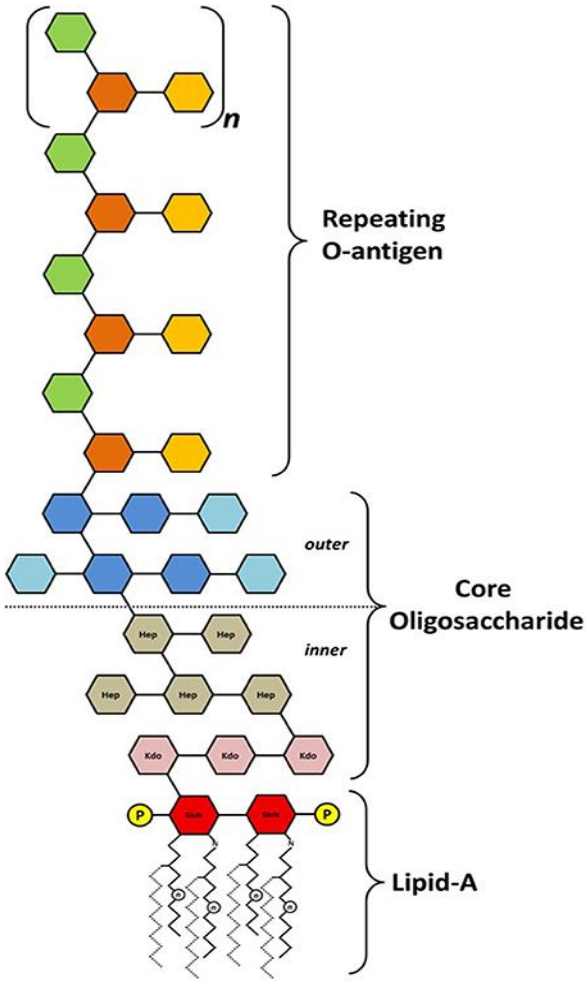

Figure 1.3.1: General architecture of lipopolysaccharides

1.3.1 O-antigen: structure and function

The O-antigen, also known as O-chain, is the hydrophilic portion of LPS exposed on the bacterial surface. It can be homo- or hetero-polymeric, linear or branched, build up to 50 identical repeating units consisting of one to eight sugars.

The O-antigen region is can also contain unusual monosaccharides or non-carbohydrate substituents, thus increasing its structural heterogeneity.[9]

During the early stage of host invasion, bacteria use variation mechanisms to mask themselves to the host and escape the immune response, through the change of the length of polysaccharide region or primary structure of the whole LPS structure.[10,11,12]

[9] Silipo A. et al, *Angew. Chem. Int. Ed.*, **2011**, *50*, 12610 –12612.
[10] Lukacova M., Barak I., Kazar J., *European society of clinical microbiology and infectious disease,* **2007**, *14*, 200-206.
[11] Jansson P.E., Brade H., Morrison D.C., Opal S., Vogel S., *Endotoxin in Health and Disease*, **1999**, New York, 155-178.
[12] Whitfield C. *Annu Rev Biochem,* **2006**, *75*, 39-68.

The O-chain is important not only for bacterial interactions with immune system, but has also a protective role.

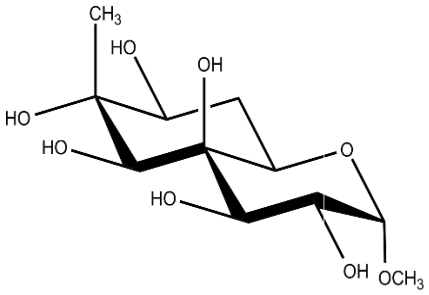

Figure 1.3.2: The structure of Bradyrhizose

1.3.2 Core Oligosaccharide

Core oligosaccharide is typically composed up to fifteen residues and can be divided in inner core and outer core regions. The inner core consists of typical monosaccharides, such as heptoses[13] (L-glycero-D-mannoheptose or D-glycero-D-mannoheptose) and Kdo (3-deoxy-D-*manno*-octulosonic acid), a monose marker of Gram-negative bacteria that connects the core oligosaccharide to lipid A backbone. The outer core is usually constituted by neutral carbohydrates as uronic acids and aminosugars. It is the most exposed portion, often branched, and it is characterized by a higher structural variability than the inner core.

1.3.3 Lipid A: structure and activity

The lipid A represents the hydrophobic domain of LPS, responsible of the anchorage of the macromolecule on the bacteria outer membrane. Its general structure is formed by a 2-amino-2-deoxy-D-glucopyranose (D-Glc*p*N, glucosamine) α-(1→6) disaccharide phosphorylated at position 1 and 4' and acylated by 3- hydroxy fatty acid residues, called ―primary fatty acid, linked with ester bonds at positions 3 and 3' and with amide bonds at positions 2 and 2' of the disaccharide skeleton. These fatty acids can be further acylated at hydroxyl position with secondary fatty acids, usually no hydroxylated and with different length.

[13] De Soyza A., Silipo A., Lanzetta R., Govan J.R., Molinaro A., *Innate Immun.*,**2008**, *14*, 127-144.

The first lipid A structure elucidation was achieved from *E. coli* and *S. enterica* LPS in 1983.[14](Fig. 1.3.3)

Despite the lipid A has a general architecture, often displays subtle structural variations often strain dependent, as as different acylation and phosphorylation patterns

E.coli lipid A (**A**)

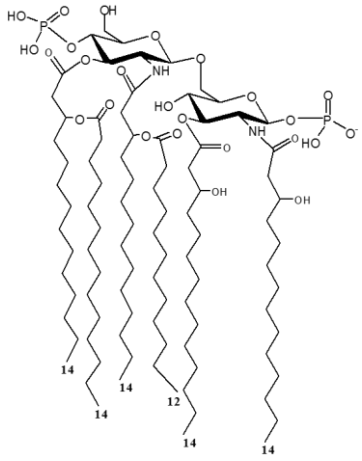

Figure 1.3.3: Lipid A structure from E. coli

1.4 Communication system among plant: pathogenesis and symbiosis

The natural ecosystem is founded on plants, animals, and humans coexistence. This cohabitation results in countless interactions with beneficial and pathogenic organisms. Very close relationships have evolved in host-specific symbioses, usually beneficial for both partners. In most cases, symbiosis derives from metabolic complementation between the host and microbe, in which one partner provides missing nutrients to the other. Moreover, microbes can contribute in many ways to host development by synthesizing hormone-like compounds[15] and affecting host immunity[16]. The symbiotic associations can be facultative or obligate, that is due to the absent biosynthetic pathways in the host cell, essential for free living of bacteria.

In plants, obligate symbiosis is more rare, on the contrary, facultative mutualistic interactions are more common as fungal-plant and *Rhizobium*-legume interactions.

[14] Wollenweber H.W., Schlecht S., Luderiz O., Rietschel E.T., *Eur. J. Biochem.,* **1983**, *130*, 167-171.
[15] Shin S.C. et al, *Science*, **2011**, *334*, 670–74.
[16] Moreira L.A. et al, *Cell.,* **2009**,*139*,1268–78.

Plants innate immune system is the line of defense against external attack of pathogen microorganisms. As in mammals, plants immunity has acquired the ability to recognize specific molecular structures, known as MAMPs (Microbe Associated Molecular Patterns),[17] indispensable for the microbial life; responsible for MAMPs recognition are PRRs receptors (Pattern Recognition Receptors). Flagellin, lipopolysaccharides and peptidoglycan are all MAMPs and their structures and molecular affinity to the receptors precisely modulated host immune responses.

During the infection, there is a consequent activation of the immune system, with the development of necrotic tissues caused by Hypersenitive response (HR). During HR there is a rapid decline of bacterial proliferation and a suppression of pathogen growth, protecting in this way the plant from infection. The plant response is accompanied by rapid cell death in the site of the infection and follows a rapid necrosis of plant tissue representing the final stage of resistance, when stress signals request strong defensive responses.

LPS can be responsible of suppression and this phenomenon is well known with the name of LIR (localized induced resistance). The mechanism of activation of LIR is strictly connected to LPS structure. In fact, several studies demonstrated that the minimum requirement for activity is having the lipid A-core region, minimum structure able to trigger the immune response.[18]

It is possible that the effects of LPS in HR prevention and in triggering basal defense may allow the plants to express resistance without devastation of tissue.[19]

Generally, lipid A and the core oligosaccharide, are able to elicit the defense-related genes *PR1* and *PR2* preventing HR in *A.thaliana*. Although LOS stimulate the gene transcription in two temporal phases, the core oligosaccharide induced only the earlier phase and lipid A induced only the later phase.

Thus, the O-chain fraction should not have a specific role in plant pathogenesis suggested by finding of rough type LPS isolated from diseased plants. Conversely, mutants for biosynthesis of inner or outer core showed reduced virulence degree and they are no longer able to survive *in vivo* owing to chemical and physical stress.

On the other hand, in the natural ecosystem exist plants, which are able to directly interact with various microorganisms in a mutually beneficial way. One of the most studied relationship between plant and microorganisms is represented by Rhizobia species, which fix nitrogen in ammonia. Nitrogen is an essential source for plant life, because it is always required to biosynthetize nucleotides

[17] Shazia N.A. et al., *Molecular Plant Pathology,* **2009***, 10,* 375–387.
[18]Dow M.J., Newman M-A., von Roepenack E., *Annu. Rew, Phytopathol.* **2000**, *38*,241-261.
[19] Dow M.J., Molinaro A., Cooper R.M., Newman M-A., *In Microbial Glycobiology Structures, Relevance and Applications.*

and amino acids. Indeed, bacteria species belonging to Rhizobia are used as biofertilizers in order to decrease the environmental impact due to pesticides commonly used in agriculture field.

From the biological point of view, the symbiotic process is based on two main mechanisms: NF-dependent and NF-independent process (Nod Factor (NF).. In the first, plant signals as flavonoids, polyphenol compounds like apigenin and narigenin, are perceived by bacteria, that induce the transcription of Nod genes and resulting in the transduction of lipochitooligosaccharides, known as Nod Factor (NF). These last molecules are perceived by plant that in turn activate pathways leading to nodules organogenesis on the plant root.[20] Instead, the NF-independent process depends on production of cytokine–like receptor compounds followed by plants epidermidis lesions that likely directly by-pass the early NF-signaling pathway and trigger the nodule organogenensis.

The strategy chosen by bacteria depends on host plant and in any case lead to specific organs on root, termed nodules. Recently data show that in two strain of *Bradyrhizobium* (BTAi1 and ORS278) the canonical *nod*-ABC genes responsible for the biosynthesis of the nod factors are absent although bacteria are still able to induce the nodule formation in plants as *Aeschyomene sensitive* and *Aeschyomeneindica*.[21] This finding suggest the existance of alternative strategies, used by bacteria, to establish the symbiosis and actually there are many studies in progress in order to understand which molecular patterns are involved in this nod factors independent mechanism**.**

Many publications revealed that LPS is essential for diverse stages of symbiosis such as nodules invasion, physiological adaptation and stress resistance.[22] As in the animal innate immune system, also in plants, the recognition of the lipid A moiety may be at least responsible for many of the effects of LPS in plants.[23]

[20] Oldroyd J.E.D., Downie J.M., *Annual Rew. Plant Biol*.,**2008**, *59*, 519-546.
[21] Giraud E., Xu L., Chaintreuil C., Gargani D., Gully D., Sadowsky J.M., *Applied and Environmental Microbiology*, **2013**, 2459–2462.
[22] Silipo A. et al, *Glycobiol.*, **2010**,*20***,** 406-419.
[23] Dow M., Molinaro A., Cooper R.M., Newman M-A., Microbialglycosylatedcomponents in plant disease. In:*MicrobialGlycobiology: Structures Relevance and Applications*, **2009**, (Eds.: Moran A., Brennan P., Holst O.), Elsevier, 803–820.

Chapter II

Structural elucidation of lipopolysaccharides

2.1 Extraction and purification of lipopolysaccharides

The first step to evaluate the structure and function of glyco-conjugates from the bacterial cell envelope is their extraction Two different approaches are used for a selective extraction from intact cells: PCP (phenol/chloroform/petroleum ether 5/8/2) extraction,[24] more useful for selective isolation of lipooligosaccharide (LOS) or rough-type LPS, and phenol/water extraction suitable for smooth-type LPSs isolation.[25] The determining factor of the extraction is the distribution of the hydrophilic portion (O-antigen) of LPS in the aqueous phase, instead the hydrophobic portion of LOS is better disperded in organic phase of PCP.

Usually the LPS once extracted undergoes an enzymatic treatment /nuclease (DNAse and RNAse) and protease) to get rid of nucleic acids and proteins released during the extraction. . To check the purification degree of the extracted phases, the LPS or LOS molecules are then analyzed by polyacrylamide SDS electrophoresis gel (PAGE) and stained with silver nitrate.[26]

The presence of LPS is confirmed by a typical ladder-like profile on the gel at high molecular masses, on contrary LOS is evaluated by a dark region at low molecular masses on the bottom of the gel.

2.2 Structural analysis of LPS

The most common procedure to isolate the major components of LPSs is a mild acid hydrolysis, which lead to cleavage of the ketosidic linkage between Kdo and non-reducing glucosamine of the lipid A.

[24] Galanos C., Luderitz O., Westphal O., *Eur. J. Biochem*., **1969**, *9*, 245-249.
[25] Westphal O., Jann K., *Methods Carbohydr. Chem*., **1965**, *5*, 83-91.
[26] Kittelberger R., Hilbink F., *J. Biochem. Biophys. Methods*, **1993**, *26* (1), 81-86.

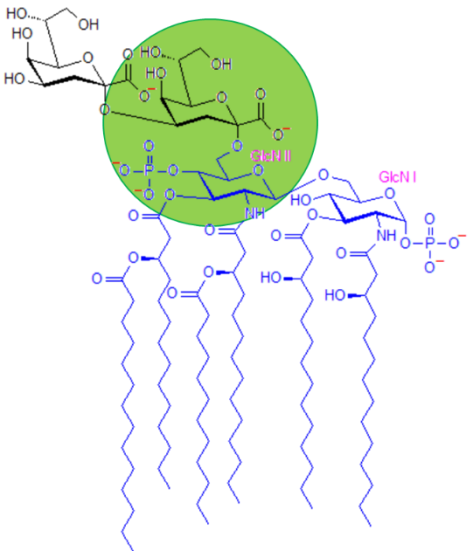

Figure 2.1: Structure of lipid A from *E.coli* (blue), where glucosamine II is linked by Kdo residue (black). The ketosidic linkage is highlighted by the green spot.

After the acid treatment, the insoluble portion, the lipid A, is removed through centrifugation. This linkage is very labile due to several reasons:

The absence of a whichever electron withdrawing group at position adjacent to anomeric C-3 favors the formation of the reaction intermediate oxonium carbocation.

The conversion from chair to half-chair conformation is fastened by the presence of non substituted carbons (less eclipsed interactions in changing conformation.

The presence of an axial hydroxyl group at C-5 contributes to a steric energy release in the formation of intermediate carbocation.

This methodology leads to formation of a Kdo reducing unit with a various conformations (α and β anomers of pyranose and furanose rings, condensed or anhydro forms) that can render the study of the oligosaccharide by NMR spectroscopy particularly difficult.

Thus, typically, the procedure to determine the primary structure of the core oligosaccharide portion is based on de-lipidation of the lipid A by means of alkaline treatment, consisting in adding anhydrous hydrazine to the LOS in order to remove ester-linked fatty acids followed by a hydrolysis in alkaline condition with KOH solution to cleave the amide-linked lipids.[27]

When the sample, contained poly/oligo-saccharide, is ready for chemical analysis, we can implement ad hoc procedures, which allow to determine their primary structure.

[27] Holst O., *Methods Mol. Biol.*, **2000**, *145*, 345 –353.

the quali-quantitative composition of sugar residues
the absolute configuration of each monosaccharide
the ring closure of monosaccharide
the glycosilation points of each monosaccharide
the anomeric configuration of the linkages
the monosaccharide sequence
the location of non-carbohydrates substituents
Additional information on the nature and sequence of monosaccharides can be obtained from diverse treatment such as acetolysis, Smith degradation and β-elimination.

2.2.1 Chemical analysis of LPS

Chemical analyses are very useful to obtain preliminary information about composition of glycoconjugates.
The sample is previously chemical derivatized in volatile compounds and then analysed to Gas-Chromatographer coupled with Mass-Spectrometer (GC-MS). There are numerous methods for the identification of monosaccharide composition as well as glycosilation positions, thus the appropriate choice of the derivatization method can highlight specific features of the sugar residues within the native LPS/LOS structure.
In order to elucidate the compositional analysis of LPS/LOS, dry sample is treated with MeOH/HCl to obtain O-methyl-glycosides, which are later derivatized as per acetylated O-methyl-glycosides (MGA) and finally analyzed via GC-MS.
Comparison of the retention times and the fragmentation pattern with standards allow to the identification of the monosaccharide residues. Quantification analysis can then be obtained by using an internal standard, that usually is per-acetylated inositol.
A further protocol, based on chemical derivatization, is used for distinction between enantiomers with determination of their absolute configuration. The enantiomerically pure alcohol as 2-(+)-octanol or 2-(+)-buthanol is used to obtain O-octyl glycosides, thus the absolute configuration of each monosaccharide residues can be determined.[28] The comparison of retention times with standards derivatized with racemic mixture of 2-octanol or 2-butanol allows to determine the final absolute configuration for each monosaccharide.
Instead, the determination of ring size and the glycosylation positions are performed via methylation analysis.[29]

[28] Leontein K., Lonngren J., *Methods Carbohydr. Chem.,* **1978**, *62*, 359-362.
[29] Hakomori S., *J. Biochem.*, **1964**, *55*, 205-208.

The procedure consists in a double methylation of the polysaccharide with CH_3I and a successive hydrolysis, then the sample is reducted over night with $NaBD_4$ and finally acetylated.and analysed via GC-MS; the fragments observed in the mass spectra are diagnostic for specific substitution patterns

The reduction of the carbonyl function with sodium borodeuteride discriminates the fragments originated from the reduced position (even masses) form those originated from the last position (odd masses). Information obtained from these chemical analyses helps and confirms the interpretation of subsequent NMR and MS experiments.

Chemical analysis can be useful to determinate also the fatty acid composition in LPS and LOS.

Even fatty acid can be derivatized as methyl-ester can be easily analyzed on GC-MS.[30]

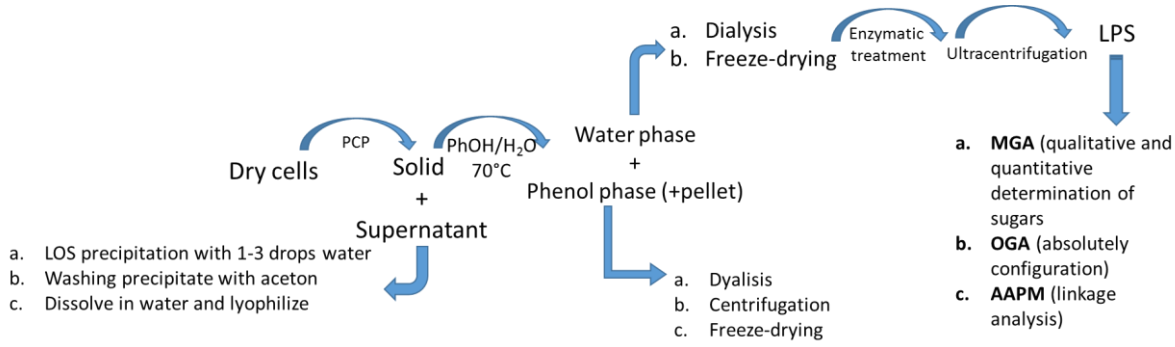

Figure 2.2.1: Isolation and compositional analysis of LPS

2.2.2 NMR spectroscopy

NMR spectroscopy represents among the most useful techniques in the structural characterization of carbohydrates.[31]

The region of ^1H NMR spectrum can be divided in different part:

The region between 5.5 and 4.6 ppm relative to the anomeric protons signals

The region between 4.6 and 2.6 ppm where the ring proton signals are located

The region between 2.5 and 1.0 ppm that is typical of the deoxy positions signals

Furthermore, from a ^{13}C NMR spectrum it is possible to obtain information about:

104-105 ppm : anomeric carbon atoms involved in a glycosidic linkage

80-60 ppm : oxymethylene or carbinolic carbon atoms

60-45 ppm : carbon atoms linked to nitrogen

[30] Rietschel E.T., *Eur. J. Biochem.*, **1976**,*64*, 423-428.
[31] Silverstein R. M., Webster F.X., KiemleJohn D. J., *Wiley & Sons*, **2005**.

~ 30 ppm : aliphatic methylene carbons of deoxy-sugar residues

20-17 ppm : methylene carbon atoms of 6-deoxy-sugar residues and of acetyl residue

In 2D NMR, indeed, a combination of homo- and hetero-nuclear experiments (such as DQF-COSY, TOCSY, NOESY, $^{1}H,^{31}P$-HSQC, $^{1}H,^{13}C$-HSQC, $^{1}H,^{13}C$-HMBC) are required in order to assign all the spin systems, to determine the glycosylation position and the nature of non-carbohydrate substituents.

In sugar having the H-2 axial (glucose, galactose), a $^{3}J_{H1,H2}$ around 8 Hz is indicative of an α-configuration, whereas below 3 Hz of an β- configuration. Sugars with the H-2 equatorial (mannose) show both $^{3}J_{H1,H2}$below 3 Hz. The $^{1}J_{C1,H1}$values are also indicative of the anomeric configuration of pyranose rings, a $^{1}J_{C1,H2}$ below 165 indicates α-anomer, whereas above 170 Hz it indicates the presence a β-anomer. The down-field shift of carbon resonances (glycosylation shift) prove the positions of glycosylation.

NOESY and ROESY together spectra are very useful in confirming the *intra*-residue assignment and the anomeric configuration (e.g. *gluco* or *manno* configuration). In fact, in β-configured sugar is visible NOE contact between H-1 and H-3 and H-1 and H-5, whereas in α-configured H-1 gives NOE effect only with H-2. In addition, *inter*-residual NOE contacts, together with the long range correlations present in HMBC experiments, are crucial to understand the sugar sequence in the saccharide chain.

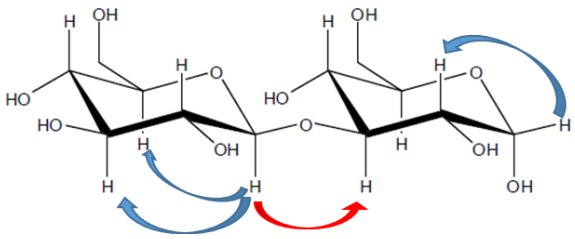

Figure 2.2.2:*Intra*-residual (blue) and *inter*-residual (red) NOE contacts.

2.2.3 Mass spectrometry

Mass spectrometry is a complementary method for structural analysis of lipopolysaccharides and lipooligosaccharides. The most used techniques are MALDI (Matrix Assisted Laser Desorption Ionisation), ESI (Electro Spray Ionisation).

Generally, for carbohydrates, MALDI and ESI MS spectra are performed in negative ion mode, due to the presence of the hydroxyl groups that can lose a proton and acquire a negative charge; even if spectra in positive ion mode are also performed as in case of *Bradyrhizobiums* lipid A.

In MALDI technique, the methodology consists in a soft ionization of a sample that is suspended in a specific matrix that helps the analyte in ionization step. The matrix has double role: the protection of the sample from the laser energy and the capacity to form single charged ions.

In case of LOS, the use of high laser power settings in MALDI spectra permits to obtain fragments derives from the cleavage of the labile ketosidic linkage of the Kdo. In the deriving spectra three regions of signals can be observed, the one of the lipid A, the core oligosaccharide and the intact LOS. In LPS, instead, the spectra displays an information on the size of the repeating unit.

Section I

Plant pathogens

Chapter III

Structural characterization of O-chain of LPS isolated from Burkholderia gladioli pv. cocovenenans

3.1 *Burkholderia gladioli pv. cocovenenans*

Burkholderia spp. are ubiquitous Gram-negative, motile, obligate aerobic rod-shaped bacteria that have the unique ability to adapt to and survive in many different environments. *Burkholderia gladioli* pv. *cocovenenans*, (BGC) isolated from cultures of the mucoralean fungus *Rhizopus microsporus*var.*oligosporus*, plays a key role in the context of plant disease, agriculture and food processing. The *Rhizopusmicrosporus* group consists of various taxa, which are responsible of toxin production, pathogenesis[32],[33] and several lethal intoxications.[34]*R. microsporus* var. *oligosporus* is traditionally used to prepare fermented foods such as tempe, a typical Indonesian dish, however, its consumption has occasionally led to severe intoxications due to the presence of bacterial contaminants in the fungal starter culture.[35] Among these, BGC[36] is responsible for producing the polyketide bongkrekic acid,[37] a respiratory toxin that causes hyperglycaemia followed by hypoglycaemia, which may cause death of consumer.[38,39] Bongkrekic acid is an unsaturated tricarboxylic acid, which inhibits oxidative phosphorylation by blocking the mitochondrial adenine nucleotide translocator.[4041] In addition, several studies demonstrated that also the azapteridine toxoflavin and other complex polyketides, enacyloxins, may contribute to the toxic properties of contaminated tempe.[42]

To gain insights into the recognition events at the basis of bacteria-fungi symbiotic relationships,[43] we performed a structural analysis of the lipopolysaccharide (LPS in particular focusing on the structure of the O-specific side chain, which may have a role in the infection? process above described.

The O-specific polysaccharide, also named O-chain, is a highly variable portion, in the genus *Burkholderia* generally composed of deoxy- or amino-sugars, and further bearing unusual residues and/or non-saccharidic substituents.[44] The number of residues in the repeating unit goes from 2 to 8 monoses and can reach high molecular masses (up to 60000 Da).

---

[32] Walther G., et al., *Persoonia***2013**, *30*, 11–47.
[33] Tintelnot K., Nitsche B., *Mycoses*, **1989**, *32*, 115–8.
[34] Buckle K.A., Kartadarma E.K., *J Appl Bacteriol,***1990**, *68*, 571–6.
[35] Garcia R.A., Hotchkiss J.H., Steinkraus K.H., *Food Addit.Contam.*, **1999**, *16*, 63–69.
[36] Coenye T., Holmes B., Kersters K., Govan J.R., Vandamme P., Urakami et al., *Int J. Syst. Bacteriol*.,**1999**, *49*, 1, 37–42.
[37] Moebius N., Ross C., Scherlach K., Rohm B., Roth M., Hertweck C., *Chem. Biol.,***2012**, *21*,19(9),1164-74.
[38] de Bruijn J., Frost D.J., Nugteren DH., Gaudemer A., Lijmbach G.W.M., Cox H.C., *Tetrahedron*, **1973**, *29*, 1541–7.
[39] K. Scherlach, K. Graupner, C. Hertweck, *Annu. Rev. Microbiol*., **2013**, *67*, 375-97.
[40] Henderson P.J., Lardy H.A., *J. Biol. Chem.*, **1970**, *245*, 1319–26.
[41] Rohm B., Scherlach K., Hertweck C., *Org. Biomol. Chem*., **2010,***7*,8(7),1520-2.
[42] Ross C., Opel V., Scherlach K., Hertweck C., *Mycoses*, **2014**, *3*,48-55.
[43] Uzum Z., Silipo A., Lackner G., De Felice A., Molinaro A., Hertweck C., *Chembiochem*., **2015,***9*,16(3),387-92.
[44] Ieranò T. et al *Chemistry*. **2009**, *20*, 15(29), 7156-66.

The LPS was purified after bacterial cell extraction and then characterized through chemical analysis and 2D NMR spectroscopy. Moreover, the spatial arrangements of the polymer was evaluated by a combined approach of NMR spectroscopy, molecular mechanics (MM) and dynamic (MD) calculations to investigate the conformational space available to the sugar units.
The study of the conformational features of the O-chain region of LPS can improve the understanding of molecular shape of bacterial external surface that deeply influences bacterial invasion and virulence.

Results and Discussion

3.2 Structural isolation and purification of LPS from *Burkholderia gladioli pv. cocovenenans*

LPS of *Burkholderia gladioli* is obtained by a phenol/water extraction; the water phase, in which the LPS was abundant, is submitted to enzymatic treatment followed by an extensive dialysis.
The recovered phase is further purified using gel permeation chromatography, the total lipopolisaccharide fraction was detected by SDS-PAGE. On the latter was visible the typical ladder-like motif of LPS at high molecular weight.

Figure 3.2.1: SDS-PAGE 13.5% on total extract derives from phenol/water extraction. **1**. LPS from E. coli standard; **2**. Water phase; **3**. Phenol phase

3.2.1 Preliminary chemical analysis

Compositional analysis of the LPS fraction showed the presence of 2-O-methyl-D-galactose (Gal2Me), L-rhamnose (Rha), and 3-*O*-methyl-L-rhamnose (L-acofriose, Aco) as carbohydrate components. Fatty-acid analysis detected (R)-3-hydroxyhexadecanoic acid [16:0(3-OH)] with an amide linkage, and (R)-3-hydroxytetradecanoic acid [14:0(3-OH)] and hexadecanoic acid [16:0] with ester linkages. To study the O-chain, a complete deacylation was carried out. The absolute configuration of each monosaccharide unit was assigned on the basis of 2-*O*-octyl glycoside

derivatization using GC–MS, and comparison with appropriate standards. The results of this analysis, taken together with the results of methylation analysis of the delipidated LPS, showed the presence of 2-substituted- L-Rha*p*, 4-substituted-D-Gal*p*, 4-substituted-D-Gal2Me*p*,and 2-substituted-L-Aco*p*.

3.3 Full characterization of O-chain from LPS of *Burkholderia gladioli pv. cocovenenans* wild type

3.3.1 NMR Analysis

The de-O-acylated product is then studied by NMR spectroscopy. 2D NMR experiments (DQF-COSY, TOCSY, ROESY, NOESY, 1H,13C HSQC, 1H,13C HSQC-TOCSY, and 1H,13C HMBC) were performed to assign all spin systems; the anomeric configuration of each monosaccharide was attributed on the basis of the $^{3}J_{\text{H-1,H-2}}$ coupling constant values obtained by DQF-COSY, whereas the relative configuration of the sugar residues was assigned on the basis of the $^{3}J_{\text{H,H}}$ ring coupling constants; finally, the *intra*-residue pattern of dipolar correlations gave further confirmation of the anomeric configurations.

The 1H NMR spectrum of the O-chain moiety is shown in Figure 3.3.1.

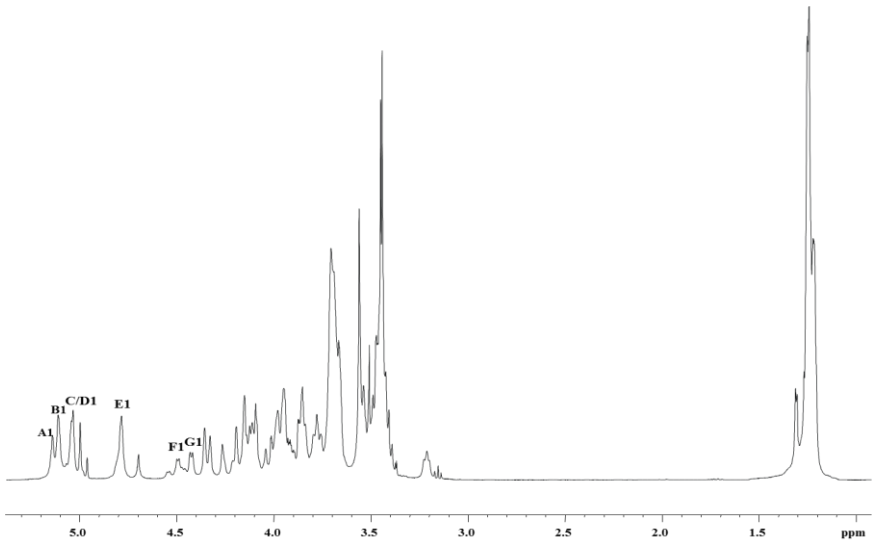

Figure 3.3.1: 1H NMR spectrum (600 MHz) of the O-chain fraction from *Burkholderia gladioli* pv. *cocovenenans*. The low-intensity signals in the anomeric region at 5.00 and 4.97 might be related to the core oligosaccharide region or to minor components, and are not assigned.

The anomeric region of the ^{1}H NMR spectrum (Figure 3.3.1) contained several signals (**A**–**G**, Table 3.3.1) that corresponded, as demonstrated below, to two tetrasaccharide repeating units.

Unit	1	2	3	4	5	6
A	5.14	4.35	3.53	3.47	3.67	1.24
2- α -Aco	100.72	73.18	79.41	70.2	69.3	16.5
	$^1J_{CH}$176.9 Hz		O-CH_3 3.44/56.9			
B	5.11	4.327	3.53	3.47	3.67	1.24
2- α -Aco	100.72	73.18	79.41	70.2	69.3	16.5
	$^1J_{CH}$176.9 Hz		O-CH_3 3.44/56.9			
C	5.04	4.19	3.78	3.43	3.67	1.24
2- α -Rha	99.37	77.46	69.3	71.3	69.3	16.5
	$^1J_{CH}$175.6 Hz					
D	5.03	4.15	3.76	3.40	3.66	1.24
2- α -Rha	99.37	77.8	69.3	71.3	69.3	16.5
	$^1J_{CH}$175.6 Hz					
E	4.78	3.98	3.85	3.44	4.11	1.21
2-α-Rha	101.13	77.6	69.2	72.2	69.2	16.3
	$^1J_{CH}$174.9 Hz					
F	4.49	3.2	3.69	3.94	3.69	3.69
4-β-Gal-2OMe	101.7	80.2	71.14	77.2	75.2	60.5
	$^1J_{CH}$164.8 Hz	O-CH_3 3.55/60.49				
G	4.42	3.51	3.69	3.94	3.60	3.60
4-β-Gal	102.6	70.3	71	77	75	60.5
	$^1J_{CH}$164.8 Hz					

Table 3.3.1: 1H and 13C NMR chemical shifts (ppm) of the O-antigen from *B. gladioli* **X** [→2)-α-Rha-**(**1→2)-α-Aco-**(**1→2)-α-Rha-(1→4)-β-Gal2Me-(1→]*n* and **Y** [→2)-α-Rha-**(**1→2)-α-Aco-**(**1→2)-α-Rha-(1→4)-β-Gal-(1→]*n*. The 1H and 13C chemical shifts for the methoxy groups are at δ= 3.44/56.9 ppm and δ= 3.55/60.4 ppm,respectively.

Spin systems **C**/**D** and **E** (Figures 3.3.1, 3.3.2, and 3.3.3) were identified as 2-substituted α-rhamnose residues due to the scalar correlations, evident in the TOCSY spectrum, of the ring protons with

methyl signals resonating in the shielded region of the spectrum. Their α-anomeric configuration was established on the basis of the $^{1}J_{C,H}$ values (see Table 3.3.1), and of the *intra*-residual NOE correlation of 1-H with 2-H. Their *manno* configuration was assigned by evaluation of the $^{3}J_{H,H}$ coupling constants.

Spin systems **A** and **B** corresponded to 2-substituted acofriose residues, as deduced by the downfield shift of C-3 of **A**/**B** (δ=79.4 ppm, Table 3.3.1), by the NOE correlation of 2-H and 3-H of **A**/**B** with a methoxy group resonating at δ= 3.44 ppm, and by the long-range correlation present in the HMBC spectrum of **A**/**B** (3-H/C-3) with the methoxy group. (Figure 3.3.2-3.3.3).

The final spin systems, **F** and **G** (1-H at δ= 4.49 and4.42 ppm, Figure 3.3.1) were identified as 4-substituted 2-*O*-methyl-β-galactose and 4-substituted-β-galactose, respectively.

The *galacto* configuration was assigned on the basis of the low$^{3}J_{3\text{-}H,4\text{-}H}$ and $^{3}J_{4\text{-}H,5\text{-}H}$ coupling constants. The β-anomeric configuration was inferred from the $^{1}J_{C,H}$ values, and was confirmed by the *intra*-residue correlations of 1-H with 3-H and 5-H in the NOESY spectrum. Furthermore, the downfield shift of C-2 of **F** (δ= 80.2 ppm, Table 3.3.1), and the long-range correlation in the HMBC spectrum of 2-H and C-2 of **F** with a methoxy group at 3.55/60.4 ppm were all proof of *O*-methylation at the 2-positionof residue **F** (Figure 3.3.2).

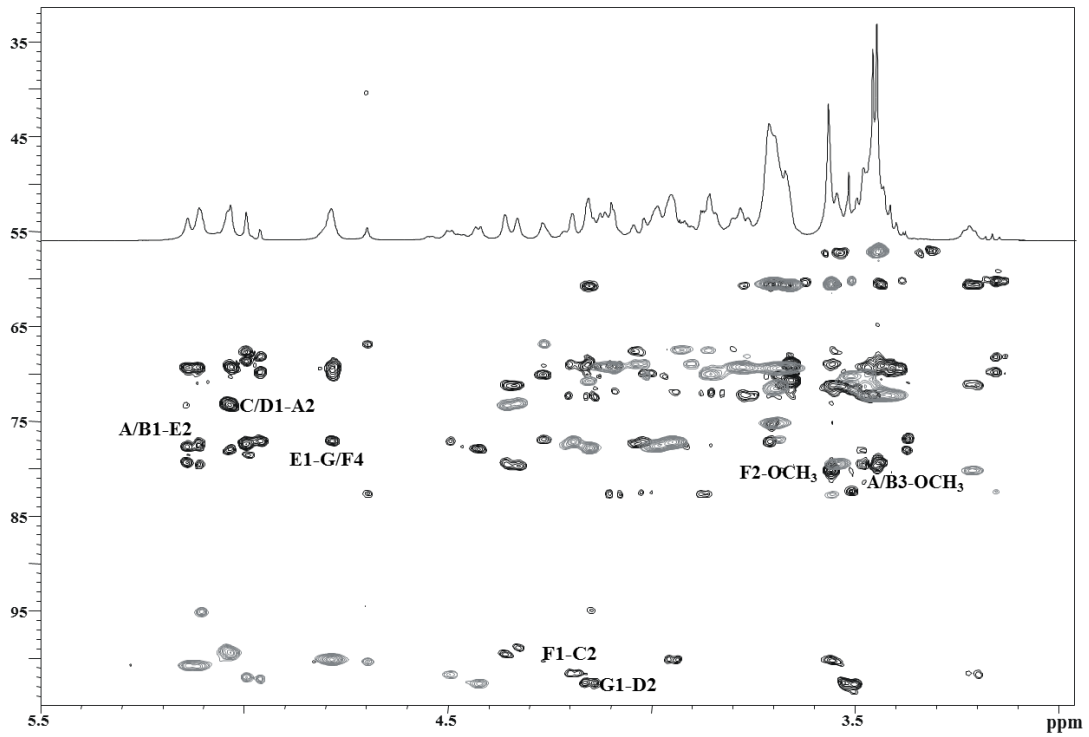

Figure 3.3.2: HMBC (black) and HSQC (grey) spectra of the O-chain fraction from *Burkholderia gladioli* pv. *cocovenenans*.

The sequence of the sugar residues in the repeating unit was determined by NOESY and HMBC experiments. Downfield shifts of the carbon resonances identified the glycosylated positions: C-2 of residues **A**, **B**, **C**, **D**, and **E**, and C-4 of residues **F** and **G**, which was in full agreement with the methylation analysis.

Analysis of the *inter*-residue correlations in the HMBC spectrum revealed the presence of two polysaccharide repeating units. Thus, spin system **E** was glycosylated at O-2 by both residues **A** and **B**, as proved by the long-range correlations **A** (1-H/C-1)‑**E**(2-H/C-2) and **B**(1-H/C-1)‑**E**(2-H/C-2) (Fig. 3.3.3), and by the corresponding NOE contacts. This indicates the coexistence of two different polysaccharides. Spin system **A** was in turn glycosylated at O-2 by residue **C**, while spin system **B** was substituted at O-2 by residue **D** (Fig. 3.3.2-3.3.3, see HMBC and NOE contacts). Spin system **D** was in turn glycosylated at O-2by residue **G**, as shown by the long-range and NOE correlations between **G**(1-H/C-1) and **D**(2-H/C-2) (Figures 3.3.2 and3.3.3). Similarly,α-rhamnose residue **C** was glycosylated at O-2 by residue **G** (Figures 3.3.3 and 3.3.4). Residues **F** and **G** were both glycosylated by residue **E** at O-4, as indicated by long-range correlations and NOE contacts (Figures 3.3.2 and 3.3.3).

To summarize, the pattern of long-range correlations derived from the HMBC spectrum, and of NOE dipolar correlations showed that the O-chain isolated from BGC was characterized by the coexistence of two polysaccharide repeating units **X** and **Y**, which differed in the non-stoichiometric methylation at position O-2 of the β-galactose residue.[45]

[45]De Felice A.,Silipo A., Scherlach K., Ross C., Hertweck C., Molinaro A., *Eur. J. Org. Chem*.,**2016**, 748–755.

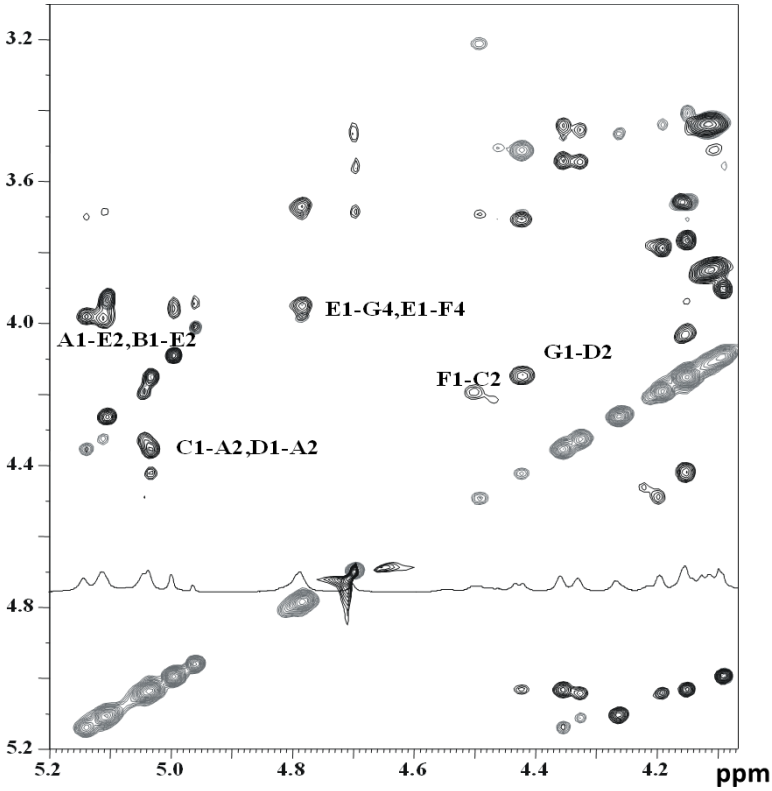

Figure 3.3.3: A section of ROESY (black) and TOCSY (grey) spectra of the O-chain fraction from *Burkholderia gladioli* pv. *cocovenenans*.

Definitely, the polysaccharide displayed two species reported here below:

Species X

C **A** **E** **F**

[→2)-α-Rha-**(**1→2)-α-Aco-**(**1→2)-α-Rha-(1→4)-β-GalMe-(1→]$_n$

Species Y

D **B** **E** **G**

[→2)-α-Rha-**(**1→2)-α-Aco-**(**1→2)-α-Rha-(1→4)-β-Gal-(1→]$_n$

3.3.2 Conformational analysis: Molecular Mechanic and Dynamic calculations on the O-chain moiety

In order the gain information on the solution conformation of the two polysaccharide repeating units, we firstly built the potential energy surfaces for each disaccharide connected by a glycosidic linkage; Φ represents the torsion angle about H1-C1-O-CX' whereas Ψ about C1-O-CX'-HX'. For both repeating units the following disaccharides Gal→2Rha or GalMe→2Rha, Rha→2Aco, Aco→2Rha and Rha→4Gal or Rha→4GalMe were constructed and subjected to calculations using MM3* force field to provide a first estimation of the conformational regions energetically accessible. The resulting adiabatic energy maps indicating global and local minima are reported in Fig. 3.3.4. All glycosidic torsions adopted exo-anomeric conformations in the main energetic minima, the presence of the O-

methyl group at position 2 of the galactose unit did not affect the resulting adiabatic map. A certain flexibility around Ψ angle was evident for the α–(1→2) glycosidic units.[46]

For both polymers, a dodecasaccharide fragment containing three repeating units was built from the global minima of the energy maps and the conformational behavior was studied by using molecular dynamic simulation:

$A_1 \rightarrow 2E_1 \rightarrow 4F_1 \rightarrow 2C_1 \rightarrow 2A_2 \rightarrow 2E_2 \rightarrow 4F_2 \rightarrow 2C_2 \rightarrow 2A_3 \rightarrow 2E_3 \rightarrow 4F_3 \rightarrow 2C_3$ **Dodecasaccharide X**

$B_1 \rightarrow 2E_1 \rightarrow 4G_1 \rightarrow 2D_1 \rightarrow 2B_2 \rightarrow 2E_2 \rightarrow 4G_2 \rightarrow 2D_2 \rightarrow 2B_3 \rightarrow 2E_3 \rightarrow 4G_3 \rightarrow 2D_3$ **Dodecasaccharide Y**

The initial structures were extensively minimized and trajectory coordinates were sampled every ps; 10,000 simulations were performed in GB/SA water solvation model as implemented in MacroModel (MMOD). Trajectories and Φ/Ψ scatter plots of the different glycosidic linkages, together with the population of each conformational family are shown in Fig. 3.3.5.

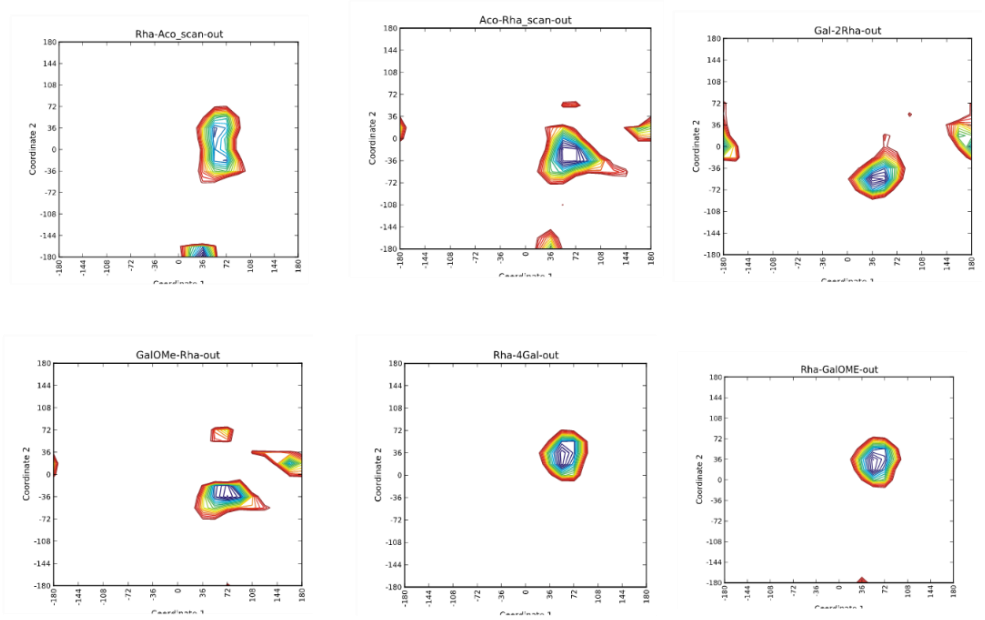

Figure 3.3.4: Relaxed energy maps for the disaccharide fragments composing the O-polysaccharide from *Burkholderia gladioli*

[46]Clément M.J. , Imberty A., Phalipon A., Pérez S., Simenel C., Mulard L.A., Delepierre M., *J. Biol. Chem.*,**2003,** *278 (48)*, 47928–47936.

A)

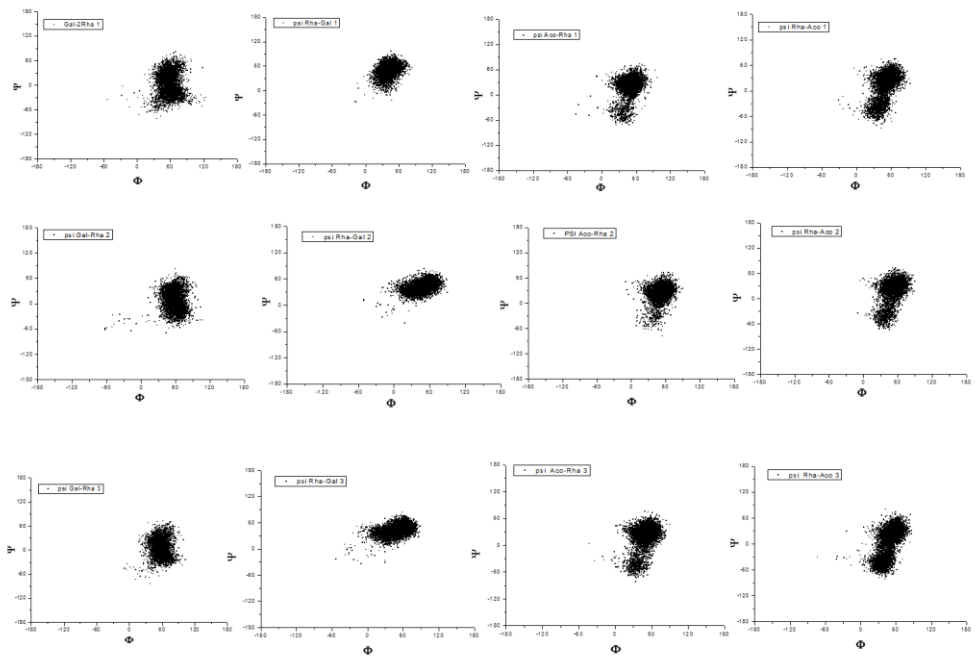

B)

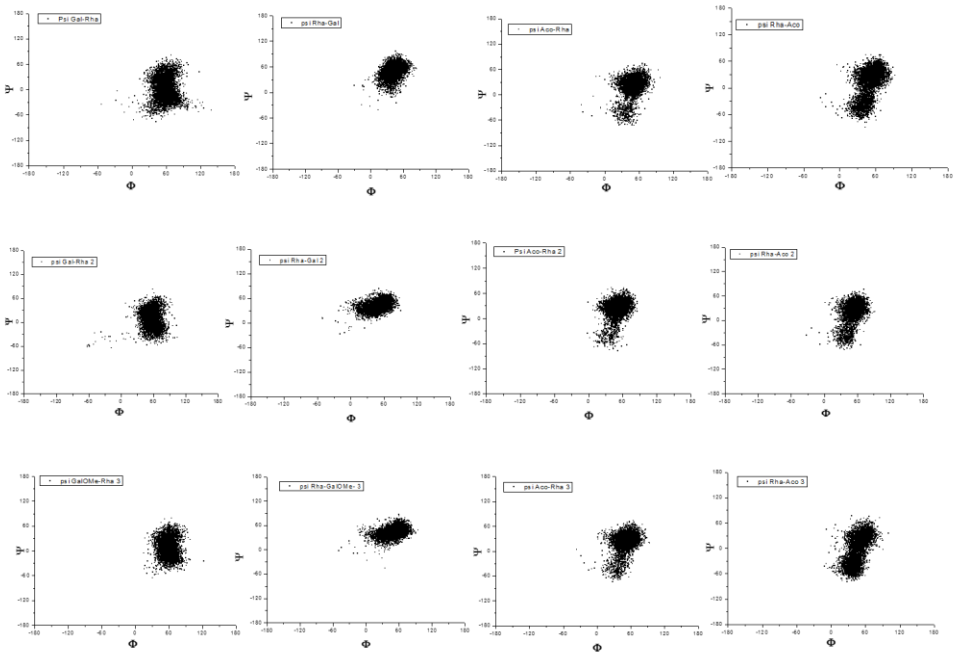

Figure 3.3.5: Scatter plots of φ vs. ψ values for the disaccharide fragments that compose the two O-chain sequences, a) species **X** and b) species **Y**.

Specie X					
	Experimental (Obs. NOE)	**Pentasaccharide**	**Dodecasaccharide**		
Gal-2Rha	2.55	2.55±0.28	2.55±0.28	2.55±0.26	2.54±0.26
Rha-4Gal	2.77	2.76±0.35	2.79±0.32	2.76±0.32	2.75±0.33
Aco-2Rha	2.57	2.54±0.30	2.55±0.27	2.58±0.27	2.54±0.28
Rha-2Aco	2.58	2.47±0.31	2.58±0.30	2.60±0.30	2.48±0.30

Specie Y					
	Experimental (Obs. NOE)	**Pentasaccharide**	**Dodecasaccharide**		
Gal-2Rha	2.56	2.57±0.28	2.55±0.28	2.55±0.26	2.55±0.26
Rha-4GalOMe	2.77	2.82±0.339	2.79±0.32	2.76±0.32	2.78±0.32
Aco-2Rha	2.56	2.54±0.30	2.54±0.27	2.58±0.27	2.56±0.28
Rha-2Aco	2.57	2.46±0.30	2.58±0.31	2.60±0.29	2.46±0.30

Table 3.3.2: Experimental (from NOESY experiments) and calculated (from MD calculations) interresidue proton–proton distances {1-H–X′-H distances [Å] for a (1→X′) linkage} for oligomers built with two and three repeating units. The experimental values were obtained as described in the experimental part by applying the isolated spin-pair approximation.

MD results showed that trajectories remained in the broad low energy regions previously predicted by the MM calculations and all glycosidic linkages mainly adopted Φ/Ψ values in accordance with the exo-syn anomeric conformation, in agreement with the MM results and the experimental data. The simulation showed a higher flexibility for the α-(1→2) linkages involving α-manno configured sugar moieties and for the β-(1→2) linkage of the β-Gal→Rha units. Conversely, the examination of MD data showed the existence of a rather compact energy well for the α-(1→4) glycosidic linkages (linkages E→4F for species X, E→4G for species Y). The computational models obtained from the MD data were then compared to the experimental results. Ensemble average inter-proton distances for each molecule were extracted from dynamic simulations and translated into NOE contacts according to a full-matrix relaxation approach. The corresponding average distances obtained for the simulation from $\langle r^{-6} \rangle$ values were compared to those collected experimentally (Table 3.3.2). A. satisfactory agreement was observed between the calculated and the experimental values.

Given the good flexibility around the glycosidic linkages of both O-chain structures, as expected both polysaccharides adopted a variety of three-dimensional shapes in rapid interchange. Snapshots of the most representative conformers of O-chain species **X** and **Y** are depicted in Figure 3.3.6 a and 3.3.6 b; both adopted a helicoidal shape even though with a different extensions, more constricted in case of dodecasaccharide X and more extended in case of dodecasaccharide Y.

A)

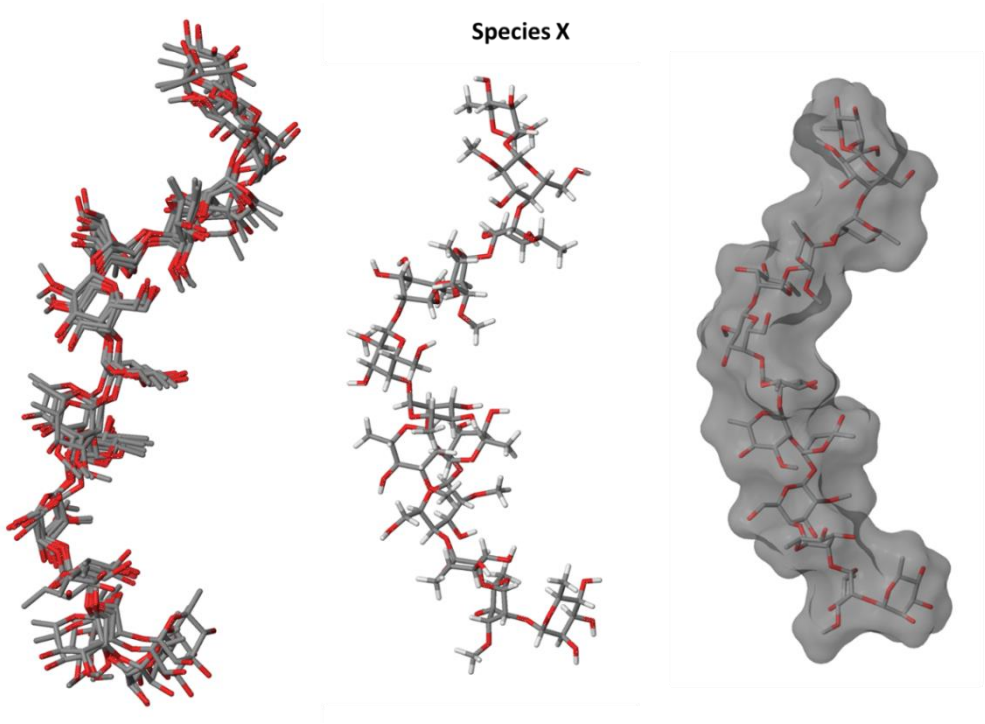

B)

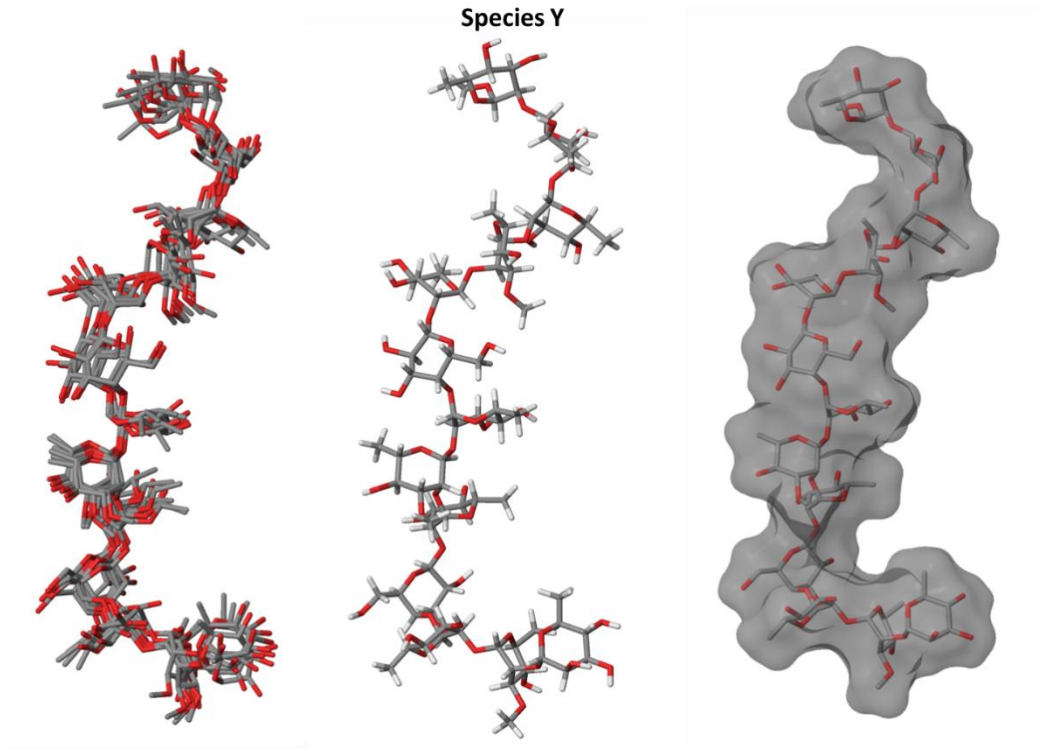

Figure 3.3.6. View of representative structures and Connelly surfaces of the conformers for species **X** and **Y**.

3.4 Structural characterization by MALDI mass spectrometry of LPS and the lipid A

The intact LPS and lipid A were analyzed by MALDI mass spectrometry to gain further information on lipid A in both conditions. This first approach is very useful as it allows the study of intact molecules[47,48] without any chemical manipulation, thus preventing the loss (either by alkaline or acid treatment) of labile groups (e.g., phosphate, acetyl), typically present on LPSs. The complete LPS undergo to negative-ion MALDI mass spectrometry showed, in addition to the molecular ions related to the native LPS mixture (*m/z* 3400-4000), fragments between *m/z* 1400 and 2300.

[47] Sturiale L., Garozzo D., Silipo A., Lanzetta R., Parrilli M., Molinaro A., *Rapid Communications in Mass Spectrometry*, **2005**,*19*, 1829–1834.
[48] Sturiale L., Palmigiano A., Silipo A., Knirel Y.A., Anisimov A.P., Lanzetta R., Parrilli M., Molinaro A., Garozzo D., *J. Mass Spectrom*., **2011**, *46*, 1135-1142.

The MALDI-TOF mass spectrum of the *Burkholderia gladioli* LPS (Fig. 3.4.1) obtained in the linear negative mode contained three distinct clusters of ions, corresponding to lipid A fragments, core fragments and intact LPS, respectively.

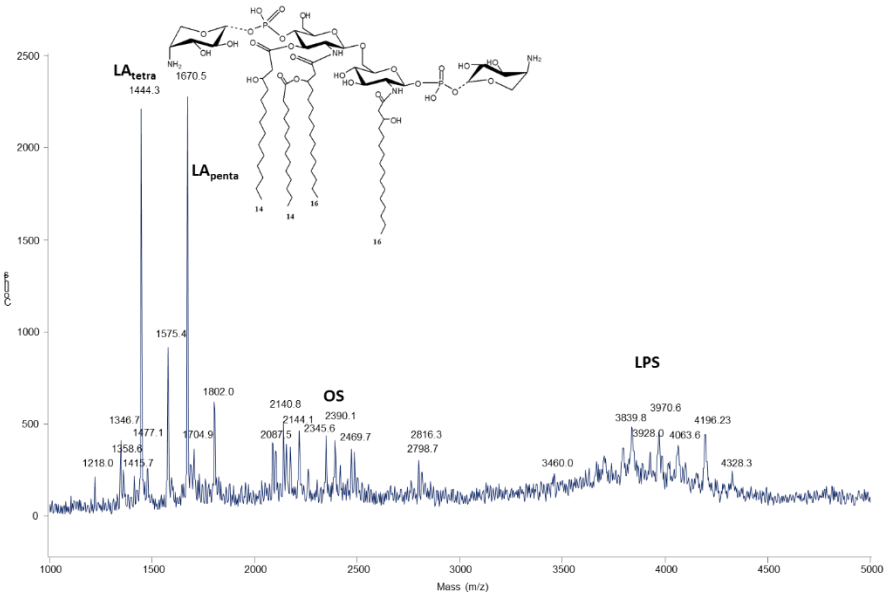

Figure 3.4.1: MALDI TOF MS analysis of total from *Burkholderia gladioli*; Negative-ion mass spectrum showing both LPS molecular ions and their ion fragments, attributable to the core oligosaccharides and to the reported lipid A structure.

The chemical structure of lipid A from *B. gladioli* was also analyzed after mild acetic acid hydrolysis. Penta-acylated lipid A species (*m*/*z* 1670.5) includes two N-linked C_{16}:3OH residues of and two C_{14}:3OH *O*-linked residues of as primary acyl groups and one secondary residue of C14 fatty acid. The tetra-acylated form (*m*/*z* 1444.3) is present in equal amounts and lacked one residue of C_{14}:3OH. A characteristic feature of this LPS is the presence of significant amount of tetra- and penta-acylated lipid A species (*m*/*z* 1494.44 and 1721.54, respectively), bearing one residue of 4-amino-4-deoxyarabinose (Ara4N) attached to one of the phosphate groups.

Frequently, acetic treatment partially induce cleavage of the phoshpate group on lipid A backbone. In particular, MALDI MS (Fig. 3.4.2) revealed the presence of ion cluster at *m/z* 1364.34 and 1590.43 corresponding to mono-phosphorylated tetra and penta-acylated lipid A species.

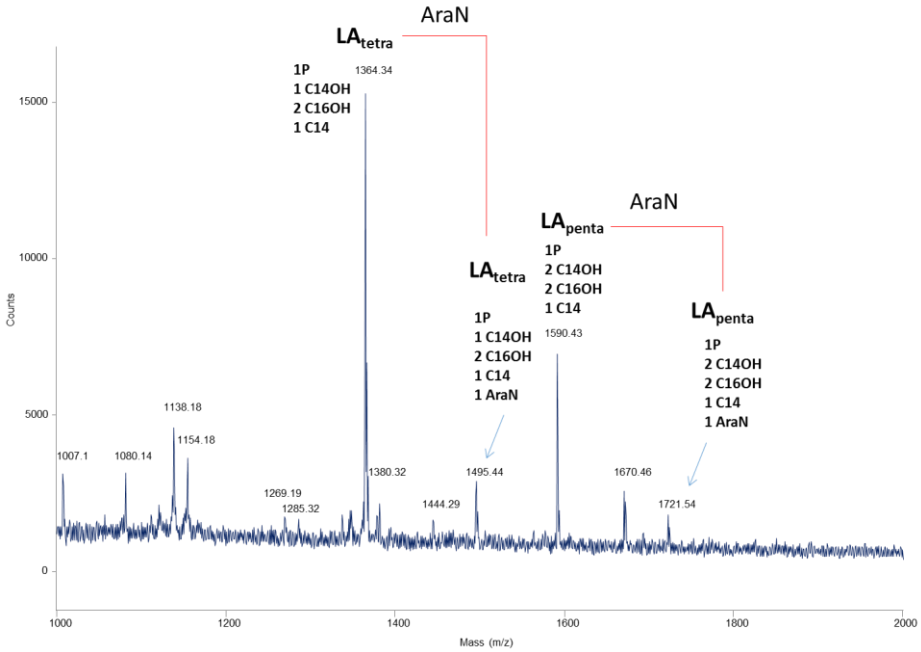

Figure 3.4.2: MALDI MS spectrum in negative ion mode dispalys pattern of the mono-phosphorylated, tetra and penta-acylated lipid A moiety obtained by acetate buffer hydrolysis

3.5 Conclusions

The LPS O-chain structure of *B. gladioli* pv. *cocovenenans* HKI 10521 (DSM 11318) consists of a mixture of two repeating units/polymers characterized by a tetrasaccharide (Figure 3.3.6 a and b) with the galactose unit non-stoichiometrically methylated at position O-2.

A combined approach based on NMR spectroscopy and MD simulation was used to study the conformational properties of the two O-polysaccharides. The data indicated a limited flexibility of the α-(1→4) glycosidic linkage, and a remarkable flexibility of the (1→2) glycosidic linkages. The surfaces of the two dodecasaccharides were built according to the Connelly method to gain additional information about the overall shape of these species. The two species adopted comparable shapes with a helicoidal extension. The existence of two repeating units implies different three-dimensional shapes giving rise to structures with different packings and extension.

The NMR spectroscopic data did not give clear evidence as to whether the O-chain structure is a mixture of two different O-chain polymers or whether it was a single polymer with a blockwise repeating unit organization. The presence of two different O-antigens for *Burkholderia* LPSs is common, especially for plant-associated bacteria.[49,50]

[49] De Castro C., Molinaro A., Lanzetta R., Silipo A., Parrilli M., *Carbohydr. Res.*, **2008**, *343*, 1924‑1933.
[50] Silipo A. et al., *Glycobiology,* **2010**, *20*, 406‑419.

However, it is very rare for other bacterial LPSs. Most of the monosaccharide residues found in O-chains are 6-deoxysugars, either rare monosaccharide residues or more typically rhamnose and fucose. This is also true of the O-antigens reported here: both repeating units contain L-rhamnose and 3-*O*-methyl-L-rhamnose. The non carbohydrate appendages and the deoxysugars help to confer a hydrophobic character to bacterial cell surface, which is probably important in its interaction with eukaryotic plant cells. In fact, it has been shown that the O-antigens from different planta associated bacteria have a pivotal role in the context of the innate immune response of the host to the bacterial cell. The O-antigen can either suppress the immune response (as for symbiosis), or trigger it (pathogenesis).[51,52]

[51] Seltmann G., Holst O., *The Bacterial Cell Wall*, **2001**, Springer, Heidelberg, Germany,
[52] Alexander C., Rietschel E.T., *J. Endotoxin Res.,* **2001**, *7*, 167‑202.

Chapter IV

Determination of O-antigen structure from Gram-negative bacterium Burkholderia fungorum

4.1 *Burkholderia fungorum*

Burkholderia fungorum strain DSM 17061 is a Gram-negative bacterium isolated respectively from an oil refinery discharge and rhizosphere of hybrid poplar. It is rod-shaped, strictly aerobic, catalase positive and oxidase negative. It is capable of transforming polycyclic aromatic hydrocarbon (PAHs), which are an extended class of organic compounds containing two or more condensed aromatic rings. Their molecular stability and hydrophobicity are among the prominent factors that contribute to the persistence of these pollutants in the environment.[53] Preliminary studies carried out on *Burkholderia fungorum* strain has revealed that this bacterium plays a key role in phytoremediation of organic contaminants. Infact, the inoculation of *B. fungorum* into hybrid poplar planted in non-contaminated soil could cause a negative e effect on biomass index, whereas inoculated plants in contaminated soil, result to have a better tolerance against toxic effects of PHAs.[54] Recently, many studies have been focusing on microbe-assisted phytoremediation, where the presence of endophytic micro-organisms enhances plants growth.[55,56]

Thanks to the study of the LPS structure disposed on the bacteria's outer membrane[57],it was possible to explain the elementary mechanism of plant pathogen recognition.

Results and Discussion

4.2 Structural characterization of LPS from *Burkholderia fungorum*

The bacterial pellet was extracted with a phenol/water solution 90%, and the LPS was obtained in water phase. From preliminary chemical analysis, the water phase resulted to be abundant in nucleic acid and proteins as well, so we proceeded with enzymatic

[53] Cerniglia C.E., *Biodegradation*, **1992**, *3*, 351–368.
[54] Andreolli M. et al, *Chemosphere*, **2013**, *92*, 688-694.
[55] GermaineK.J., KeoghE., RyanD., DowlingD.N., *FEMS Microbiol. Lett.*, **2009**, *296*, 226–234.
[56] SoleimaniM. et al. *Chemosphere*, **2010**, *81*,1084–1090.
[57] Silipo A., De Castro C., Lanzetta R., Parrilli M., Molinaro A., Lipopolysaccharides. In: *Prokaryotic Cell WallCompounds - Structure and Biochemistry*. **2010**, König, H., Claus, H., Varma A., Eds.; Springer, Heidelberg.

treatment followed by a consecutive ultracentrifugation. The obtained product, resulted to contain pure LPS, which was the subject of the following chemical analysis.

Figure 4.2.1: SDS-PAGE 13.5% on total extract derives from phenol/water extraction. **1**. Water phase; **2**. Phenol phase

4.2.1 Preliminary analysis

The compositional analysis of LPS fraction showed the presence of a huge amount of L-rhamnose (Rha) and L-xylose (Xyl) as carbohydrate components whereas fatty acids analysis detected (*R*)-3-hydroxyhexadecanoic acid [16:0(3-OH)] in amide linkage and (*R*)-3-hydroxytetradecanoic [14:0(3-OH)] acid and hexadecanoic acid [16:0] in ester linkage. With the purpose of isolating and characterizing the O-chain structure, a mild acid hydrolysis on pure LPS was performed. On the supernatant, containing the O-polysaccharide, was performed a swift chemical analysis to determine monosaccharides composition and then the same sample was treated with 2-octanol to assign the absolute configuration of each monosaccharide using GC-MS compared with appropriate standards. Linkage analysis performed on the free O-polysaccharide revealed the presence of 2-substituted-L-Rha*p*; 4-substituted-L-Rha*p*; 2,3-substituted-L-Rha*p* and terminal-L-Xyl*p*.

4.3 NMR characterization of O-polysaccharide isolated from LPS of *Burkholderia fungorum* wild type

Mono and bi-dimensional NMR were performed on the supernatant of acetic acid product. The anomeric configuration of each monosaccharide unit was assigned on the basis of the $^{3}J_{\text{H-1,H-2}}$ and $^{1}J_{\text{C,H}}$ coupling constant values, whereas the values of the vicinal $^{3}J_{\text{H,H}}$ ring coupling constants allowed the identification of the relative configuration of each sugar residue. The region of spectrum that goes from 5.30-4.30 ppm contained several anomeric signals. Actually, some of them were due to the O-polysaccharide and the others belonged to by-products of the acid hydrolysis reaction. The intense signals shown in (Figure 4.3.1) were part of the O-chain (**A-G,** table 4.3.1) and they matched, as

demonstrated below, with tetrasaccharide-repeating units with a non-stoichiometric terminal xylose as appendage.

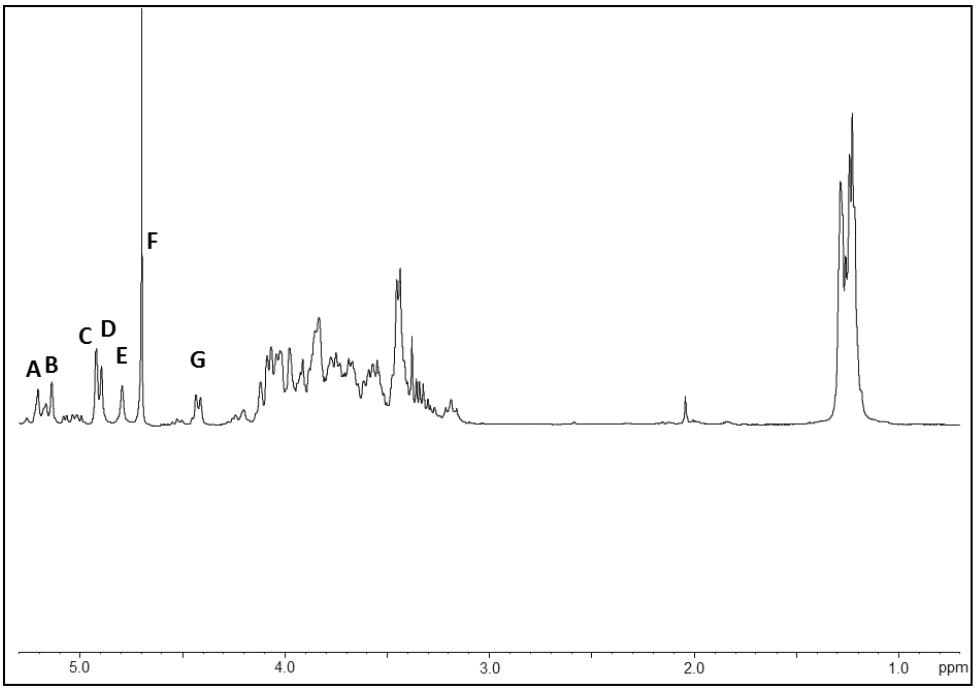

Figure 4.3.1: ^{1}H NMR spectrum (400 MHz) of the O-chain fraction from*Burkholderia fungorum.*

Spin system **A** H-1/**B** H-1at 5.20/100.9 and 5.14/102 ppm (Fig. 4.3.2 and tab. 4.3.1) were identified as 2-substituted α-rhamnose residue on the basis of scalar correlation between ring protons and methyl group resonating at low value of chemical shift. The residue **A/B** displayed an α-anomeric configuration established from the $^{1}J_{C\text{-}H}$ values and the *intra*-residual NOE contact of H-1 with H-2, even the *manno* configuration was assigned by evaluation of $^{3}J_{H,H}$ coupling constants. An additional α-*manno*-configurated spin systems was **C** (H-1/C-1 at 4.92/101.9), which was identified as 4-substituted-α-rhamnose for the chemical shift value of C-4 at downfield region of spectrum. (Figure 4.3.2 and table 4.3.1)

Unit	1	2	3	4	5	6
A	5.20	3.97	3.85	3.44	3.85	1.24
2- α -Rha	100.9	78.3	69.8	71.9	69.0	16.7
	$^{1}J_{CH}$ 176.9 Hz					
B	5.14	4.01	3.89	3.44	3.78	1.24
2- α -Rha	102.0	78.3	69.8	71.9	69.2	16.7
	$^{1}J_{CH}$ 176.9 Hz					
C	4.91	4.08	3.84	3.55	3.74	1.22
4- α -Rha	101.9	69.5	69.9	82.5	67.5	16.7
	$^{1}J_{CH}$ 175.6 Hz					
D	4.89	4.07	3.84	3.55	3.74	1.22
4-α-Rha	102.0	69.5	69.9	82.5	67.5	16.7
	$^{1}J_{CH}$ 175.6 Hz					
E	4.79	4.11	3.68	3.44	3.44	1.28
2,3-β-Rha	100.1	79.3	76.1	71.2	71.9	16.8
	$^{1}J_{CH}$ 174.9 Hz					
F	4.69	4.04	3.60	3.44	3.44	1.27
3-β-Rha	101.1	70.4	79.5	71.2	71.9	16.8
	$^{1}J_{CH}$ 164.8 Hz	O-CH_3 3.55/60.49				
G	4.42	3.31	3.38	3.58	3.18/3.93	
β-Xyl	104.5	73.5	75.3	69.3	64.9	
	$^{1}J_{CH}$ 164.8 Hz					

Table 4.3.1: ^{1}H and ^{13}C NMR chemical shifts (ppm) of O-antigen from *B. fungorum.*

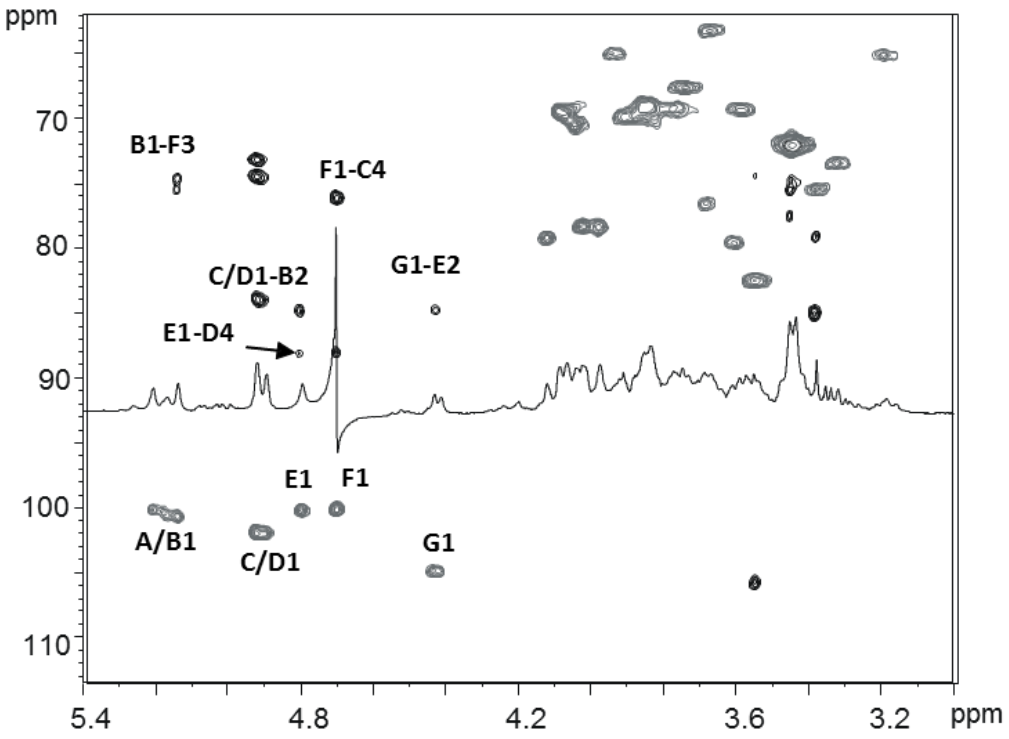

Figure 4.3.2: HSQC (grey) and HMBC (black) spectra of O-polysaccharide isolated from *B. fungorum*.

Instead, spin system **E** was assigned as 2,3-substituted β-rhamnose residue, as deduced by high glycosylation shift at position C-2 and C-3 respectively at 79.3 and 76.1 ppm. (Fig. 4.3.2 and tab. 4.3.1). These data were also confirmed by linkage analysis. Residue **E** was glycosylated at O-3 and O-2 respectively by residues **A** and **G** as shown by *inter*-residual NOE contact between **A1**-**E3** and **G1**-**E2** and in turn residues **C**/**D** was glycosylated at O-4 by residue **F/E** respectively. (Figure 4.3.3) The last spin system **G** H-1/C-1 at 4.42/104.5 ppm corresponded to a terminal β-xylose residue, as suggested by chemical analysis. The anomeric signal gave all long range correlations with protons ring and both H-5 resonating at 3.92/3.17 ppm peculiar for methylene group of a pentose residue. (Fig. 4.3.3) All data proved the presence of the β-*gluco*-configurated monosaccharide.

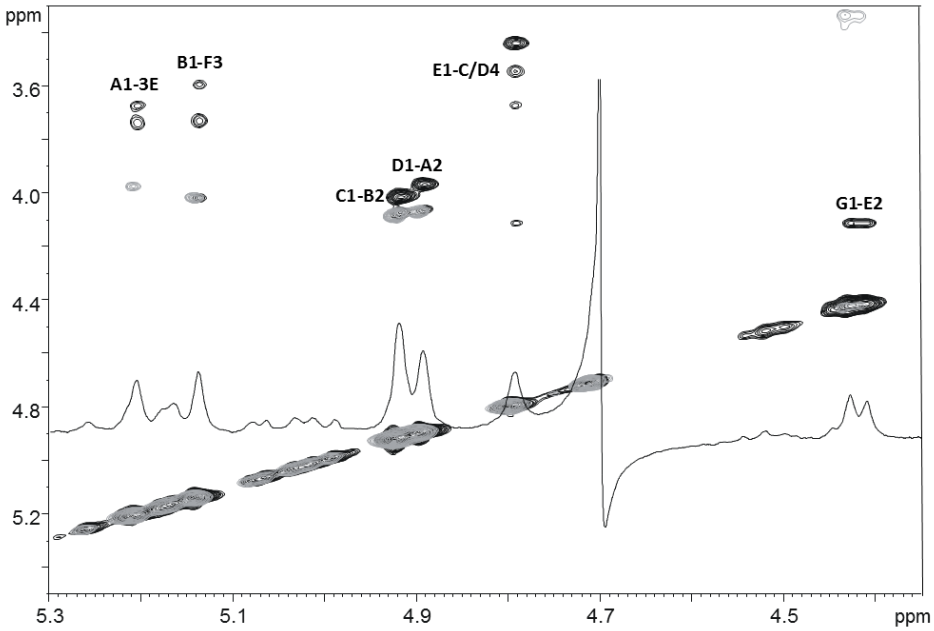

Figure 4.3.3: A section of NOESY (black) and TOCSY (grey) spectra of the O-chain fraction from *Burkholderia fungorum.*

The sequence of the sugar residues in the repeating unit were determined by NOESY and HMBC experiments, which were allowed to determine the following O-polysaccharide structures (Figure 4.3.4):

A **E** **D**

X [→2)-α-Rha-**(**1→3)-β-Rha-**(**1→4)-α-Rha-(1→]$_n$

2

↑

1)-β-Xyl **G**

B **F** **C**

Y [→2)-α-Rha-**(**1→3)-β-Rha-**(**1→4)-α-Rha-(1→]$_n$

Figure 4.3.4: Structures of the O-chain isolated from *Burkholderia fungorum*

4.4 Structural characterization by MALDI mass spectrometry of LPS and the lipid A

As previously discussed (paragraph 3.4 section I), lipid A was characterized by a combination of chemical analysis and MALDI mass spectrometry. The lipid A fraction under review was recovered by a mild acid hydrolysis. Chemical analyses showed the presence of 6-substituted-GlcN and terminal-GlcN, both in D-configuration and a further residue, terminal-4-amino-4-deoxy-arabinose, with L-configuration. The negative ion MALDI spectrum is reported in Fig. 4.4.1. In analogy with lipid A structures from *Burkholderia*,[58]also this specie has the classical β-(1→6)-GlcN*p* carbohydrate backbone phosphorylated at the α-anomeric position of the reducing GlcN and at O-4 of the non-reducing β-GlcN. At these phosphate groups were attached through a phosphodiester linkage to β-Ara4N residues. Ion peaks at *m/z* 1012.8 and 1670.6 were identified as tri-acylated and penta-acylated lipid A respectively, possess in ester linkage two 14:0 (3-OH) and one 14:0 residues, and in amide linkage two 16:0 (3-OH) residues. Instead, at *m/z* 1444.3corresponded to a minority species of tetra-acylated lipid A, that carried a less C14:3OH respect to the LA_{penta} specie. In addition to the signals attributable to the lipid A, in MALDI spectrum are detected also core and total LPS signals.

[58] De Soyza A., Silipo A., Lanzetta R., Govan J.R., Molinaro A.,*Innate Immunity,* **2008**, *14*,127-144.

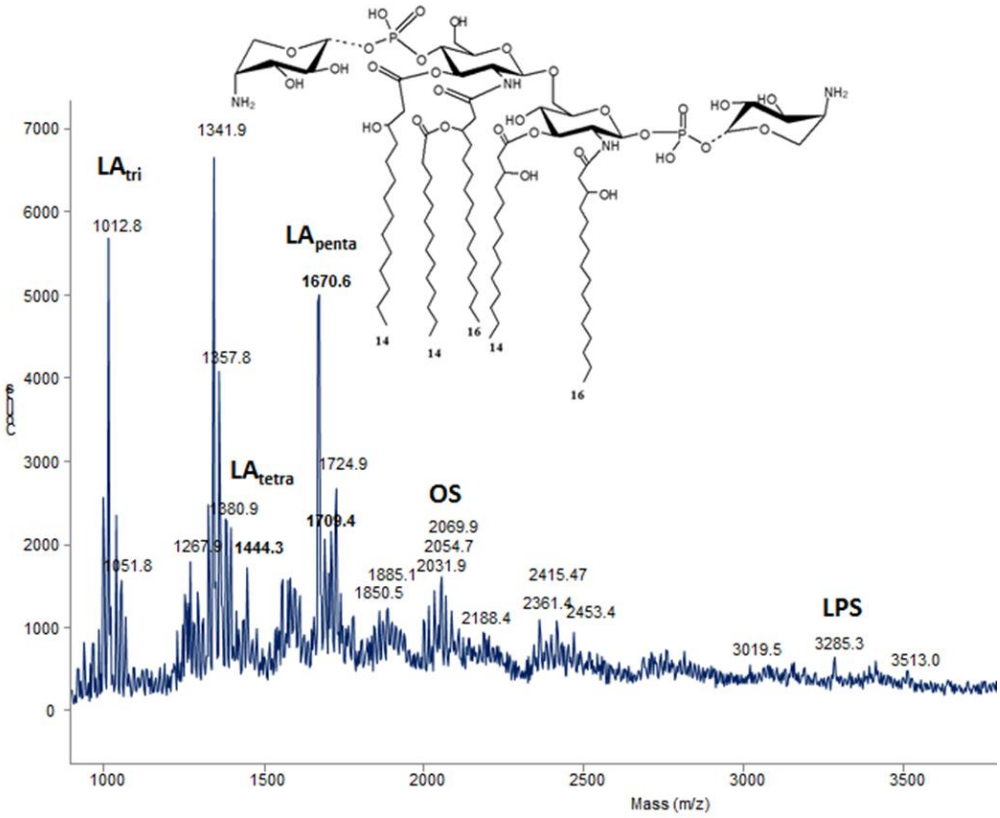

Figure 4.4.1: MALDI TOF MS analysis of total LPS from *Burkholderia fungorum*; Negative-ion mass spectrum showing both LPS molecular ions and their ion fragments, attributable to the core oligosaccharides and to the reported lipid A structure.

In summary, MS analysis of the intact LPS completed and confirmed the previous structural hypotheses and allowed the full assignment of the lipid A structure from *Burkholderia fungorum*

Chapter V

Elucidation of LPS structure isolated from Pantoea ananatis strain M408

5.1 *Pantoea ananatis* strain M408

Pantoea ananatis is a natural ubiquitous Gram-negative bacterium. In many cases, bacteria are associated with plants and they are responsible of positive effects on the growth promotion. However, several Pantoea strains, among which strain M408, cause plant diseases in maize and rice, the most abundant product farmed in Europe.[59]

Maize is not only the most used source of methanol and biomass for direct burning, but has an agricultural significance for the fodder production for animals nutrition and grains for human consumption. The occurrence of bacterial pathogens of maize is reported from different parts of the world. [60,61] Some pathogenic tests confirm that *P. ananatis* stimulate a hypersensitivity reaction, producing brown lesions and necrotic tissue on leaves of maize.[62]

In order to elucidate the recognition at molecular level between plant-bacteria, it is pivotal to investigate structure of lipopolysaccharide (LPS), the major component of the outer membrane of Gram-negative bacteria, and in particular the polysaccharides portion, exposed on the bacterial external surface.[63]

5.2 Structural characterization of LPS from *Pantoea ananatis* strain M408

P. ananatis M408 was grown in TSB medium.[64] The lipopolysaccharide was extracted by the hot phenol–water method and then purified by enzymatic treatment. The LPS was found in the water phase as confirmed by SDS-PAGE showing the characteristic ladder LPS profile (Figure 5.2.1). A further purification by ultracentrifugation was conducted to remove glucan contaminant and afterward, the hydrolysis under mild acidic conditions of LPS released the O-antigen and lipid A sediment. The latter was removed by centrifugation and the supernatant was loaded onto a size exclusion chromatography on TSK50 column (Toyopearl HW-50).

[59]Krawczyk K., Kamasa J.,Zwolinska A.,Pospieszny H. *J., Plant Pathol*., **2010**, *92* (3), 807-811.
[60] Cother E. J. et al *Austr.PlantPathol*., **2004**, *33*, 495–503.
[61] Coutinho T.A. et al *PlantDis*., **2002**, *86*, 20–25.
[62] Goszczynska T., Botha W.J., Venter S.N.,Coutinho T.A.,*Plant Dis*., **2007**, *91*, 711–718.
[63] Silipo A., De Castro C., Lanzetta R., Parrilli M., Molinaro A.,Lipopolysaccharides. In: *Prokaryotic Cell Wall Compounds - Structure and Biochemistry.* König, H., Claus, H., Varma A., Eds.; Springer, Heidelberg, **2010**
[64] Lisowicz F., et al *OchronaRoslin,* **1995**, *39*, 10-11.

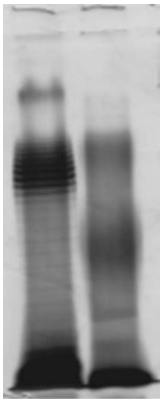

Figure 5.2.1: SDS-PAGE of the LPS isolated from *Pantoea ananatis* after enzymatic treatment.**1**) LPS from E.coli; **2**) water phase

5.2.1 Preliminary analysis

The polysaccharide moiety underwent GC-MS analyses as acetylated *O*-methyl glycosides derivative and revealed the presence of rhamnose and galactose as major components. Their absolute configuration was established by using *O*-octyl glycoside derivatives in which it was possible to find rhamnose in L-configuration and galactose in D-configuration. Linkage analysis revealed the presence of terminal galactose, 2-substituted rhamnose and 2,3-di-substituted rhamnose. The polysaccharide obtained was fully characterized by 2D NMR spectroscopy.

5.3 NMR characterization of O-chain isolated from LPS of *Pantoea ananatis* strain M408

The O-antigen was studied by 2D NMR (Tab. 5.3.1). From the ^{1}H NMR spectrum (Fig. 5.3.1), the presence of five different spin systems was evident. Four of them, labeled **A**, **B**, **C** and **D**, were typical *manno*-pyranose rings on the basis of small vicinal $^{3}J_{1,2}$ and$^{3}J_{2,3}$ coupling constants of about 2 Hz and 3.2 Hz respectively and of large $^{3}J_{3,4}$ and $^{3}J_{4,5}$ around 10 Hz. These data, together with chemical analyses, suggested that the O-chain portion was mainly constituted by a differently substituted Rha*p* chain.

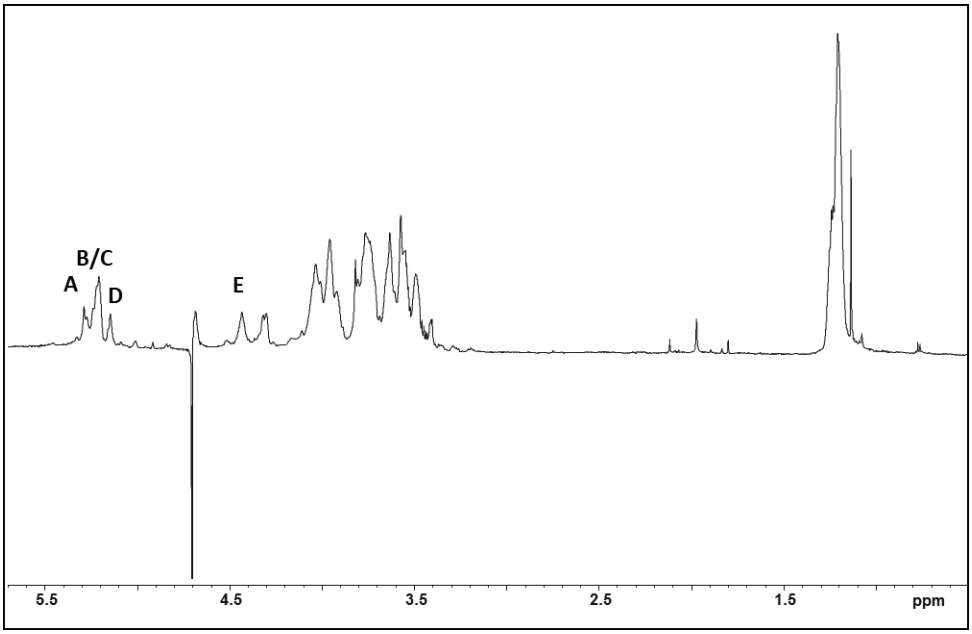

Figure 5.3.1:[1]H NMR spectrum (600 MHz) of the O-chain fraction from *Pantoea ananatis* M408.

The α-anomeric configuration of all of these four residues was assigned on the basis of their H-5 and C-5 chemical shift.[65]

Spin system **E** (H-1/C-1) at 4.42/106.3 ppm was identified as terminal β-Gal*p* residue. The *galacto* configuration was established by the low values of $^{3}J_{3,4}$ and $^{3}J_{4,5}$ coupling constants, while the β-anomeric configuration of **E** was inferred by anomeric resonances and by $^{1}J_{C,H}$ values and also confirmed by the *intra*-residue correlations of H-1 with H-3 and H-5 in the ROESY spectrum. Furthermore, the ^{13}C resonances showed a non-substituted monosaccharide, as also confirmed by linkage analysis.

Spin system **D** (H-1/C-1) at was identified as a 2,3-substituted Rha*p* as confirmed by a relevant glycosylation shift of C-2 and C-3, respectively at 75.8 and 81.4 ppm (see Tab.5.3.1 and Fig. 5.3.2).

[65] Lipkind G. M., Shashkov A. S., Knirel Y. A., Vinogradov E. V., Kochetkov N. K.,*Carbohydr. Res.*, **1988**, *175*, 59-75.

Residue	1	2	3	4	5	6
A	5.28	4.03	3.96	3.54	3.79	1.26
2-α-Rha	99.1	74.4	69.9	69.7	70.1	17.5
B	5.22	3.95	4.00	3.50	3.76	1.20
2-α-Rha	98.7	76.4	69.8	69.7	70.1	16.8
C	5.20	3.92	4.01	3.53	3.75	1.21
2-α-Rha	99.2	76.7	69.9	69.7	70.3	15.5
D	5.14	4.32	4.06	3.55	3.74	1.21
2,3-α-Rha	99.5	75.8	81.4	71.0	70.0	16.5
E	4.42	3.57	3.81	3.72	3.62	3.63/3.72
t-β-Gal	106.3	72.7	68.8	70.0	75.5	60.8

Table 5.3.1: ^{1}H and ^{13}C NMR chemical shifts (ppm) of O-antigen isolated from *Pantoea ananatis*. All rhamnose residues are in L-configuration, while the galactose residue is in D-configuration.

Residue **D** was in turn glycosylated at O-2 by residues **B** (H-1/C-1) at 5.22/98.7 ppm and at O-3 by **E** (H-1/C-1) at 4.42/106.3 ppm, which respectively were identified as 2-substituted Rha*p* and t-Gal*p* (see Tab. 5.3.1), as shown by *inter*-residual NOE contact between **B1-D2** and **E1-D3** (Fig. 5.3.3). Likewise, residue **A** (H-1/C-1) at 5.28/99.1 ppm and residue **C** (H-1/C-1) at 5.20/99.2 ppm were both identified as 2-substituted Rha*p* residues as shown by the downfield displacement of ^{13}C chemical shift of both C-2, respectively at 74.4 and 76.7 ppm (see Fig. 5.3.2).

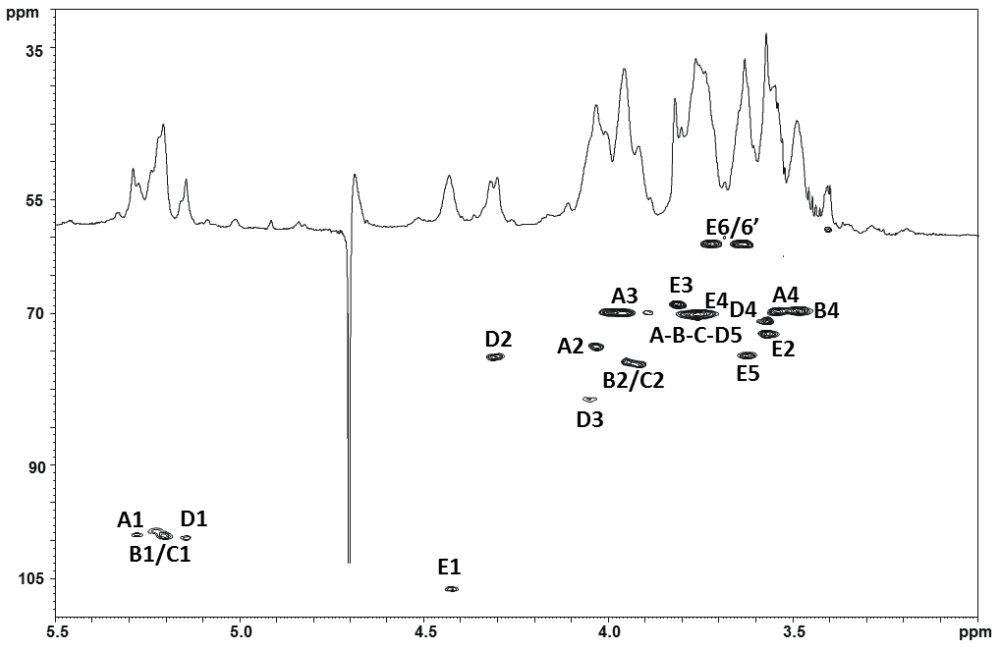

Figure 5.2.2: ^{1}H NMR and HSQC (black) spectra the O-chain fraction from *Pantoea ananatis* M408

Residue **A** was in turn glycosylated by residue **C** at O-2 and was linked at O-2 of **B** residue. In fact, by means of ROESY experiment, the NOE contacts between **C1-A2**, **A1-B2** and **D1-C2** (see Fig. 5.3.3) were identified.

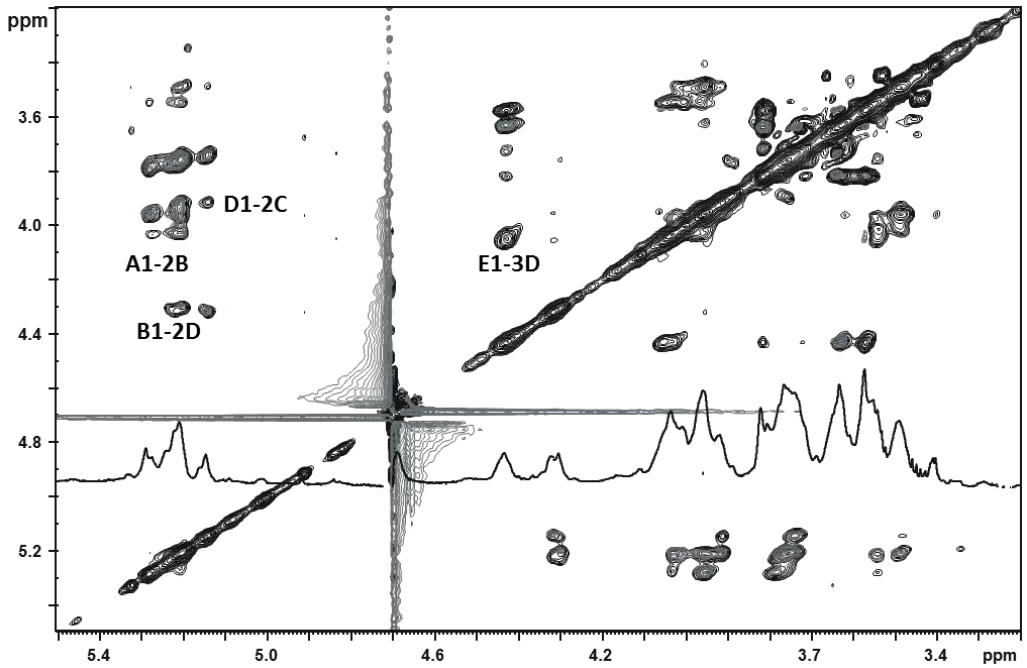

Figure 3: ROESY and TOCSY spectra (black and grey respectively) of the O-chain fraction from *Pantoea ananatis* M408.

All of the above data confirmed the presence of a linear tetrasaccharidic rhamnose chain carrying a galactose as appendage, as shown below.

D **C** **A** **B**

[→2)-L-α-Rha(1→2)-L-α-Rha(1→2)-L-α-Rha(1→2)-L-α-Rha(1→]$_n$

3

↑

1)-D-β-Gal **E**

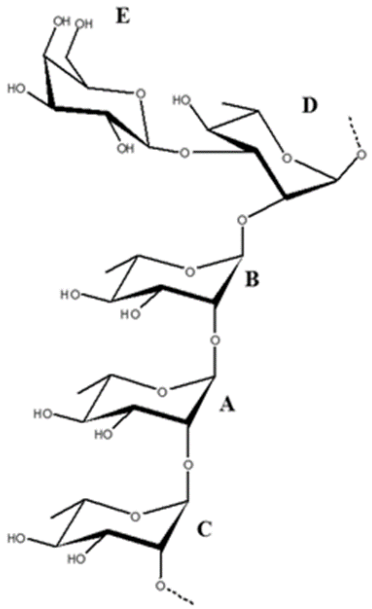

In conclusion, the structure of the LPS O-antigen from *P. ananatis* M408 was established by a combination of chemical and NMR analyses. It is built up of a tetrasaccharide rhamnose chain to which is linked a single branching galactose residue. The rhamnose chains are quite common moieties of Gram negative bacterial LPS especially those associated with plants,[66,67,68,69] and we deem that LPS O-antigen plays a major role in bacteria plant association, either positive or negative.

5.4 Mass spectrometry on LPS and lipid A portion

A negative ion mode MALDI spectrum was performed on the crude lipid A, obtained as pellet after acetic acid hydrolysis. The spectrum in negative ion mode (Fig. 5.4.1) showed clearly abundant molecular ion at *m/z* 1279.84 and several minor ion cluster at *m/z* 1506.03, 1716.22 and 1798.17; which corresponded respectively to tetra-acylated lipid A, penta and hexa-acylated lipid A. The detected molecular mass of tetra-acylated lipid A (**L_1**) suggested the following composition: two glucosamine residues, one C12:0, three C14:3OH and one phosphate group. A second specie (**L_2**)at *m/z* 1359.80 showed the mass increment of 79.96 uma respect to (**L_1**), which is attributable to additional phosphate group on the backbone. Therefore, **L_2**results to be a bis-phosphorylated lipid A specie.

A second ion cluster was also detectable in a mass range between 1450-1550, the ion peak at *m/z* 1506.03 is associated to penta-acylated lipid A (**L_3**) shaped by two glucosamine, four C_{14}:3OH, one C_{12}:0 and one phosphate substituent, otherwise the lipid A composition is altered in terms of fatty

[66] De Felice A. et al *Eur. J. Org. Chem.,***2016**, 748–755.
[67] Silipo A. et al*Glycobiol.*, **2010,***20***,** 406-419.
[68] Molinaro A., Newman M. A., Lanzetta R., Parrilli M.,*Eur. J. Org. Chem.*,**2009**, 5887-5896.
[69] De Castro C., Molinaro, A., Lanzetta R., Silipo A., Parrilli M., *Carbohyd. Res*., **2008**, *343*, 1924-1933.

acids distribution(two glucosamine, three C_{14}:3OH, one C_{14}:2OH,one C_{12}:3OH, one C_{12}:O and one phosphate group).

Moreover, mass difference of 226.19 uma in mass spectrum between (**L**$_1$) and (**L**$_3$) disclosed the presence of one C14:3OH more in lipid A structure; and in addition the hexa-acylated specie detected at *m/z* 1798.17 carrying a further C_{14}:3OH and C_{14}:0. As tetra-acylated lipid A (**L**$_2$), also hexa-acylated lipid A displayed mass loss of 79.96 uma, attributable to mono-phosphorylated lipid A (**L**$_4$). Both losses of phosphate groups depended on mild acid treatment on LPS, because these groups were generally acid labile substituents.

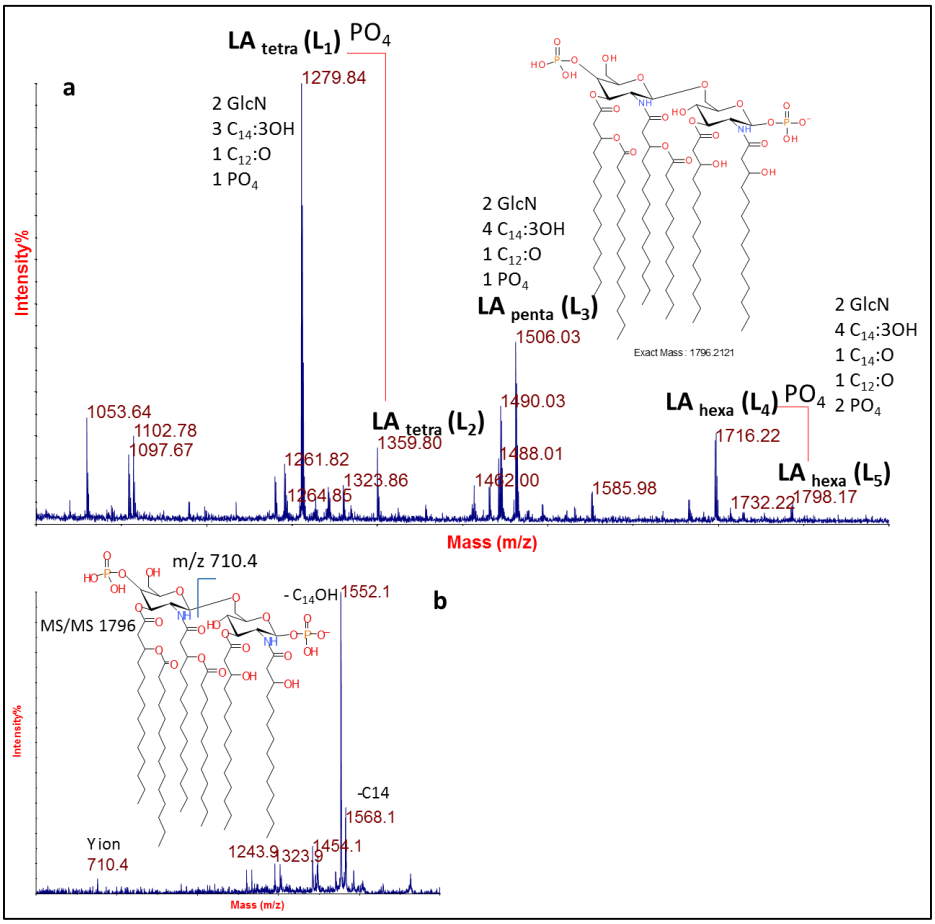

Figure 5.4.1:**a**) Mass spectrum on the crude lipid A obtained after acetic acid buffer hydrolysis; **b**) MS/MS spectrum on bis-phosphorylated lipid A hexa-acylated.

To bypass this inconvenience the complete LPS was undergo to mass spectrometry analysis. Adjusting of laser intensity was possible to cleave the labile linkage between lipid A and Kdo, so in the linear spectrum (Fig. 5.4.2 a) was already clearly visible a division between lipid A signals around 1200-1800 and total LPS signals around 3500-4000. (Fig. 5.4.2 b)

Once identified the ion cluster of intact LPS, was performed also a MS/MS experiment in order to distinguished precisely lipid A portion and saccharide portion of LPS and propose a structure hypothesis of oligosaccharide portion. (Fig. 5.4.2 c)

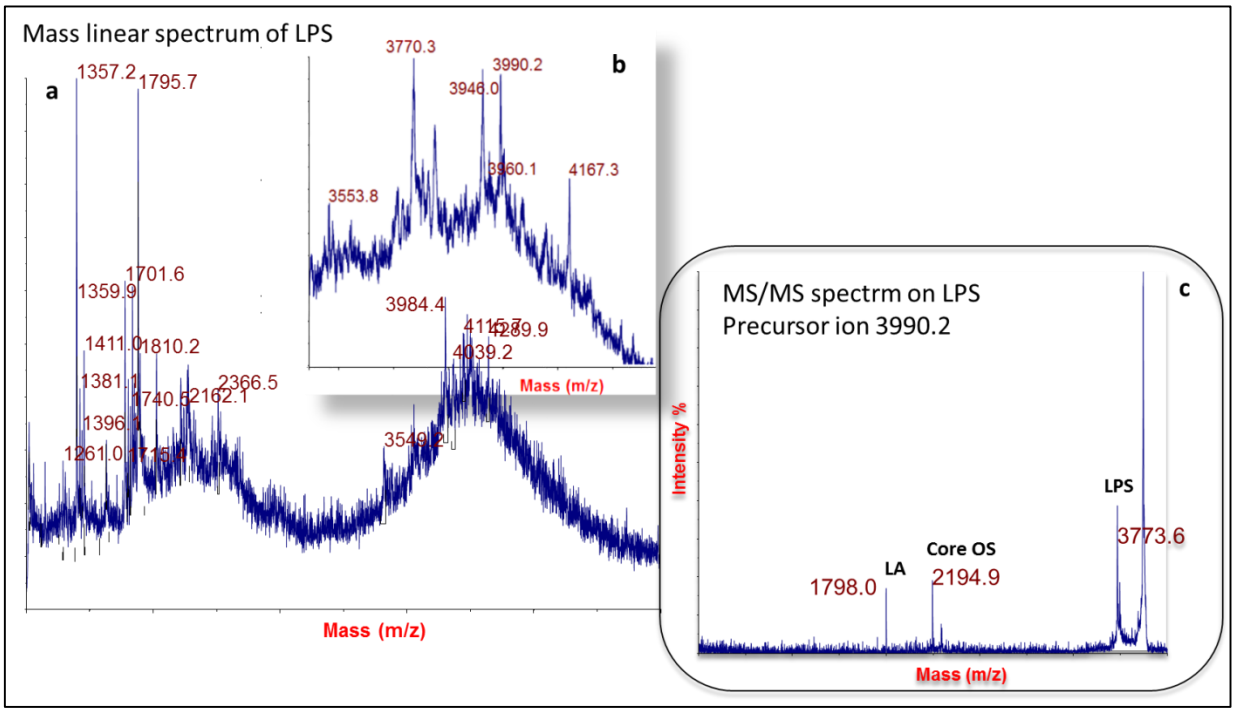

Figure 5.4.2:**a**) Mass linear spectrum of whole LPS; **b**) zoom region of mass spectrum at high masses; **c**) MS/MS spectrum on the complete LPS.

Core OS turns out to be formed by two hexoses, one N-acetyl-hexosamine, three heptoses, three kdo, two uronic acid, one phosphate group. It was evident that the lipid A structure above reported, was comparable with *E.coli* lipid A. as expected since *Pantoea ananatis* M408 belong to *Enterobacteriaceae*

Section II

Plant symbionts

Chapter VI

Structural elucidation of LPS from Bradyrhizobia bacteria

6.1 Introduction

Bradyrhizobium species are Gram-negative nitrogen-fixing bacteria capable to establish a mutualistic symbiotic relationship with plants of *Leguminosae* genus. As a consequence of the endosymbiotic process, bacteria, most commonly *Rhizobiaceae*, cause the development of root nodules in which they can fix atmospheric nitrogen into ammonia available as energy for nucleotide building blocks biosynthesis.

Generally, legume plants sticked by bacteria belongs to *Aeschynomene* genus and they cannot survive in absence of Rhizobia (as *Mesorhizobium*, *Sinorhizobium*, and *Azorhizobium*), therefore they have been largely used in agriculture system to enhance the natural nitrogen sources avoiding the use of chemical fertilizer.[70]

The molecule that effectively carry out an important role during the interaction with the legume host is the lipopolysaccharide (LPS) disposed on the bacterial surface.[71,72]

Among the three regions constituting the LPS, the lipid A, the core oligosaccharide and the O-antigen side chain, the last one directly enters in contact with the host plant during the symbiotic interaction and it is the most variable among the bacteria. This structural diversity of the O-antigen region could modulate or suppress the plant defense reactions, in order to facilitate the establishment of the symbiosis.[73]Interestingly, it has been described that the LPS O-antigen of photosynthetic BradyrhizobiumBTAi1 is a homo-polymer built up on a unique bicyclic α-(1→7)-linked monosaccharide that had never been described before in nature, named bradyrhizose.[74]

Furthermore, it has been shown that this *Bradyrhizobium* O-antigen does not trigger the innate immunity in different plant families, including the host plant *A. indica*.

In fact, recently data show that in two strain of *Bradyrhizobium* (BTAi1 and ORS278) the canonical *nod*-ABC genes, and thus the nod factor, are absent although bacteria are still able to induce the nodule formation in plants as *Aeschyomene sensitive* and *Aeschyomene indica*.[75]

This finding overturns the previous hypothesis and suggests an alternative strategy, where bacteria have evolved a modification in non-immunogenic O-antigen structure to avoid the induction of the plant immune system in order to facilitate the establishment of the symbiosis.

Actually, there are many studies in progress in order to understand which molecular patterns are involved in this nod factors independent mechanism.

---

[70] OgutcuH., AdiguzelA., GulluceM., KaradayiM., SahinF.,*Romanian Biotechnological Letters,* **2009**, *14*, 4294-4300.
[71] Fraysse N., Couderc F., Poinsot V.,*Eur J Biochem*.,**2003**,*270*(7), 1365–80.
[72] Lerouge I., Vanderleyden J., *FEMS Microbiol Rev.,* **2002**, *26*(1), 17–47.
[73] Carlson R.W., Forsberg L.S., Kannenberg E.L., *Subcell.Biochem*., **2010**,*53*, 339–86.
[74] Silipo A., et al., *AngewChemInt Edit*., **2011**, *50*(52),12610–2.
[75] GiraudE., XuL., ChaintreuilC., GarganiD., GullyD., Michael SadowskyJ., *Applied and Environmental Microbiology*, **2013**, 2459–2462.

Overall, the plant immune system, as in mammals, has acquired the ability to recognize the molecular structures of MAMPs, but their receptors recognition happens into the plasma membrane.

The plant immune response is usually followed by a necrosis of plant tissues, termed Hypersensitive Response (HR) thanks to whom the plant contains the infection. Around the infection site, there is a sudden cellular death and a simultaneous reduction in the number of viable bacteria, which represents the final stage of resistance. From previous studies,[76] LPS from plant symbiont results to be involved in suppression of innate immunity, preventing the HR by means of a "localized induced resistance" (LIR), which consists in the production of antimicrobial compounds as peroxidase and cationic peptides. The structural requirements of LPS to provoke LIR are still under studying, but much progress has done in recent years.

From biological point of view the symbiotic process is based on two main mechanisms (Fig. 6.1): using NF-dependent and NF-independent process. In the first, several plant signals as flavonoids, polyphenol compounds, like apigenin and narigenin, were perceived by bacteria NodD proteins, that induce the transcription of Nod genes and they are resulting in transduction of lipochitooligosaccharides, known as Nod Factor (NF). These last molecules are able to activate a LysM-RLK kinase enzyme, which is in turn involved in phosphorylation of calcium channel. The increment of intracellular calcium concentration enhanced the formation of calcium-calmodulin complex, which it could be recognized by cytokine receptors that translocated in the nucleus and activated the transcription of symbiotic genes that lead to nodules organogenesis on the plant root.[77]

Instead, the NF-independent process depends on the production of several cytokine–like receptors compounds after plants epidermidis lesions and they might directly by-pass the early NF-signaling pathway and finally trigger the nodule organogenensis.[78]

Therefore, NF-dependent and independent bacteria are able anyway to set up right conditions to give rise to symbiosis.

A key role during the symbiosis also took place from lipid A. Despite the general architecture of lipid A is conserved among individuals belongings to the same family, the lipids A isolated from several strains as *Rhizobia* turn out to be different for: nature of glycidic backbone, being substituted non stochiometrically with phosphate or with other residues; high fatty acids distribution with acyl chain in various length and in some case they also displayed an hepta-acylayted lipid A due to a triterpenoid lipid, termed hopanoid, which may has a pivotal role in regulation of cellular homeostasis.

It is obvious that in most cases, symbiosis derives from metabolic complementation between the host and microbe, in which one partner provides missing nutrients for the other. Moreover, microbes can

[76] SequeiraL., HillL.M., *Physiol. Plant Pathol.,***1974**, *4*, 447-455.
[77] OldroydJ.E.D., DownieJ.M., *Annual Rew. Plant Biol*., **2008**, *59*, 519-546.
[78] GiraudE. et al. *Science,* **2007**, *316*, 1307-1312.

contribute in many ways to host development by synthesizing hormone-like compounds[79]and affecting host immunity.[80]The symbiotic associations can be facultative or obligate due to many absent biosynthetic pathways. In plants, obligate symbiosis is effectively rare, on the contrary, facultative mutualistic interactions are more common as the fungal-plant and the *Rhizobium-Aeschynomene* interactions.

Since that time, the *Rhizobia* genus have generated a considerable interest for their new properties; the principal goal of the this PhD project was the extraction, structural analysis and also biological activity studies of several Rhizobium LPS and in particular lipids A isolated from *Bradyrhizobia*strains.

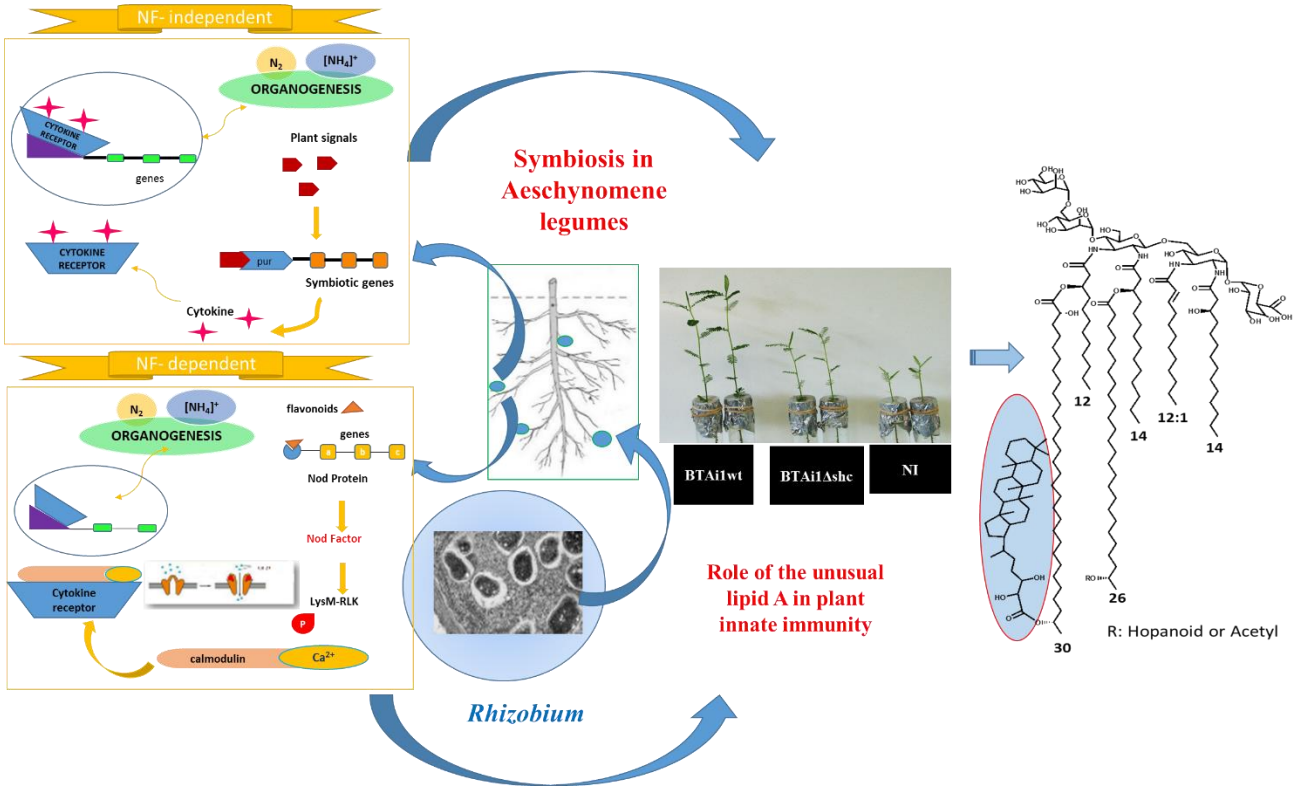

Figure 6.1: Activation systems during symbiosis process, which lead to nodule formation.

[79] Shin S.C.et al., *Science*, **2011**, *334*, 670–74.
[80] MoreiraL.A.et al.,*Cell.,* **2009**, *139*,1268–78.

Results and Discussion

6.2 Purification and characterization of LPS from *Bradyrhizobium sp* ORS 285

Bradyrhizobia belong to the slow growing bacteria group. Thus, during the growth there is a high risk of contaminations by other bacteria that grow quickly. The bacterial pellet submitted to analysis were ORS 285 (Br1) and ORS 285 rfaL (Br2) mutant, which produced respectively LPS and LOS.
It was performed a usual hot phenol/water protocol, followed by enzymatic treatment and ultracentrifugation in order to remove all contaminants. The SDS-PAGE analysis disclosed the presence of typical ladder pattern for Br1 and a sticked spot at low molecular masses for Br2 (Fig. 6.2). This was the first confirmation of the selective production of LPS and LOS from two strains.
Then oligosaccharide fractions were studied via MALDI mass spectrometry and NMR spectroscopy after a selective acetic acid hydrolysis and a further purification of species by means of exchange ion chromatography.

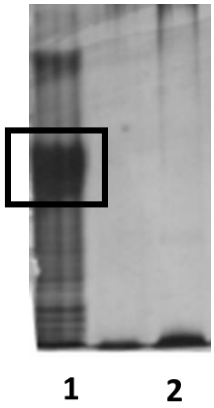

Figure 6.2: SDS-PAGE gel scan of the LPS of ORS 285 wt (**1**), O-antigen mutant (**2**). The black box shows the canonical high molecular weight band of Br1 LPS (with the O-antigen). Br2 mutant strain displayed LPS lacking the complete O-antigen region with low molecular weight.

6.2.1 Chemical analysis and preliminary results

To confirm that the selected mutants were affected in the O-antigen-synthesis, we compared the LPS GC-MS profile of Br1 and Br2. As shown in (Fig 6.2.1 a-c), ion peaks belonging to bradyrhizose (ion peaks from 25 to 32min) present in spectrum of WT LPS were not observed in the mutant LPS. Further, the compositional analysis indicate that the LPS of the selected mutant completely lack the O-antigen region and only display sugar residues belonging to the core region.

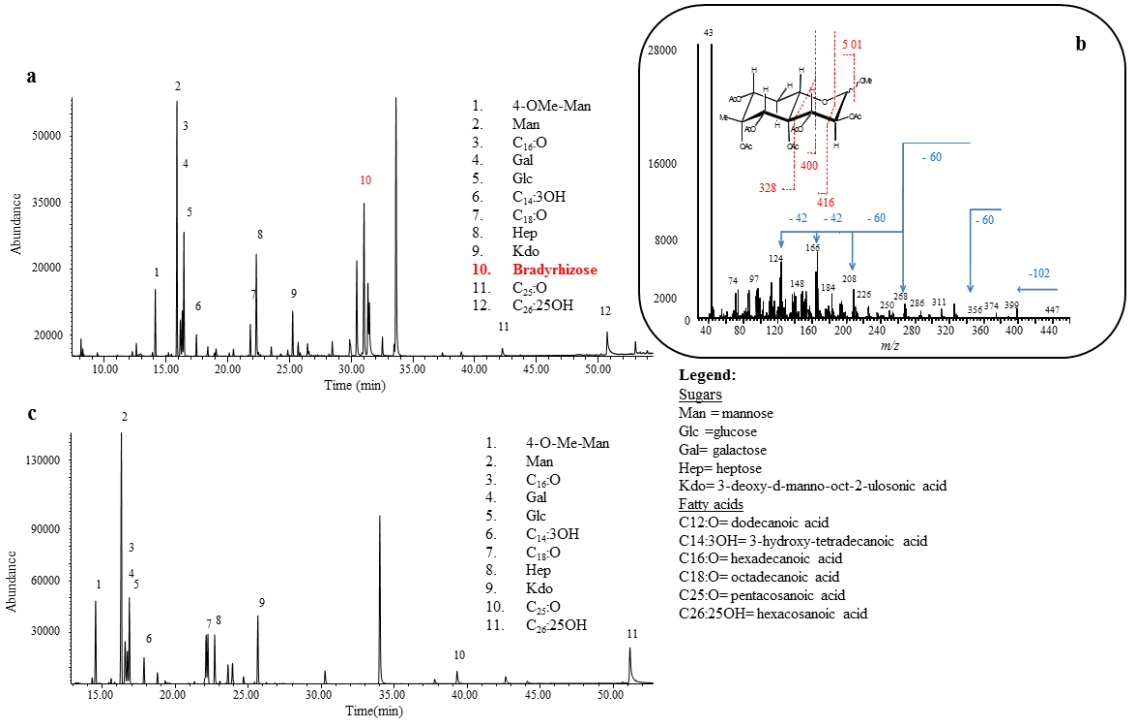

Figure 6.2.1: GC-MS chromatogram of LPS from ORS285wt(**a**) and Δ*rfal*(**c**).The inset reasumes the compositional analysis, between 25-30 min ion peaks belonging to Bradyrhizose were present. On the right the mass spectrum (**b**) and fragmentation pattern of one of the ion peaks belonging to Bradyrhizose, (numebered as **10**)is also shown.
The mutant LPS (**c**) does not display O-antigen region at about 30 min retention time.

Since the O-antigen structure of wt strain Br1 was already reported as a homo-polymer repeating unit of bradyrhizose, the most of the project was spent in determination of oligosaccharide core.

On the crude LOS (Br2) was performed a permethylation analysis, that revealed the presence of 3-substituted-D-4-O-Methyl-mannose, 7-substituted heptose, 3-substituted-D-glucose, 3-substituted-D-mannose, 5-substituted-Kdo ant terminal N-methyl-hexosammine.

The absolute configuration of all residues were determined from GC-MS analysis comparing the peracetylated octil-glycosides standards and they result to be D.

Nevertheless, the structure of core is currently under studying.

In parallel, also the lipid A portion isolated from both Br1 and Br2 strain was analyzed, using mass spectrometry in positive ion mode. From previous results, it was evident that both strains displayed the same ion distribution reconductable to the same lipid A species.

The first information on the lipid A structure were obtained from positive-ion MS spectrum performed on the intact lipid A in which we identified an heterogeneous mixture of peaks, that differed for the long chain fatty acid distribution on the sugar backbone.

Based on the compositional analyses we assigned the peak at *m/z* 2595.7(Fig. 6.2.2) to a hexa-acylated species with the following composition:

two residues of GlcN3N

two residues of Man

one unit of GalA

two C14:0 (3-OH)

one C12:0 (3-OH)

one C12:1

one C30:0 (2,29-OH)

one C26:0 (25-OH)

Moreover, it was possible to detect a new ion cluster at *m/z* 2271.6 that corresponded to hexa-acylated lipid A lacking the disaccharide mannose residue, which usually labile linked to the rest of molecule. The presence of two residues of mannose in mass spectra confirmed that they were both linked to the non reducing DAG of the lipid A saccharide backbone while the GalA unit was located on reducing DAG.

Furthermore, the molecular ion that represented the hexa-acylated lipid A was also useful to identify the fatty acid distribution on each DAG residue of sugar backbone. In fact, the peaks at *m/z* 2129.36corresponded to penta-acylated lipid A fragments, lacking a residue of C30:0 (29-OH), this suggested that the last fatty acid was in ester linkage, more labile respect to amide-linked fatty acids. A third ion group localized at *m/z* 3106.2 in MALDI spectrum of crude lipid A (Fig. 6.2.2) corresponding to an equivalent structure of *m/z* 2595.7 (LA_{hexa}), but with a difference in mass of 512.4. This last peak was attributable to a hepta-acylated specie carrying a macromolecule, named hopanoid, that confers unusual feature to the lipid A. Further investigations were done in order to identify the chemical structure, variation and biological relevance of this residue.

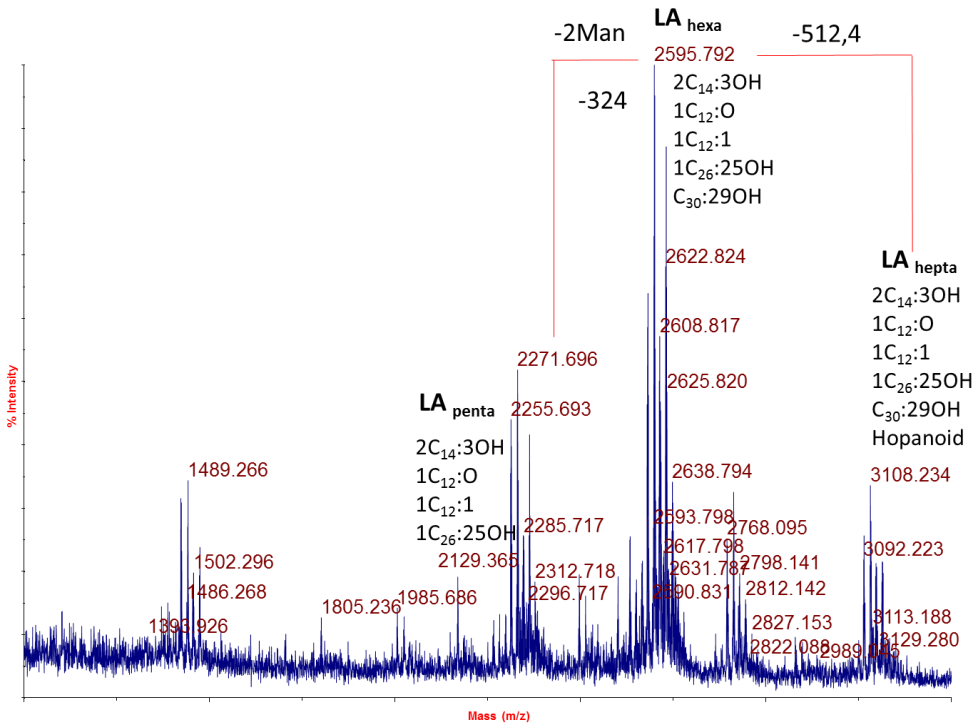

Figure 6.2.2: MALDI mass spectrum of crude lipid A obtained after mild hydrolysis in acetate buffer.

6.3 Biological significance of O-antigen portion

Bradyrhizobium bacteria, as discussed above, display a unique LPS O-antigen composed of a new sugar, the bradyrhizose that is regarded as a key symbiotic factor due to its non-immunogenic character. To check this hypothesis, were isolated mutants affected in the O-antigen synthesis by screening a transposon mutant library of the ORS285 strain for clones altered in colony morphology. Five mutants were selected and found to be mutated in two genes, rfaL, encoding for a putative O-antigen ligase and gdh encoding for a putative dTDP-glucose 4,6-dehydratase (Fig. 6.3.1).

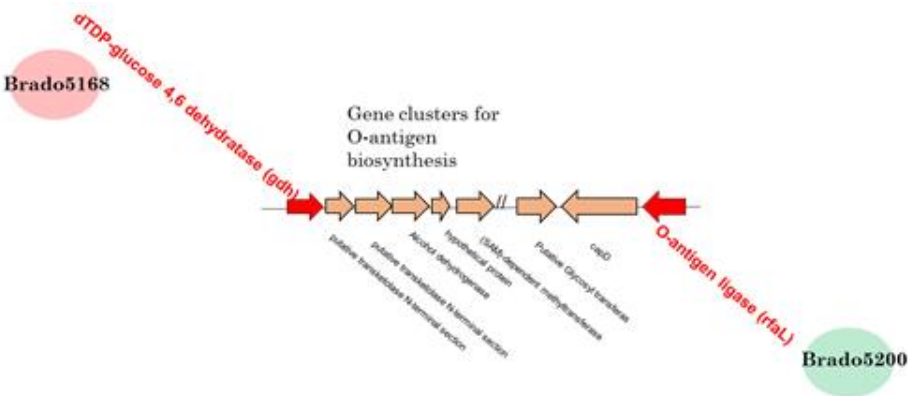

Figure 6.3.1: Identification of ORS285 mutants affected in the O-antigen synthesis in genomic context of *Bradyrhizobium* strains

As confirmed by chemical analysis the LPS of these mutants result to be completely lack the O-antigen region. However, no effect of the mutations could be detected on the symbiotic properties of the mutants indicating that the O-antigen region of photosynthetic *Bradyrhizobium* strains is not required for the establishment of symbiosis with *Aeschynomene*.

This kind of mutation can lead to a sweeping change of the colonies aspect, it has been reported that the removal of the O-antigen region could alter the sensitivity of some mutants to various stresses.[81,82] This higher sensitivity can compromise the success of the symbiotic interaction because all along the process the bacteria has to cope with various stressful conditions such as acidic pH, high osmolarity, reactive oxygen species, and peptide antibiotics.(Fig. 6.3.2)

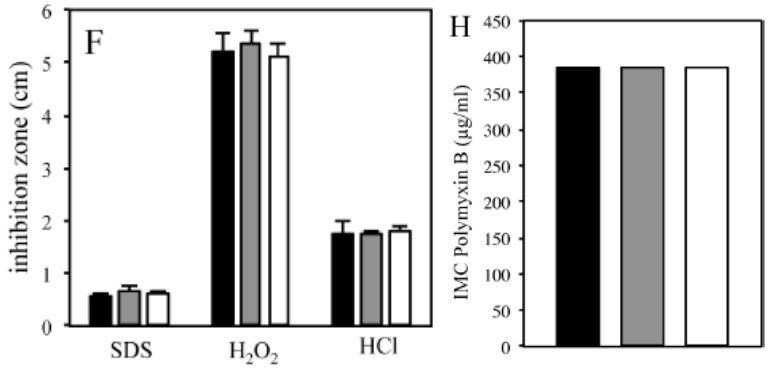

Figure 6.3.2:The lack of O-antigen has no impact on the free life of ORS285. **F**) Hydrogen peroxide (H2O2), hydrogen chloride (HCl) and sodium dodecyl sulfate (SDS) resistance of ORS285 (black bar), rfal(grey bar) and gdh (white bar) mutants, as determined by disk diffusion assays; **H**) Polymyxin B resistance of ORS285 (black bar), rfal (grey bar) and gdh (white bar) mutants, as determined by Etest (Etest1bioMérieux) on YM medium.

The mutant displayed a similar growth than the WT-strain. We also analyzed the ability of the mutant to cope with various stressors, acid (HCl), oxidant (H2O2) and detergent (Sodium dodecyl sulfate) using disk diffusion assays and also the number of the nodules on the plant root, focusing on the nitrogenase activity (ARA).

However, similarly, no significant difference was observed between the mutant and the WT-strain. (Fig. 6.3.3)

Altogether, these data suggest that the O-antigen region does not play an important role in the ability of the ORS285 strain to cope with various stressful conditions.

[81] Berry M.C., McGhee G.C., Zhao Y., Sundin G.W.,*FEMS Microbiol.Lett.*,**2009**,*291*(1), 80–7.
[82] Xu L.L., Wang Q.Y., Xiao J.F., Liu Q., Wang X., Chen T., et al., *Arch Microbiol*., **2010**,*192*(12),1039–47.

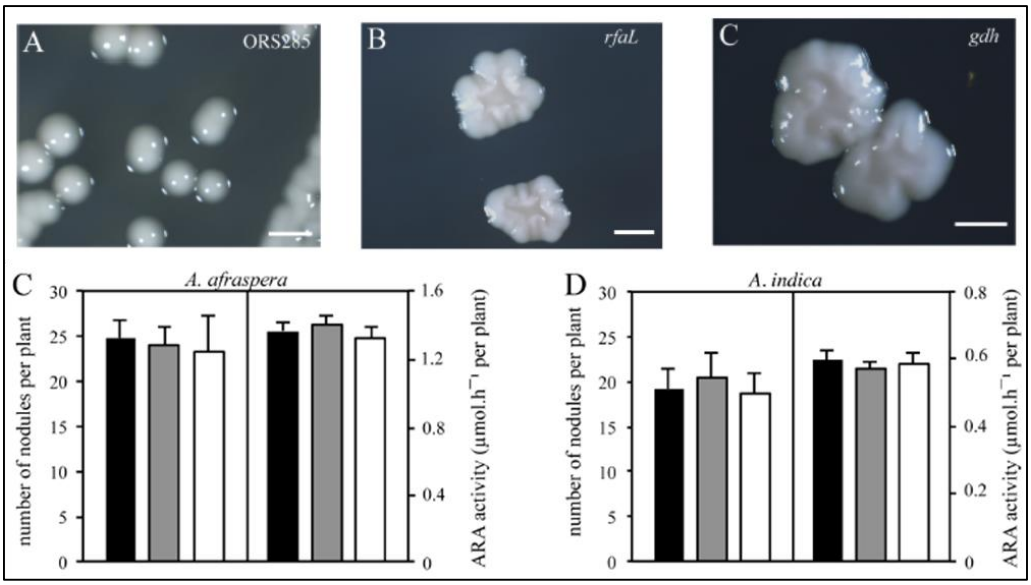

Figure 6.3.3:O-antigen minus mutants of ORS285 are not affected in their symbiotic properties with *Aeschynomene* legumes.(**A-C**) Colony morphotypes of ORS285 (A), rfal (B) and gdh (C) mutants. Quantification of acetylene reduction activity (ARA) and number of nodules per plant inoculated with ORS285 (black bars), rfal (grey bars) or gdh (white bars) mutants in A. afraspera (**C**) and A. indica (**D**).

Various hypothesis have been proposed to clarify the effect of deletion of the O-antigen region during interaction process between photosynthetic *Bradyrhizobium* strains and *Aeschynomene*.

First, the core oligosaccharide that becomes in these mutants the most external part susceptible to enter directly in contact with the host cell is also non-immunogenic. Second, the photosynthetic bradyrhizobia are coated with other non-immunogenic surface polysaccharides, such as EPS, KPS and/or cyclic glycans that mask the LPS antigenic epitopes. They are several examples indicating that such surface polysaccharides play also an important role in the establishment of the rhizobium-legume symbiosis either by suppressing the plant immunity or by masking some surface antigens or by acting directly as a symbiotic signal.[83,84,85]

Finally, we cannot exclude that the photosynthetic bradyrhizobia produce unknown non-Nod signal(s) that besides triggering the symbiotic process, suppress the plant innate immunity, such as proposed for Nod factors.[86,87]

[83] Fraysse N., Couderc F., Poinsot V.,*Eur J Biochem*., **2003**, *270*(7), 1365–80.
[84] Carlson R.W., Forsberg L.S., Kannenberg E.L.,*Subcell. Biochem.*, **2010**, *53*, 339–86.
[85] Kawaharada Y., Kelly S., Nielsen M.W., Hjuler C.T., Gysel K., Muszynski A., et al. *Nature*, **2015**,*523*(7560), 308–12.
[86] Gourion B., Berrabah F., Ratet P., Stacey G., *Trends Plant Sci.,* **2015**, *20*(3), 186–94.
[87] Liang Y., Cao Y., Tanaka K., Thibivilliers S., Wan J., Choi J., et al. *Science,* **2013**, *341*(6152), 1384–7.

Section III

Role of lipid A in Bradyrhizobium strains

6.4 Structure and function of *Bradyrhizobium* lipid A

In the following section we focused on the study of lipids A isolated from *Bradyrhizobium* strains with the aim to correlate the peculiar structure never described before to their function and biosynthetic pathways.

Despite the general architecture of lipid A is conserved among individuals belongings to the same family, the lipids A isolated from several strains as *Rhizobia* turn out to be different for: nature of glycidic backbone, being substituted non stochiometrically with phosphate or with other residues; high fatty acids distribution, the presence of Very Long Chain Fatty Acids (VLCFA),in some strain for the presence of hepta-acylated strains carrying a triterpenoid lipid, termed hopanoid, which may has a pivotal role in regulation of cellular homeostasis.

To better understand how bacteria resist stresses encountered during the progression of plant-microbe symbioses, we focus on the peculiar lipid A structures and their substituents, which contribute to hydrophobicity and stability of bacterial outer membrane.

Bradyrhizobium lipid A structure is formed by a skeleton of β-(1→6)-linked 2,3-diamino- 2,3-dideoxy-D-glucopyranose (DAG) carrying an α-GalpA on the vicinal DAG and an α-(1→6) Man*p* disaccharide on the distal DAG unit, substituted by a heterogeneous blend of lipid chains in terms of lengths and distributions. The number of carbon atoms in VLCFA is more variable each strain. Most of all are linear, mono or dimethyl branched-chain fatty acids built up of 26 to 34 carbon atoms.[88] VLCFAs can span out the entire outer membrane and play a crucial role in its stabilization. Furthermore, in *Bradyrhizobium* lipid A the two secondary VLCFAs were substituted by a hopandiolic acid and by an acetyl group.

All together these properties allowed to determine a novel lipid A skeleton, which we named HoLA (Hopanoid-Lipid A).

6.5 Hopanoids

Hopanoids are a big class of compounds, which belong to pentacyclic triterpenoid lipids, functional homolog of cholesterol in mammal cells. Hopanoids interact with glycolipids in bacterial outer membranes to form a highly ordered bilayer in a manner analogous to the interaction of sterols with sphingolipids in eukaryotic plasma membranes.[89]

The principal features contributing to lipids order are: the rotational freedom of motion and lateral packing of lipids within the bilayer. In general, sterols ordering provide the basis for membrane lateral

[88] Choma A., Komaniecka I., *Acta Biochim. Pol.,* **2011***, 58*, 51–58.

[89] Sáenz J.P., Grosser D., Bradley A.S., Lagny T.J., Lavrynenko O., Broda M., Simons K., *Proc Natl Acad Sci U S A.,* **2015**, *112*(38), 11971-6.

segregation and promote a fluid, mechanically robust plasma membrane. Hopanoids are often used by geobiologists as biomarkers, to evaluate bacteria distributions from early days to recent modern ecosystems and were also found in nitrogen-fixing bacteria especially in *Frankia*, which were among the best hopanoid producers.[90]

Hopanoids are biosynthesized by bacteria via cyclization of squalene-hopene cyclase to yield the C30 hydrocarbon compound and a following enzymatic addition of small molecules may shape hopanoids with a side chains variable in number of carbon atom. (Fig 6.5.1)

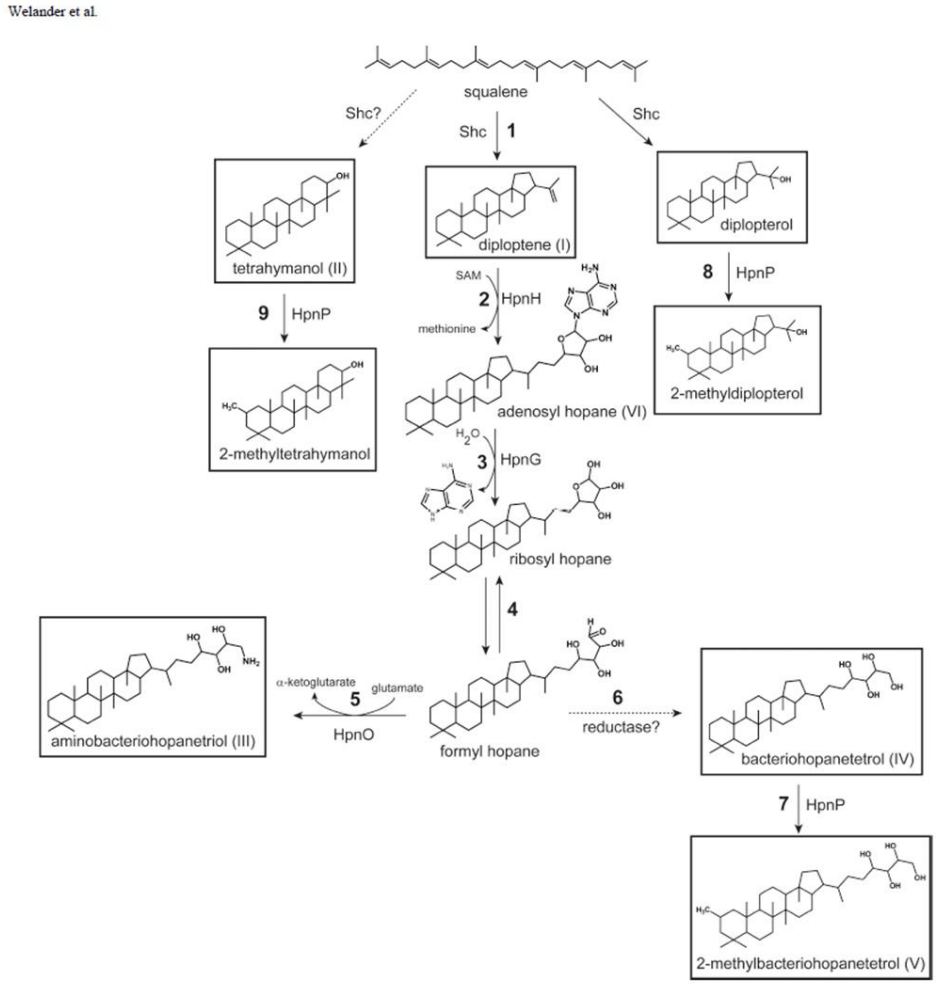

Figure 6.5.1: Biosynthetic pathway of hopanoid molecules and derivatives.

The deletion of hopanoid synthesis is non-lethal for bacteria, but hopanoid-deficient mutants have been shown to exhibit increased sensitivity to antibiotics and various stress conditions, including variation in pH, temperature, and osmotic pressure.[91,92]

[90]Berry A.M., Moreau R.A., Jones A.D., *Plant Physiol.*, **1991**, *95*, 111-11.
[91] Welander P.V. et al.,*J.Bacteriol.*, **2009**, *191*(19), 6145–6156.
[92] Kulkarni G., Wu C-H., Newman D.K, *J. Bacteriol.*, **2013**, *195*(11), 2490–2498.

It is not understood until now exactly how hopanoids are linked to resistance and tolerance to stress, but understanding the role of hopanoids in shaping membrane properties would provide an important step toward bridging this gap.

Within this frame, we produced, isolated and analyzed lipid A from mutant *Bradyrhizobium* strains with mutations in genes controlling the pivotal biosynthetic step of hopanoid moiety and the attachment of VLCFA to the lipid A, in order to deeply understand how they contribute to the lipid A's functions in symbiotic process.

Results and Discussion

6.6 Isolation and characterization of lipid A from BTAi1 wt, hopanoid minus mutant Btai1Δshc and their complemented mutants

The bacterial pellets were extracted and purified with an enzymatic treatment followed by ultracentrifugation to remove nucleic acid traces and β-glucan contaminants respectively. An acetic acid hydrolysis on LPS was performed to obtain the lipid A as precipitate, in turn further purified[93].

6.6.1 MALDI mass spectrometry on lipid A from *Bradyrhizobium* Btai1 wild type

The lipid A isolated from Btai1 wild type strain was analyzed via MALDI mass spectrometry in positive ion mode. The spectrum revealed the presence of three ions cluster at *m/z* 2128.42, 2594.93 and 3135.36, which respectively corresponded to penta, hexa and hepta-acylated lipid A. The most abundant ion cluster belongs to a hexa-acylated specie formed by two DAG residues, two Man*p* and one GalA*p*, which constituted the sugar backbone. The proximal DAG residue is linked by one C_{12}:3OH and one C_{14}:3OH through amide linkage, whereas the distal DAG displayed an amide linkage with one unsaturated fatty acid residue C_{12}:1 and a further C_{14}:3OH.

The second fatty acid intorn was characterized from the presence of one C_{32}:O (2, 31-OH) linked by the C_{12}:3OH, while the C_{14}:3OH carrying a C_{26}:25OH fatty acid and both are in ester linkage, more labile than amide. Thus, it was possible to detect in the mass linear spectrum also a penta-acylated lipid A without the secondary fatty intorn region. Moreover, a small ion cluster at high *m/z* with difference of 512.4 respect to hexa-acylated specie confirmed the presence of hepta-acylated lipid A carrying a hopanoid molecule. (Fig 6.6.1). The definitive information on the certain presence of hopanoid molecule was recovered from MS/MS experiment on the crude lipid A.

[93] Silipo A., Vitiello G., Gully D., Sturiale L., Chaintreuil C., Fardoux J., Gargani D., Lee H.I., Kulkarni G., Busset N., Marchetti R., Palmigiano A., Moll H., Engel R., Lanzetta R., Paduano L., Parrilli M., Chang W.S., Holst O., Newman D.K., Garozzo D., D'Errico G., Giraud E., Molinaro A., *Nat Commun*., **2014**, *5*, 5106.

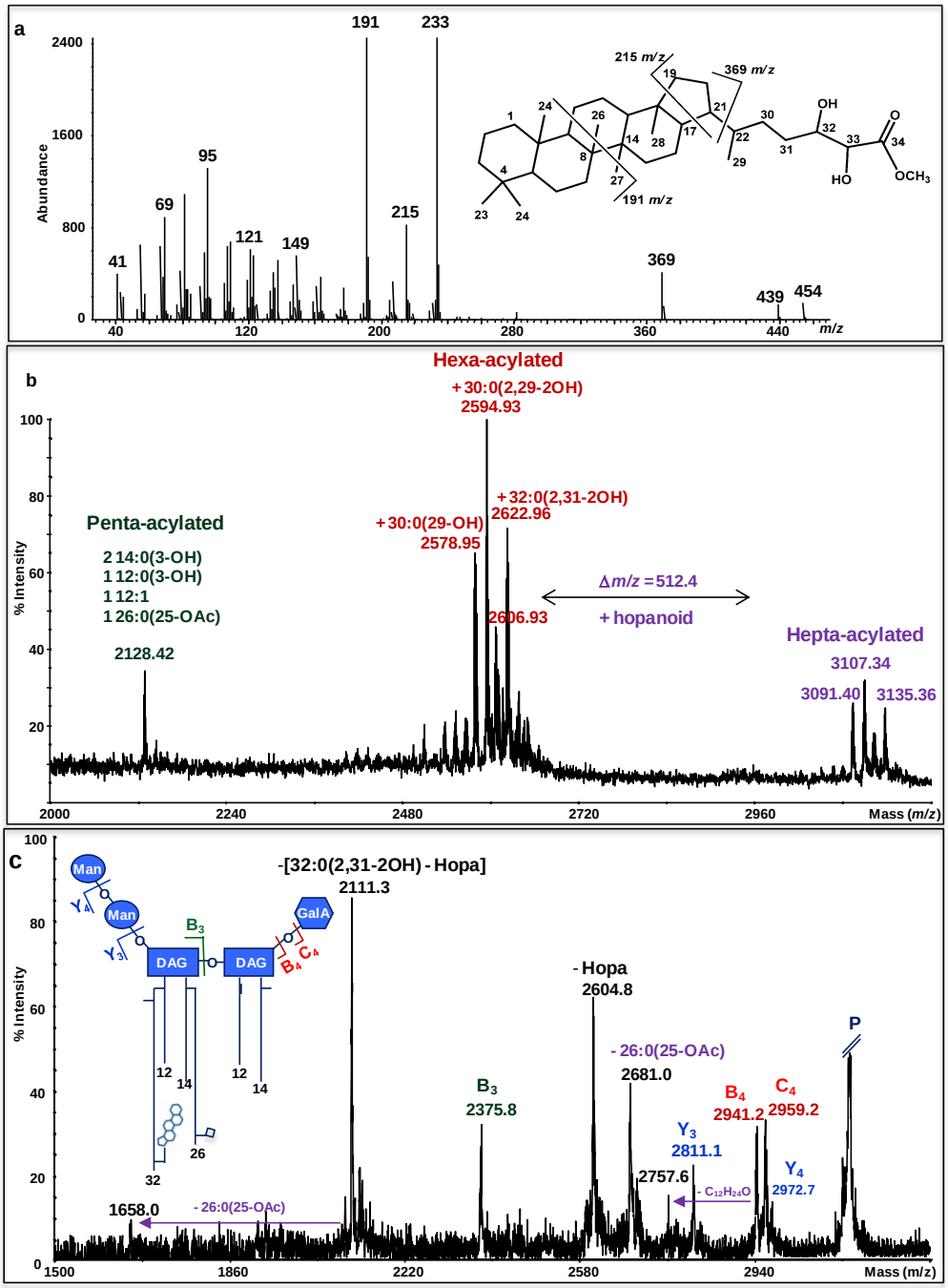

Figure 6.6.1: a) fragmentation pattern of hopanoid moiety; **b**) linear mass spectrum in positive ion mode of lipid A of Btai1 wt; **c**) MS/MS spectrum of hepta-acylated lipid A with precursor ion at *m/z* 3135

6.6.2 Lipid A from Btai1Δshc (hopanoid minus mutant)

With the same approach we analyzed the lipid A from Btai1Δshc (hopanoid minus mutant). MALDI mass spectrum (Fig. 6.6.2) highlighted the complete absence of hepta-acylated lipid A due to the lacking of gene encoding for squalene-hopene-cyclase, a key enzyme in the biosynthesis of

hopanoids, responsible for the cyclization of the linear squalene into the pentacyclic triterpenoid.[94](see biological effect in 6.7.2).

Since the *shc* gene coding an enzyme for hopanoid biosynthesis, we wanted to clarify the role of *shc* gene cluster in the covalent attachment of hopanoid to the lipid A both for NF-dependent and NF-independent Bradyrhizobia.

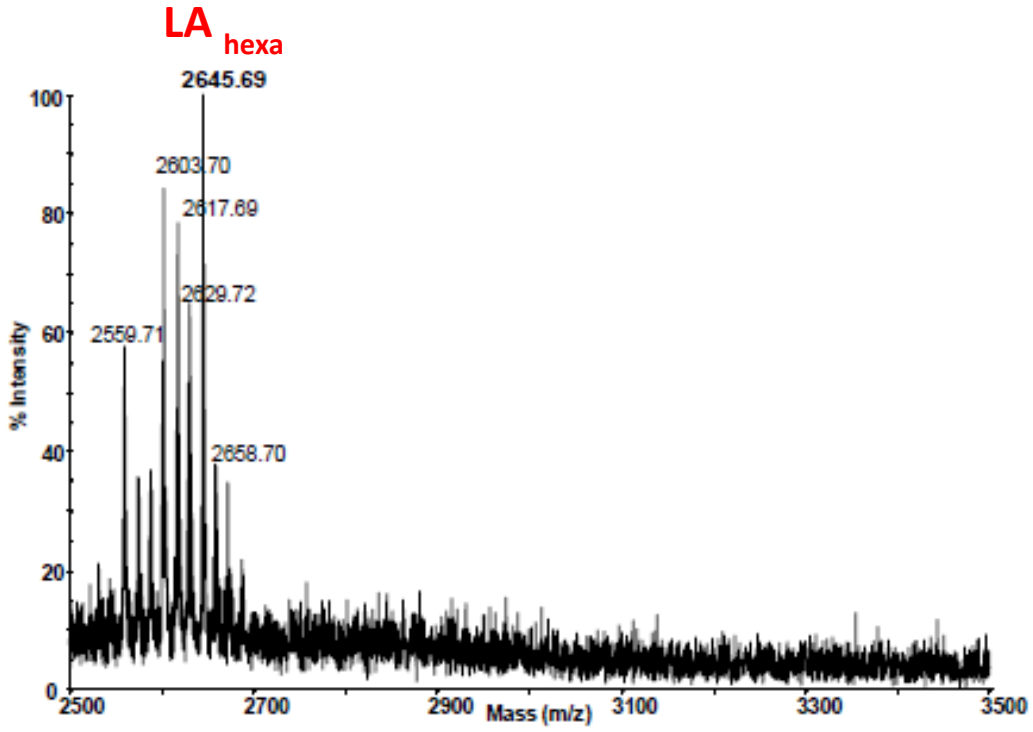

Figure 6.6.2: Reflectron MALDI TOF mass spectrum of the lipid A from BradyrhizobiumBTAi1Δshc showing the complete absence of the HoLA species. All the molecular ions were detected as di-sodiated ion adducts.

Genome sequence analysis of photosynthetic *Bradyrhizobium* strains, as *Bradyrhizobium* BTAi1 and ORS 278 wild type, revealed the presence of only one *shc* gene, which, in contrast to the non-photosynthetic strains, as *Bradyrhizobium* japonicum, was not surrounded by other genes involved in hopanoid biosynthesis.

To confirm the hypothesis that, *shc* gene is pivotal in the hopanoid biosynthesis in both Bradyrhzobia strains, Dr. Giraud and his group prepared complemented mutants between Btai1Δshc and *shc* gene from *Bradyrhizobium* ORS 278 and *Bradyrhizobium japonicum*, which belongs respectively to Nod-independent and Nod-dependent Bradyrhizobia.(Fig. 6.6.3)

[94] Siedenburg G., Jendrossek D.,*Appl. Environ. Microbiol.*, **2011**, *77*, 3905–3915.

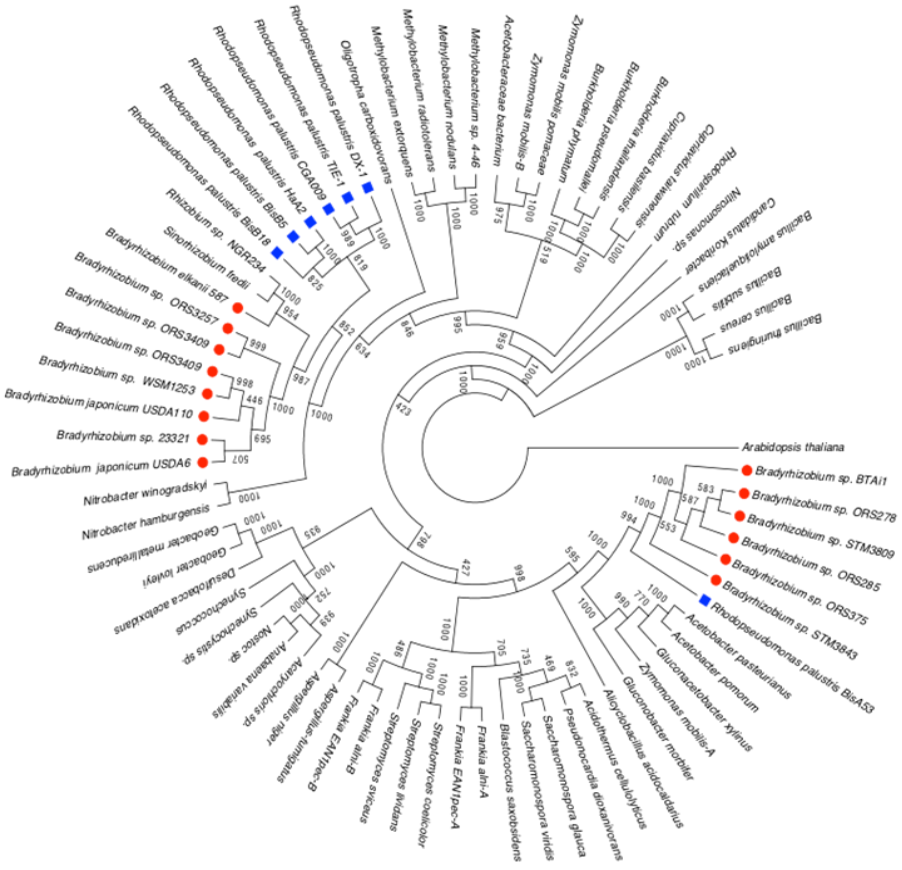

Figure 6.6.3: Phylogenetic tree of *Bradyrhizobium* strains.

6.6.3 MALDI mass spectrometry on complemented strains Bradyrhizobium Btai1Δshc with *shc* from B. japonicum and/or ORS 278

From these mutant strains were isolated lipid A and extensively analyzed their structure using MALDI mass spectrometry. Both complemented strains displayed the same blend of ion distribution of *Bradyrhizobium* Btai1 wt lipid A formed by:

two DAG

two Man

one GalA

two C_{14}:3OH

one C_{12}:3OH

one C_{12}:1

one C_{26}:25OH

one C_{32}:O (2,31-OH)

An additional feature, detectable from mass spectra (Fig.6.6.4) was the presence of small traces of hepta-acylated species bearing a second hopanoid. Based on MS data, we were able to assign the full lipid A structures.

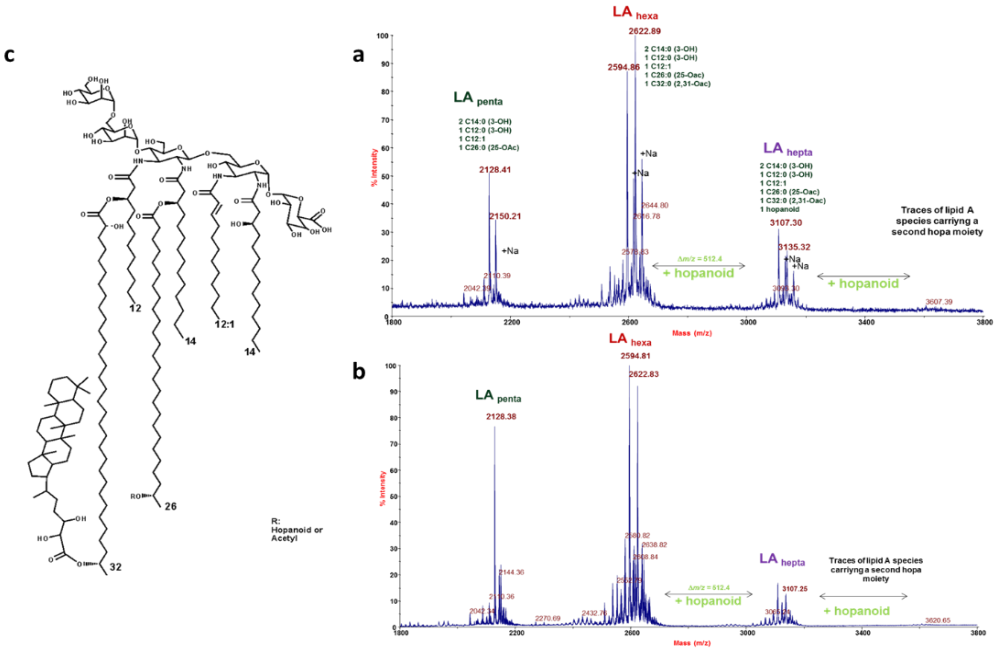

Figure 6.6.4: **a**) Mass spectrum of B*radyrhizobium* Btai1Δshc complemented with s*hc* from ORS 278; **b**) Mass spectrum of B*radyrhizobium* Btai1Δshc complemented with s*hc* from *B. japonicum;* **c**) Complete structure of lipid A from both complemented strains overlapped to wt lipid A structure

This findings suggested that lipid A biosynthesis preceded its attachment to a hopanoid moiety using squalene-hopene-cyclase, which is encoded only from *shc* gene. So, the synthesis of LA covalently linked by hopanoids is not related to an unusual shc enzyme, hypothetically present in in photosynthetic Bradyrhizobia NF-dependent strain, but probably a gene cluster exists responsible of transcription of a ligase in both NF-dependent and NF-independent Bradyrhizobia strains responsible for the linkage of hopanoid moieties and not discovered yet.

6.7 Biological features of *Bradyrhizobium* outer membrane

Is well known that, hopanoids act as membrane condensers, thus increasing bacterial resistance to various abiotic stresses. [95,96,97] The absence of hopanoids in the membranes could destabilize its regular arrangement and therefore have a profound impact on BTAi1 physiology.

Biological assays showed the effect of the *shc* mutation on the growth of BTAi1 in both rich and minimal media. As shown in Fig. 6.7.1 a-b, the growth rate of the mutant was markedly lower than that of the WT strain in both media. Further, we were also interested in evaluating the ability of BTAi1Δshc mutant to cope with various stressors. We tested oxidative, acid and detergent stresses using disk diffusion assays. Saline/osmotic stress was evaluated by comparing bacterial growth rates in the presence of increasing concentrations of NaCl. The data obtained (Fig. 6.7.1 c-d) showed that the BTAi1Δshc mutant was more sensitive than the WT strain to all stressors tested.

Instead, from morphological point of view, no significant differences were observed between plants inoculated with WT and mutant strains, the number of nodules per plants and the nitrogenase activity measured by the acetylene reduction assay (ARA) were comparable (Fig. 6.7.2 a-b). This indicated that the Δshc mutation had no effect on the ability of the bacteria to establish a symbiotic relationship.

From cytological analysis of nodules using transmission electronic microscopy (TEM) was determined also a nodule degeneracy (Fig. 6.7.2 e,f) and their up regulation during the symbiosis providing the nitrogen request.(Fig. 6.7.2 c-d)

All data reported suggest that hopanoids play an important role in the physiology of BTAi1 membrane.

[95] Welander, P. V. et al.,*J. Bacteriol.*, **2009**, *191*, 6145‑6156.
[96] Bosak T., Losick R. M., Pearson A. *Proc. Natl Acad. Sci.,* **2008**,*105*, 6725‑6729.
[97] Malott R. J., Steen-Kinnaird B. R., Lee T. D., Speert D. P., *Antimicrob. Agents Chemother*., **2012**, *56*, 464‑471.

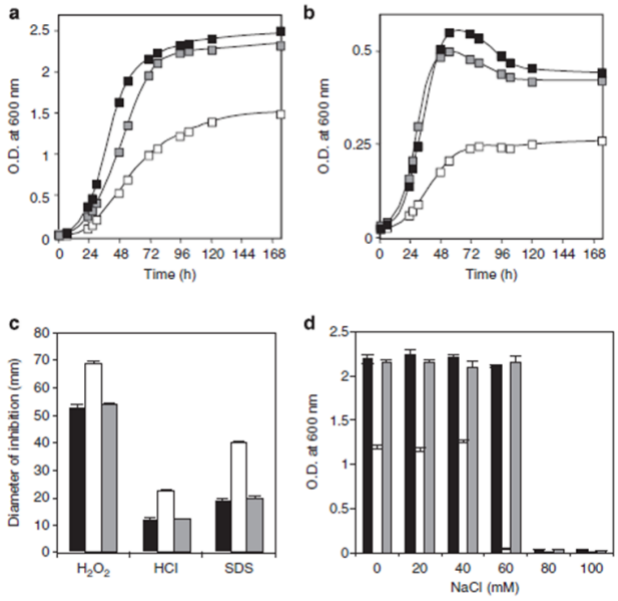

Figure 6.7.1: (**a, b**) Representative growth curves of BTAi1 (black square), BTAi1Δshc (white square) and complemented BTAi1Δshc+shc (grey square) strains cultivated in rich (**a**) or minimal medium (**b**). (**c**) Hydrogen peroxide (H2O2),hydrogen chloride (HCl) and sodium dodecyl sulfate (SDS) resistance of BTAi1 (black bar), BTAi1Δshc (white bar) and complemented BTAi1Δshc+shc(grey bar) strains, as determined by disk diffusion test (**d**) NaCl resistance of BTAi1 (black bar), BTAi1Δshc (white bar) and complemented BTAi1Δshc+shc (grey bar) strains.

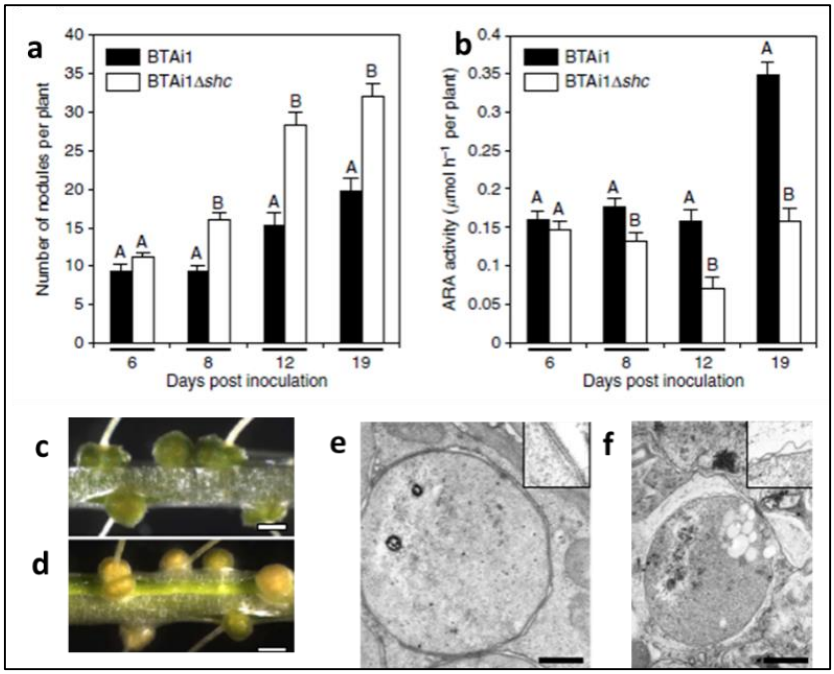

Figure 6.7.2: a) Nodulation kinetics of Bradyrhizobium BTAi1 and BTAi1Δshc strains on *A. evenia* plants. **b**) The occurrence of acetylene-reducing activity (ARA) in *A. evenia* plants inoculated with *Bradyrhizobium* BTAi1 and BTAi1Δshc mutant. **c-d**) Aspect of the nodules elicited by the WT strain BTAi1 and the BTAi1Δshc mutant respectively. **e-f**)Transmission electron micrographs of nodules elicited by the WT strain and the BTAi1Δshc mutant. Insets in **e,f** show a detail of the cell wall ultrastructure of bacteroids.

Section IV

Chemistry of Very Long Chain Fatty Acids

6.8 Role of VLCFAs as major components of *Bradyrhizobium* lipid A: analysis of mutant strains ORS278Δ*4679* and ORS278Δ*4680*

Bradyrhizobium lipid A is made up of very long chain fatty acids (VLCFA, from 26 to 32 carbon atoms.[98,99,100]) typical component of Rhizobia [101].

The presence of very long chain fatty acids is an hallmark not only of *Rhizobia* and *Bradyrhizobia* strains, but also of other of lipid A isolated from mammalian pathogens such as *Brucella abortus*,[102] *Legionella pneumophila* and *Bartonella henselae.*

Given the peculiar lipid A structure from Bradyrhizobia strains (Fig. 6.8.1) we studied the chemistry of VLCFA and their role in symbiosis. Several experiments were performed on mutants for VLCFAs biosynthesis, in order to identify the gene cluster responsible of elongation of the acyl-chains of lipid A and how the latter can bear the hopanoid moiety. The mutant strains are lacking in genes encoding for the specialized acyl carrier protein AcpXL[103,104] and LpxXL.[105,106]. They are required for VLCFA building and for the transferring of VLCFA from the AcpXL-VLCFA conjugate complex directly to the lipid A.

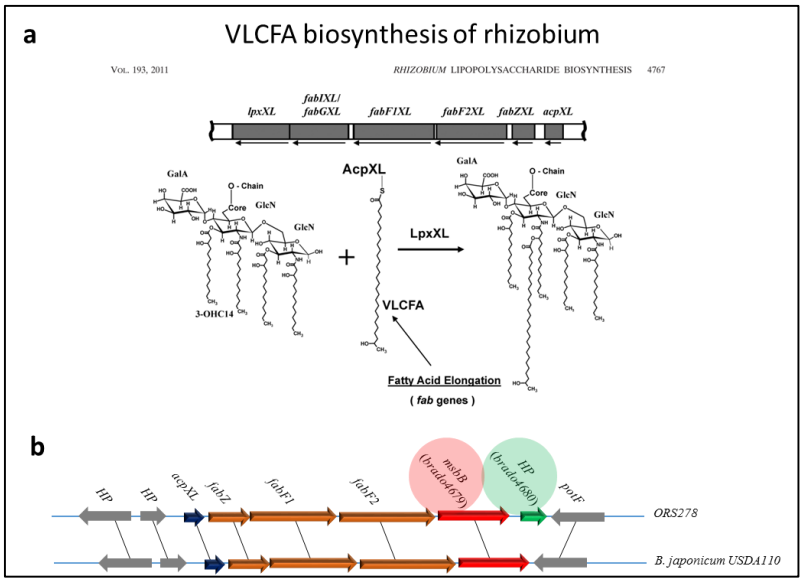

Figure 6.8.1: **a**) General scheme of VLCFA biosynthesis; **b**) Genome region in which are highlighted the specific mutated genes in order to obtain *Brado4679* (red point) and *Brado4680* (green point) mutants

[98] Corsaro M.M., De Castro C., Molinaro A., Parrilli M., *Recent Res. Devel. Phytochem*., **2001**, *5*, 119–138.
[99] de Maagd R.A. et al, *J. Bacteriol.,* **1989***, 171*, 1143–1150.
[100] Choma A., Sowinski P.,*Eur. J. Biochem.,* **2004**,*271*, 1310–1322.
[101] Gudlavalletti S.K., Forsberg L.S., *J. Biol. Chem*., **2003**, *278*, 3957–3968.
[102] Moreno E. et al.,*J. Bacteriol.* **1990**,*172*, 3569–3576.
[103] BrozekK.A. , Carlson R. W., Raetz C. R. H., *J. Biol. Chem*., **1996**, *271*, 32126–32136.
[104] Vedam V. et al., *J. Bacteriol*., **2003**, *185*,1841–1850.
[105] BasuS.S., Karbarz M. J., Raetz C. R. H., *J. Biol. Chem*., **2002**, *277*, 28959–28971.
[106] Ferguson G.P. et al, *Mol. Microbiol*., **2005**, *56*, 68–80.

VLCFA may have biological significance concerning rhizobium/legume symbiosis and pathogen/plant and animal pathogenesis. The gene likely responsible for the production of the specialized acyl carrier protein, LpxXL, has been mutated in *Bradyrhizobium* ORS 278 (*Brado*4679 the name of the mutant strain), where the bacterium is able to begin symbiotic process with *Aschynomene* legume plants.

The structural analysis, performed on both lipid A mutants, revealed the importance of the role of LpxXL protein (*Brado*4679) required for VLCFA transport on the lipid A structure; furthermore as displayed by biological data, *Brado*4679, lacking one of VLCFA, is not able to start a normal symbiotic mechanism with plant. On contrary, *Brado4680* conserving its lipid A structure can establish, as the other *Bradyrhizobium* strains like Btai1 and ORS 278, a mutualistic relationship with the legumes.

Results and Discussion

6.8.1 Preliminary analysis

Bacterial pellet of *Brado4679* and *Brado4680* were extracted with phenol/water method. The LPS were isolated and undergo to acetic acid treatment in order to obtain the lipids A.

6.8.2 Structural determination of lipid A of ORS278Δ*4679* and ORS278Δ*4680* (*Brado4679* and *Brado4680)* via MALDI mass spectrometry

From the structural point of view, lipid A isolated from *Brado*4679 displayed a pentasaccharide sugar backbone alike BTAi1, substituted by 3-hydroxy primary fatty acids and one unsaturated fatty acid chain of 12 carbon atoms. The primary fatty acid is ester linked by a C:30 (2,29-OH) fatty acid as revealed by mass spectrum Fig. 6.8.2 a, the last further substituted by bacteriohopane of 35 carbon atoms, which corresponds to hepta-acylated lipid A overmethylated at position C-2 of the hopane ring. To confirm the presence of a methylated hopanoid moiety, a MS/MS spectrum was performed on the precursor ion of hexa-acylated lipid A species at *m/z* 2668.87. The MS/MS spectrum (Fig. 6.8.2 b) revealed a loss of 526 uma, attributable to methylated hopanoid and then the loss of C_{30}:2OH in ester linkage. Unlike the wild type strain, the lipid A revealed the absence of one of VLCFA (C_{26}:25OH), which would confirm the mutation on *Brado4679*gene and the change in behavior of lipid A in the symbiotic process. (see biological test 6.9.1)

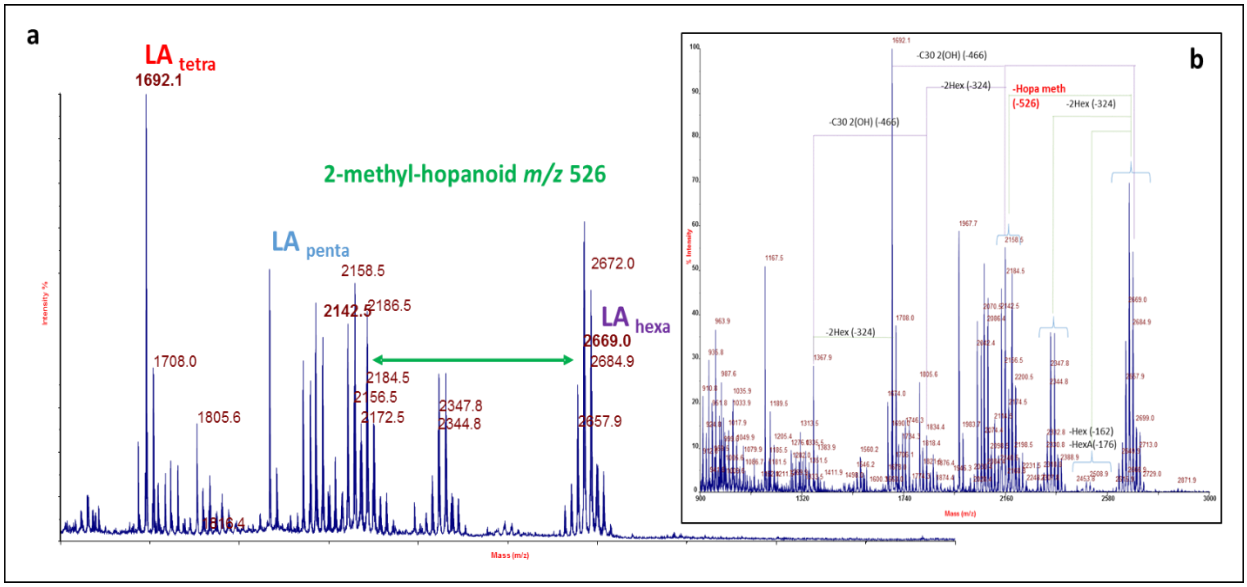

Figure 6.8.2:**a**) mass spectrum of Bradyrhizobium ORS278Δ4679; **b**) MS/MS spectrum on hexa-acylated lipid A, revealed the presence of overmethylated hopanoid moiety.

All data collected, allowed us to reach the following lipid A structure (Fig. 6.8.3):

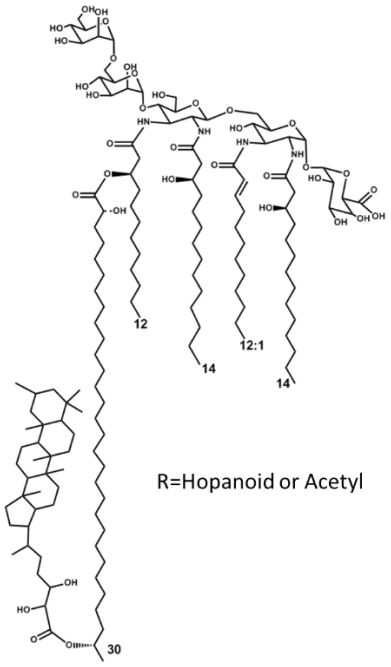

Figure 6.8.3: Complete lipid A structure isolated from *Brado*4679

We also analyzed lipid A produced from *Brado4680*, in order to elucidate the role of a second gene cluster thought to be involved in VLCFA biosynthesis.

The mass analysis displayed the usual acylation patter of *Bradyrhizobium* lipid A, no differences have been detected. Penta-, hexa-, hepta-acylated lipid A were present, containing two DAG, two Man residues, one GalA, two C14:3OH, one C12:3OH and C12:1 in amide linkage; one C12:O and VLCFA (C26:25OH, C30:29OH), hopanoic acid were also present in ester linkage (Fig. 6.8.4)

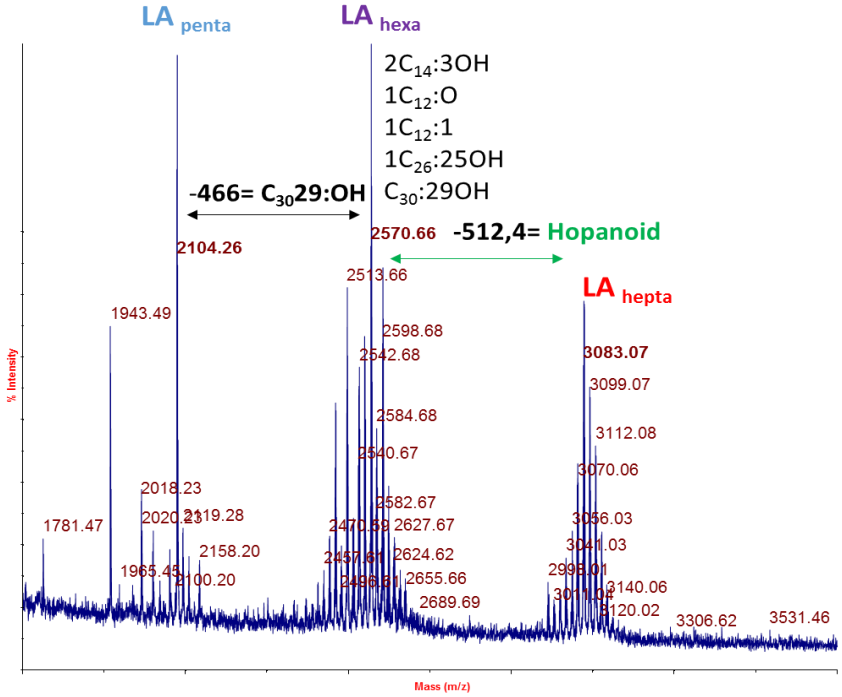

Figure 6.8.4: Mass spectrum of other mutant *Brado4680*

6.9 Biological evaluation of *Brado4679*

The lipid A of most symbionts, often containing VLCFAs,[107] are capable to adapt their hydrophobic unwieldy chains in the inner leaft of outer membrane, increasing the degree of membrane packing. From the last studies, VLCFA result to be important not only for chemical-physic properties conferred to the total membrane, but they may be important for pathogenesis and symbiosis of several organisms.

Genes involved in the synthesis of the Rhizobium VLCFA lie in a six-gene cluster on the chromosome and are widely conserved among bacteria that synthesize VLCFA.[108] In their genome, AcpXL is a

[107] Bhat U. R., Carlson R. W., Busch M., Mayer H., *Int. J. Syst. Bacteriol.*, **1991**, *41*, 213–217.
[108] Vedam V. et al., *J. Bacteriol.*, **2006**, *188*, 2126–2133.

specialized acyl carrier protein[109,110,111]on which the VLCFA is built, and LpxXL[112,113]is required for the transfer of VLCFA from the AcpXL-VLCFA conjugate to the lipid A (Fig. 6.9.1 a). These genes are specific to VLCFA synthesis. *Rhizobium* strains that contain single mutations in the *acpXL*, *fabF1XL*, and *fabF2XL*genes[114] do not synthesize VLCFA and produce lipid A which lacks VLCFA. These results show that the genes required for general fatty acid synthesis [115]do not compensate for the loss of genes required for VLCFA *in vivo*.

Here, the mutations were done at expense of particular genome region.

From biological point of view, the mutation *Brado4679*, with the consequent loss of one of VLCFA, leads to a negative effect on free symbiotic life of ORS278Δ*4679* more sensitive to various stress as shown in Fig. 6.9.1.

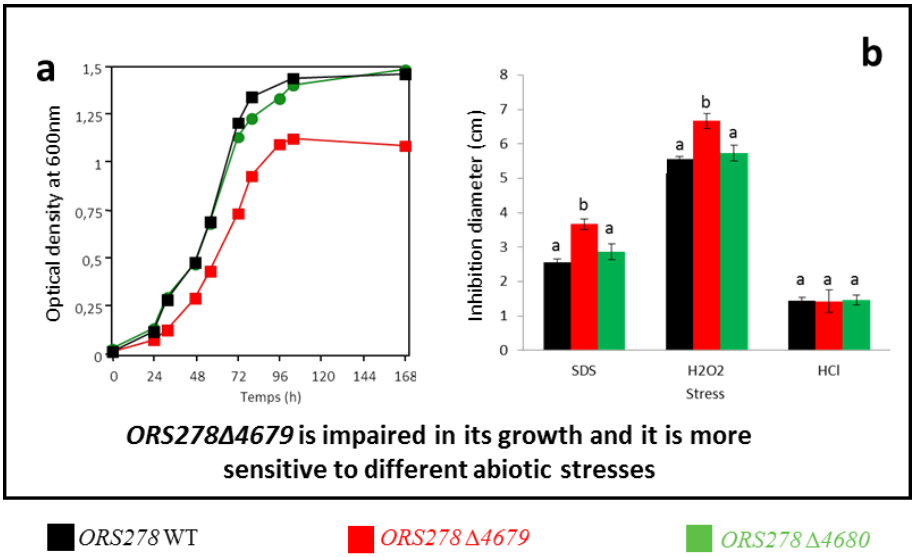

Figure 6.9.1: **a**) Optical density during the mutants growing; **b**) Disk diffusion test on mutants using several stressors.

It was also evaluated the nitrogenase activity performed by bacteria at nodule level. The ARA assays revealed a comparable activity between wt ORS278 and ORS278 *Δ4680*, instead the mutant ORS278 *Δ 4679*, displayed a strong reduction in nitrogenase activity, which corresponded to a limitate capacity to start the symbiotic process. (Fig.6.9.2)

[109] Brozek K. A., Carlson R. W., Raetz C. R. H.,*J. Biol. Chem*., **1996**, *271*, 32126–32136.
[110] Sharypova L. A., Niehaus K., Scheidle H., Holst O., Becker A.,*J. Biol. Chem*., **2003**, *278*, 12946–12954.
[111] Vedam V. et al., J. *Bacteriol*., **2003**, *185*, 1841–1850.
[112] Basu S. S., Karbarz M. J., Raetz. C. R. H., J. *Biol. Chem*., **2002**, *277*, 28959–28971.
[113] Ferguson G. P., Datta A., Carlson R. W., Walker G. C., *Mol. Microbiol*., **2005**, *56*, 68–80.
[114] Vanderlinde E. M. et al.,*Microbiology*, **2009**, *155*, 3055–3069.
[115] White S. W., Zheng J., Zhang Y.-M., Rock. C. O., *Annu. Rev. Biochem*., **2005**, *74*, 791–831.

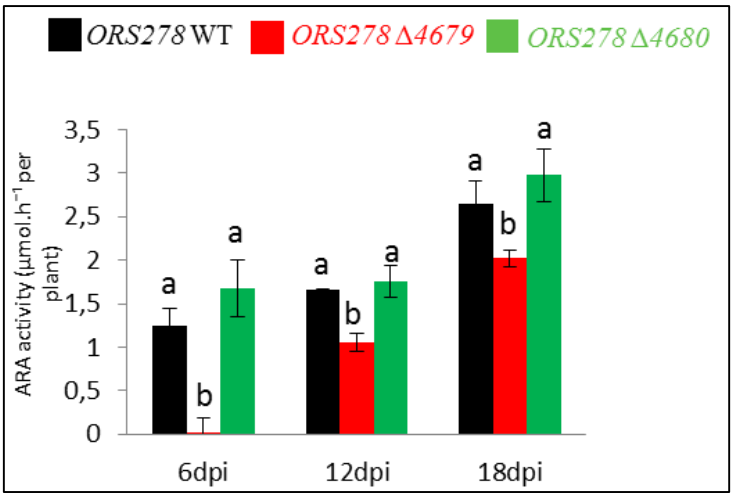

Figure 6.9.2: ARA assay to test nitrogenase activity in constructed mutants

To sum up, we showed that *Brado4679* (*lpxXL*) has an important role in the free life of the bacteria and it is necessary for the establishment of a successful symbiosis. We also demonstrated that gene *lpxXL* is involved the grafting of the only one of the two VLCFA. On the contrary, *Brado4680* not coding for *lpxXL* and/or *acpXL* proteins, because the mutation has no real effect in the lipid A structure, as showed by MALDI spectrum (Fig. 6.8.4), so *Brado4680* gene is not necessary for the symbiotic process.

Section V

Hopanoids

6.10 Structure variations on hopanoid moiety have impact on the symbiosis process

To proceed our work performed on unusual lipid A isolated from *Bradyrhizobium* strains, we characterized also the lipid A from two mutants bacteria belonging to *Bradyrhizobium diazoefficiens*, *B. japonicum* ΔhpnH and *B. japonicum* ΔhpnP, which produce lipid A lacking the side chain and the methyl group on the C-2 position of hopanoid ring, respectively.

In order to evaluate if the following modifications on the lipid A structure are indispensable for the establishment of symbiosis, we performed structural determination using mass spectrometry coupled biological evidences.

Our results showed that C35 hopanoids are necessary for symbiosis only with the host *Aeschynomene afraspera* but not with soybean. The last mutation ΔhpnH induce a drastic modification in bacterial morphology and physiology due to a less rigid membrane resulting from the absence of free or lipid A-bound C35 hopanoids or the accumulation of the C30 hopanoid diploptene.

So, the study of hopanoid mutants in plant symbionts, thus provides an opportunity to gain insight into host-microbe interactions during later stages of symbiotic progression, as well as the micro-environmental conditions for which hopanoids provide a fitness advantage.

6.11 Results and Discussion

Genes predicted to encode the C-2 methylase, *hpnP*[116]or the first enzyme catalyzing the extension of C30 hopanoids, *hpnH* were mutated[117]

WT and ΔhpnP mutant lipid A are composed of a mixture of penta- to hepta-acylated species (Fig. 6.11.1 a), differing for the presence of one C_{30}:(2,29OH) and an hopanoid resisue; whereas ΔhpnH mutant lipid A is mainly hexa-acylated (see Fig. 6.11.1 b). In WT and ΔhpnP mutant hepta-acylated species, a C35 hopanediolic acid is ester linked to hexa-acylated lipid A, and traces of a second hopanoid substitution are also detected at *m/z* 3636; conversely, the ΔhpnH mutant is missing any lipid A-bound hopanoids and displayed a single ion cluster at *m/z* 2624.

All experimental data confirmed the occurring of mutations on the hpnH and hpnP genes.

[116] Welander P.V. et al.,*Proc. Natl. Acad. Sci.* U S A, **2010**, *107*, 8537– 8542.
[117] Welander P.V., Doughty D.M., Wu C.H., Mehay S., Summons R.E., Newman D.K., *Geobiology*, **2012**, *10*, 163–177.

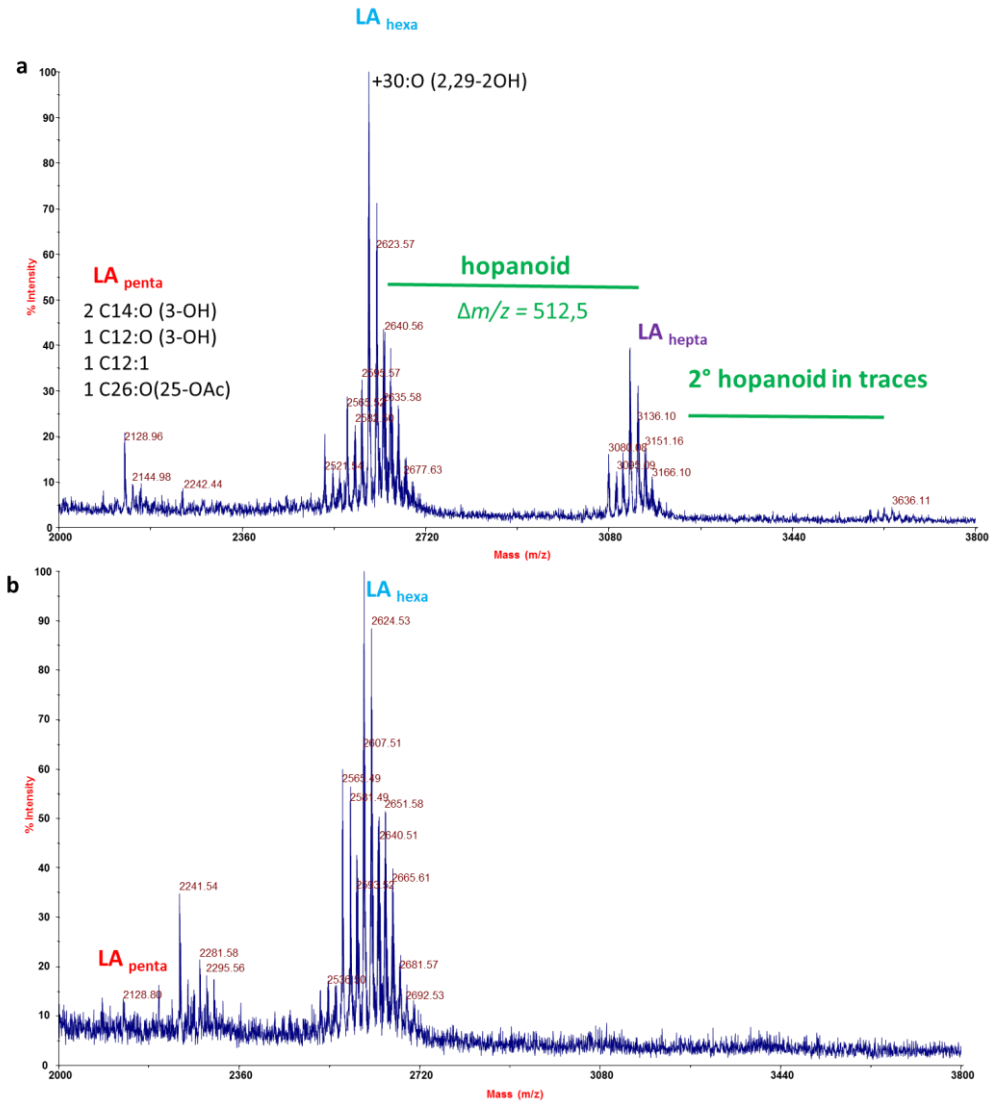

Figure 6.11.1: **a**) MALDI-MS analysis of lipid A from ΔhpnP mutant is composed of a mixture of penta-acylated and hexa-acylated species; **b**) MALDI-MS analysis of lipid A from ΔhpnH mutant lipid A is mainly hexa-acylated.

6.12 Biological assays

Then mutant strains underwent investigations to check maintenance of membrane rigidity, if stressed by various substances (Fig.6.12.1 a-b), different growth conditions at diverse temperature (Fig. 6.12.1 c), and also if the side chain play a role in the establishment of symbiosis. (Fig. 6.12.1 d)

The results showed that membranes of all strains were less rigid at higher temperature. In particular, the Δ*hpnP* mutant membrane was as rigid as the WT membrane at both temperatures, whereas the Δ*hpnH* mutant displayed a decreasing of membrane rigidity respect to wt.

Thus, C35 hopanoids are important for maintaining membrane rigidity in *B. diazoefficiens*.

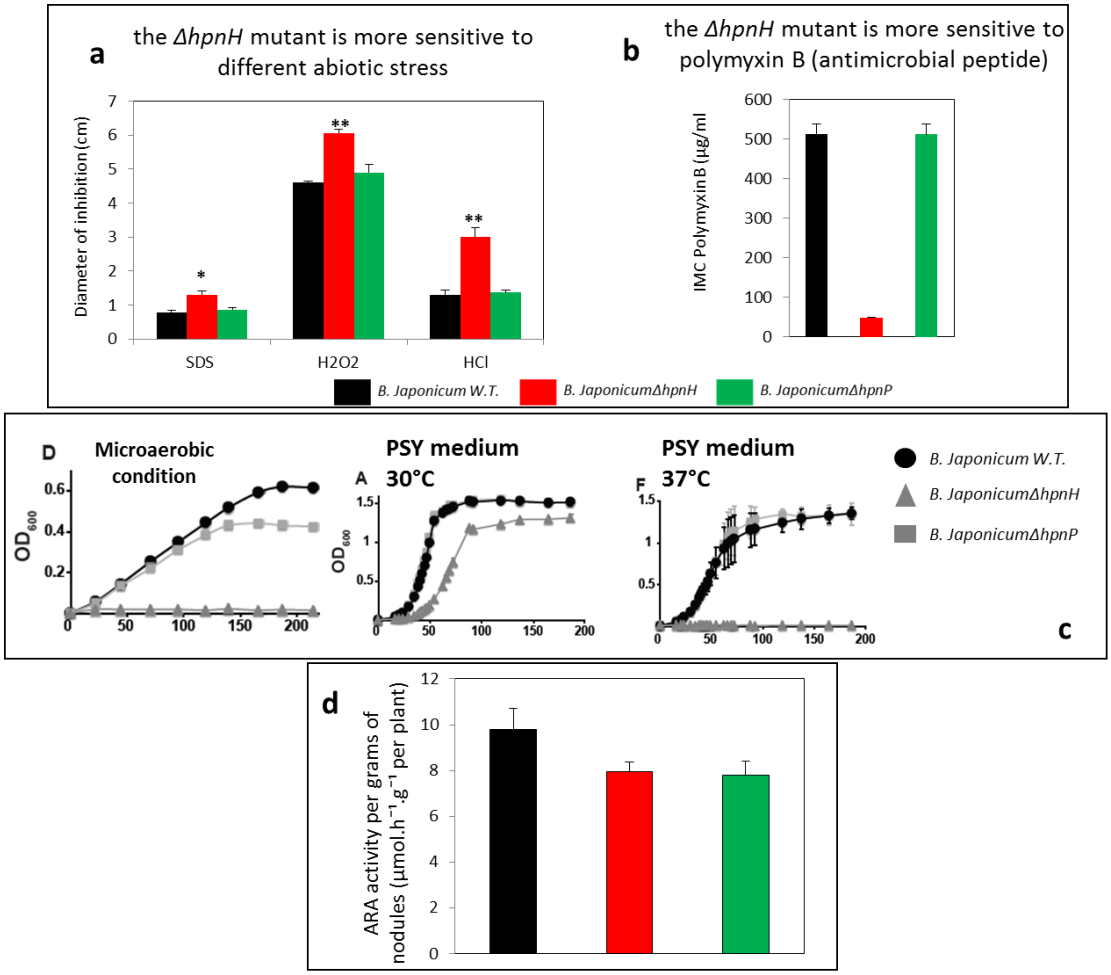

Figure 6.12.1: **a -b**) Growth of *B. diazoefficiens* strains under stress as measured in stressor gradient plates by disc diffusion assays with 10% SDS, 5.5 M H2O2, and 2 M HCl; **c**) Growth of the WT(circles), the Δ*hpnP* mutant (squares), and the Δ*hpnH* mutant (triangles) was monitored as optical density at 600 nm (OD600) in PSY at 30°C, PSY at 37°C and microaerobic PSY with 0.5%O2 at 30°C; **d**) Quantification of acetylene reduction activity (ARA) in plants inoculated with WT or Δ*hpnH* or Δ*hpnP* mutant.

The mutants mentioned above displayed also different growing in various conditions; For instance, at 30°C and 37°C the growth of WT and the ΔhpnP mutant is equivalent, instead is lower for ΔhpnH (Fig. 6.12.1 c). These results suggest that C35 hopanoids are important for growth at ambient temperature and in aerobic conditions.

Hopanoids have been shown to contribute to stress tolerance in diverse organisms.[118,119,120]

To test this hypothesis, w echallenged Δ*hpnP* and Δ*hpnH* mutants with a variety of stressors that are relevant during the initiation and progression of symbiosis, such as hypoxia, acidic pH, high

[118] Kulkarni G., Wu C.H., Newman D.K., J. *Bacteriol*., **2013**, *195*, 2490 –2498.
[119] Silipo A. et al.,*Nat. Commun*., **2014**, *5*, 5106.
[120] Welander P.V, Hunter R.C., Zhang L., Sessions A.L., Summons R.E., Newman D.K., *J. Bacteriol*, **2009**, *191*, 6145–6156.

osmolarity, reactive oxygen species, and peptide antibiotics.[121,122] In almost case, the mutant ΔhpnH revealed an high oversensitive to all stressors. (Fig. 6.12.1 a-b)

Nevertheless, there is not real impact on the nitrogenase activity respet to wt during symbiotic process. (Fig. 6.12.1 d)

So, hopanoids formed by 35 carbon atoms are required for symbiotic life of *Bradyrhizobium*strains and make membrane resistant.

In the future, it will be interesting to clarify how and where the presynthetized hopanoid, required for symbiosis, binds VLCFA during the biosynthesis of the whole lipid A.

[121] Gibson K.E., Kobayashi H., Walker G.C., *Annu. Rev. Genet.,* **2008**, *42*, 413– 441.
[122] Czernic P. et al., *Plant. Physiol.,* **2015**, *169*(2), 1254-65.

Chapter VII

Characterization O- side chain from Rhodopseudomonas strains

7.1 *Rhodopseudomonspalustris* BIS A53

Rhodopseudomonas palustris is a purple photosynthetic bacterium that able to dwell both in soil and water. Actually, it develops the ability to sense and adapt to environmental changes and can grow in a wide variety of habitats and conditions, like swine waste lagoons, earthworm droppings, marine coastal sediments and pond water.

R. palustris exhibits a surprising versatility and can switch between any of the four different metabolic states: photoautotrophic, photoheterotrophic, chemoautotrophic and chemoheterotrophic. This versatile metabolic nature has received significant attention in recent years due to the potential implications as bacterium suitable for biotechnological and industrial applications: industrial waste, inorganic and organic compounds including green plant-derived, pollutants and aromatic compounds, can be degraded by *R. palustris* and converted into either biomass or biofuel.[123]

The versatile nature of *R. palustris* and its ability to adapt to various environments prompted us to focus the attention on its membrane characteristics. Bacterial surfaces are highly decorated with saccharidic motifs responsible for mediating cell–environment interaction.[124,125] The peculiarities of R. palustris and therole likely played by cell wall components conveyed our efforts in defining the structure of membrane glyco-conjugates. In particular, we focused our attention on lipopolysaccharides (LPSs).

The O-chain of LPS is the portion more exposed to the selective pressures of the outer environment and to modifications induced by external stimuli; among its various roles, the most important appears to be protective, acting as a defensive barrier.

In detail, we have investigated the structural and conformational features of the O-chain region of LPS isolated from *R. palustris* strain BisA53. We showed that this strain produces a polymer based on a tri-saccharide repeating unit characterized by D-rhamnose, 3-deoxy-D-lyxo-2-heptulosaric acid (Dha), and a novel C-branched monosaccharide, the 4-amino-4,6-dideoxy-3-C-methyl-2-O-methyl-α-L-glucopyranose. This latter, to the best of our knowledge, has been found for the first time in Nature, thus, its absolute configuration has been determined by a combination of 2D NMR spectroscopy and molecular mechanics and dynamics.[126,127]

Moreover, a conformational study was executed on the whole polymer with the aim of evaluating its spatial arrangements by the same combined approach.

---

[123] Larimer F. W., Chain P., Hauser L., Lamerdin J., Malfatti S., Do L., et al.,*Nature Biotechnology*,**2004**,*22*, 55–61.
[124] Raetz C. R., & Whitfield C., Lipopolysaccharide endotoxins. *Annual Review ofBiochemistry*, **2002**, 71, 635–700.
[125] Silipo A., De Castro C., Lanzetta R., Parrilli M., & Molinaro A. Lipopolysaccharides., **2010** In H. König, H. Claus, & A. Varma (Eds.), Prokaryotic cell wall compounds– structure and biochemistry 133–154.
[126] Lipkind G. M., Shashkov A. S., Mamian S. S., &Kochetkov N. K.,).,*Carbohydrate Research*,**1988**,*181*, 1–12.
[127] Jimenez-Barbero J., de Castro C., Evidente A., Molinaro A., Parrilli M., &SuricoG.,*European Journal of OrganicChemistry*, **2002**,1770–1775.

Results and Discussion

7.2 Preliminary data

From dried cells were extracted LPS using hot phenol/water protocol. The SDS-PAGE analysis showed that LPS was of smooth type, according to the presence of high molecular weight species in the upper part of the gel (data not shown).

Chemical analysis of LPS fraction showed the presence of D-rhamnose, 3-deoxy-D-lyxo-2-heptulosaric acid (Dha) and of a 4-amino-4,6-dideoxy-3-C-methyl-2-O-methyl-Hex*p*.

The absolute configuration of rhamnose and DHA was determined by GLC of the acetylated (S)-2-octyl glycosides and comparison with authentic standard whereas for the new monosaccharide residue this was established by NMR and MD approach. Methylation analysis showed the presence of 3-substituted D-Rha*p*; 5-substituted D-Dha*p*; 3-substituted 4-amino-4,6-dideoxy-3-C-methyl-2-O-methyl-Hex*p*.

7.3 NMR analysis

In order to isolate the O-chain, a mild acid hydrolysis was performed and the water soluble polysaccharide was purified by gel-permeation chromatography (**PS1**) and underwent NMR analysis; however, since PS1 gave evidence of non stoichiometric O-acylation, we decided to simplify the NMR analyses by a O-deacylation performed with anhydrous hydrazine; the obtained O-deacylated polysaccharide (**PS2**) was further purified and characterized by full 2D NMR analysis. The ^{1}H NMR spectrum of the PS2 product is shown in Fig. 7.3.1.

A combination of homo- and heteronuclear 2D NMR experiment (DQF-COSY, TOCSY, ROESY, NOESY, ^{1}H–^{13}C HSQC, ^{1}H–^{13}CHMBC) was executed to assign all the spin systems and to define the saccharidic sequence.

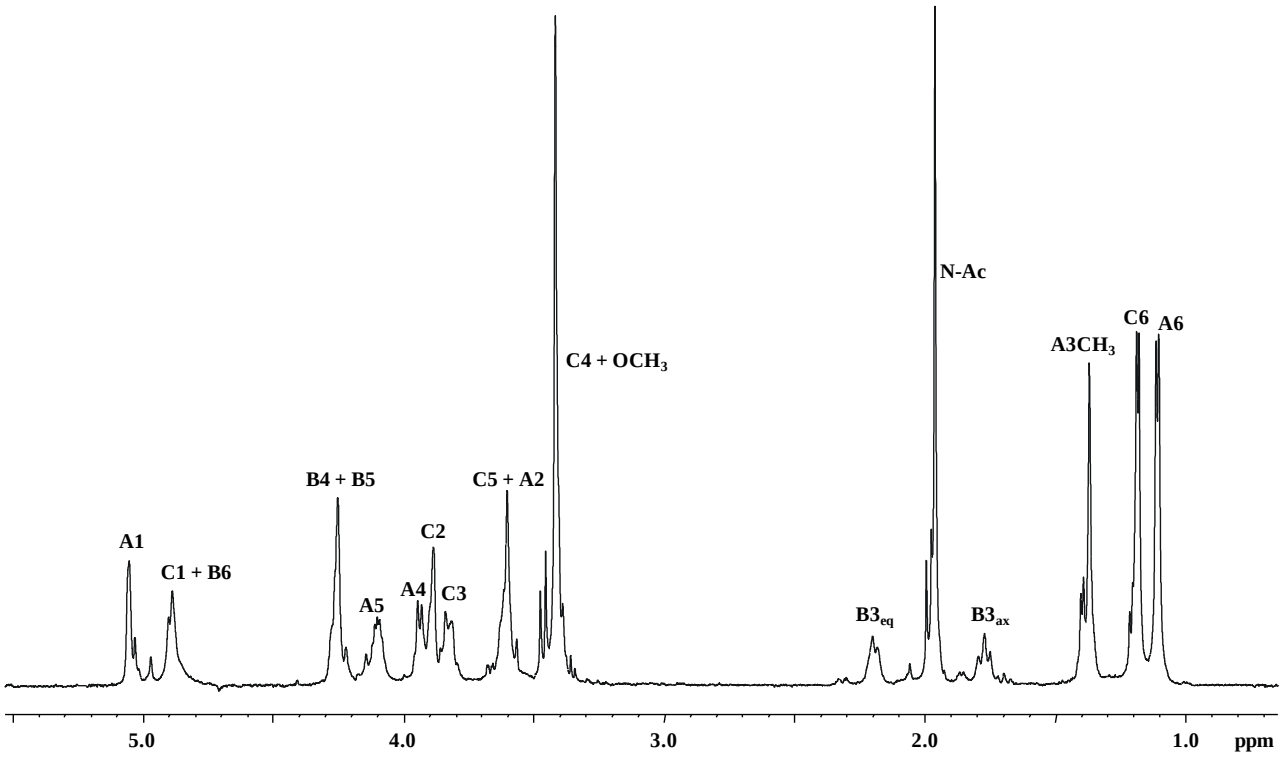

Figure 7.3.1:^{1}H NMR spectrum of PS2 product. Signals are as attributed in Table 7.3.1

The anomeric configuration of each monosaccharide unit was assigned on the basis of $^{3}J_{H\text{-}1,H\text{-}2}$ and $^{1}J_{CH}$ coupling constants, whereas the values of the vicinal $^{3}J_{H,H}$ ring coupling constants allowed the identification of the relative configuration of each sugar residue.

Residue **C** (Table 7.3.1 and Fig. 7.3.1) was recognized as α-rhamnose as indicated by the scalar correlations, in the TOCSY spectrum, of the ring protons with C-6 methyl signal (Fig. 7.3.2). The *manno*-configuration was established by$^{3}J_{H\text{-}1,H\text{-}2}and^{3}J_{H\text{-}2,H\text{-}3}$(both below 2 Hz),$^{3}J_{3,4}$(3 Hz) and$^{3}J_{H\text{-}4,H\text{-}5}$(9 Hz), the α-anomeric configuration was assigned by the$^{1}J_{CH}$coupling constant value of 175.9.

Because of the absence of the anomeric proton signal, spin system of Dha **B** was assigned starting from the diastereotopic H-3 methylene protons (Tab. 7.3.1 and Figs.7.3.1 and 7.3.2), resonating in a shielded region at 1.78 and 2.20 ppm (H-3ax and H-3eq, respectively). The lyxo-configuration of the Dha was deduced from the coupling constants$^{3}J_{H3ax,H4}$of 12.7 Hz, indicative of the axial position of H-4, and of $^{3}J_{H5,H6}$< 1 Hz, corresponding to an equatorial disposition of H-5 in a$^{5}C_{2}$ chair conformation. The α-anomeric configuration of Dha was assigned on the basis of previously published data.[128,129]

[128]Birnbaum G. I., Roy R., Brisson J. R., & Jennings H. J.,*Journalof Carbohydrate Chemistry*,**1987**,*6*, 17–39.
[129]Vinogradov E. V., Müller-Loennies S., Petersen B. O., Meshkov S., Thomas-Oates J. E., Holst O., et al., *European Journal of Biochemistry*,**1997**,*247*(1), 82–90.

Spin system **A** (Table 7.3.1) was identified as a 4-amino-4,6-dideoxy-3-C-methyl-2-O-methyl- α-glucose (3-C-methyl-2-O-methyl-4-amino-α-quinovose (further on abbreviated as 3-methyl-2-O-methyl-Qui4N). The α-anomeric configuration of **A** was supported by $^{3}J_{H-1,H-2}$ and $^{1}J_{C,H}$ coupling constant values of 2 Hz and 173.9 Hz, respectively (Table 7.3.1). The 2-O-methyl group was univocally located at C-2 **A** on the basis of the downfield shift of C-2 **A** (80.3 ppm, Table 7.3.1), by the long range correlations present in the HMBC spectrum of C-2 **A** with the proton signals of methoxy group and confirmed by the NOE contact of this latter with H-2 **A**.

The anomeric proton signal of **A** at 5.04 ppm correlated exclusively with H-2; a second spin system was present, involving scalarly correlated proton signals from position 4 to position 6.

The $^{3}J_{H-4,H-5}$ coupling constant value of 10.7 Hz was used to establish the relative axial configuration of both H-4 and H-5 protons (Table 7.3.1, Figs. 7.3.2 and 7.3.3); the scalar correlation of both H-4 and H-5 with a downfield methyl signal were indicative of the nature of 6-deoxysugar of **A**.

[→3)-**C-(**1→3)-**A-(**1→5)-**B-(**2→]$_n$							
Unit	**1**	**2**	**3**	**4**	**5**	**6**	**7**
A	5.04	3.60	-----	3.93	4.09	1.10	
3-α-Sug	96.9	80.3	77.6	54.9	65.5	16.9	
		O-CH_3 3.41/58.3	CH_3 1.37/16.9	Acetyl C=O 173.64, CH_3 1.97/22.0			
	$^{1}J_{CH}$ 173.9 Hz	$^{3}J_{H1,H2}$ 2 Hz		$^{3}J_{H4,H5}$ 10.7 Hz			
B	----	-----	2.2/1.78	4.26	4.25	4.88	----
5-α-DHA	177.3	99.0	34.9	65.0	75.9	73.9	175.8
			$^{3}J_{H3ax,H4}$ 12.7 Hz; $^{3}J_{H3aeq,H4}$ 1 Hz		$^{3}J_{H5,H6}$<1 Hz		
C	4.80	3.89	3.82	3.40	3.61	1.18	
3-α-Rha	93.1	68.6	72.5	70.6	68.9	16.9	
	$^{1}J_{CH}$ 175.9 Hz						

Table 7.3.1: ^{1}H and ^{13}C NMR chemical shifts (ppm) of PS2 measured in D_2O

Furthermore, the HSQC spectrum (Fig. 7.3.3) showed a correlation of H-4 **A** with a nitrogen bearing carbon signal at 54.9 ppm that, together with the down-field shift of H-4 proton resonance, was diagnostic of N-acyl group at this position. In fact, the presence of the amino group was also confirmed by the long range correlation in the HMBC spectrum, of H-4 **A** with the carbonyl carbon of the acetyl group and of this latter with a methyl group. The long range correlations in the HMBC spectrum (Fig. 7.3.3) were useful to completely identify residue **A**. In particular, the long range correlations of a quaternary carbon with H-1, H-2 and H-4 **A** were indicative of the presence of a quaternary carbon at position C-3 of residue **A**.

The substitution of C-3 **A** by a methyl group was identified by its long range correlations with the singlet methyl at 1.37/16.9 ppm (Fig. 7.3.3). By NOE correlations found in the NOESY spectrum, the relative configuration of monosaccharide **A** was also established.

Actually, the axial orientation of CH3on C-3 was endorsed by the *intra*-residual NOE with the syn-axial proton H-5 at 4.09 ppm (Fig. 7.3.2); likewise, the *intra*-residue NOE contacts between H-2 and H-4 indicated their syn-diaxial orientation. To summarize, the $^{3}J_{H,H}$ ring coupling constant values, NOE and HMBC correlations suggested a *gluco*-configuration for residue **A**, a 3-C-methyl-4-amino-α-quinovose carrying a methyl group at position O-2.The downfield shift of carbon resonances identified the glycosylated positions: O-3 of residues **A** and **C** and O-5 of **B**, in full agreement with the methylation analysis. The sequence of this repeating unit was defined by the long-range scalar correlations found in the HMBC spectrum and the inter-residual NOE contacts.

Residue **A** was glycosylated at O-3 by α-rhamnose **C**, as suggested by the long range scalar correlation H-1 C/C-3 A and the NOE contact of H-2 A with H-1 C (Figs. 7.3.2 and 7.3.3). Residue **C** was in turn glycosylated at its O-3 by **B** residue, as attested by the long range contact of **B**-2 with C-3; eventually, residue **B** was substituted at its C-5 by residue **A** as attested by the NOE between H-1 A and H-5 **B** (Fig.7.3.2)and by the corresponding long range contacts.

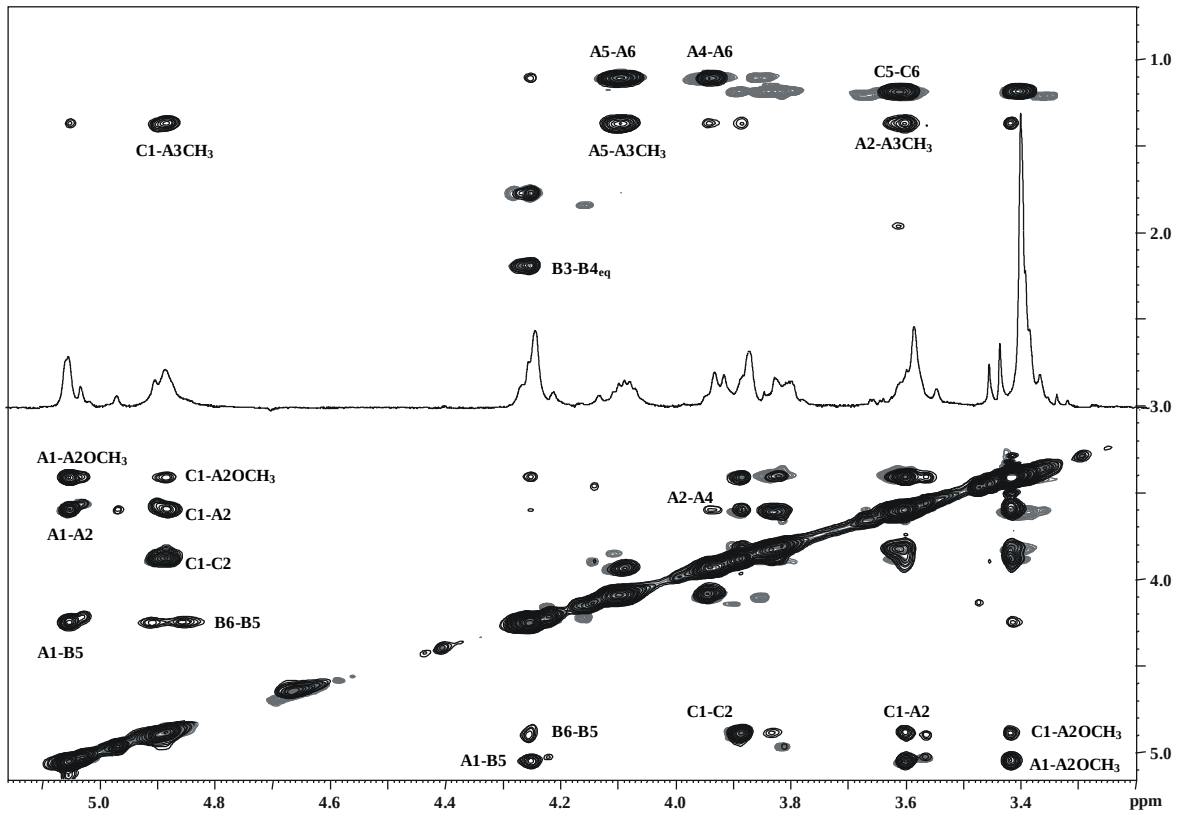

Figure 7.3.2: ROESY (black) and TOCSY (gray) spectra related to PS2 product. The main inter-residual correlations used to assign, together with the HMBC spectrum, the sugar backbone, are indicated; key intra-residual NOE correlations are also indicated.

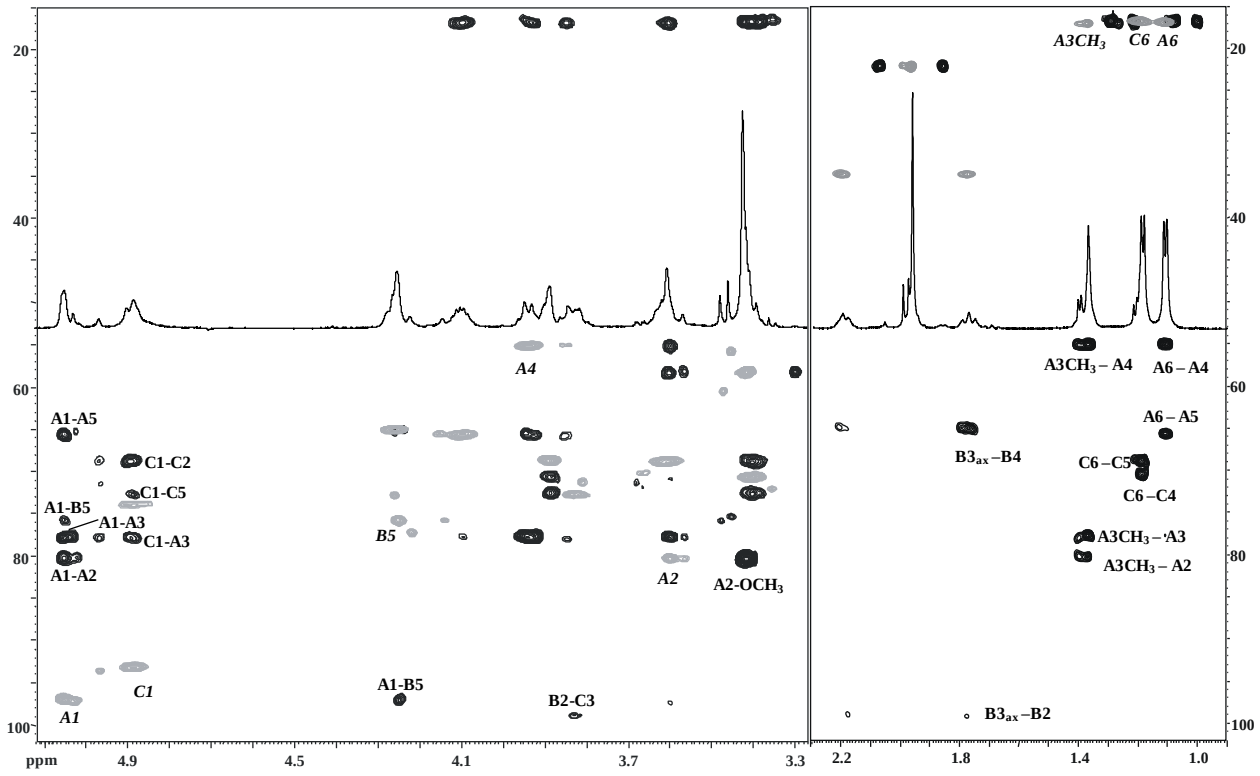

Figure 7.3.3: HSQC (gray) and HMBC (black) spectra of PS2 product; the key inter-residual and intra-residual long-range correlations are indicated.

Thus, all data were in agreement with the primary structure reported below (Fig.7.3.4)

[→3)-α-D-Rha-(1→3)-α-Sug-(1→5)-α-D-Dha-(2→]$_n$

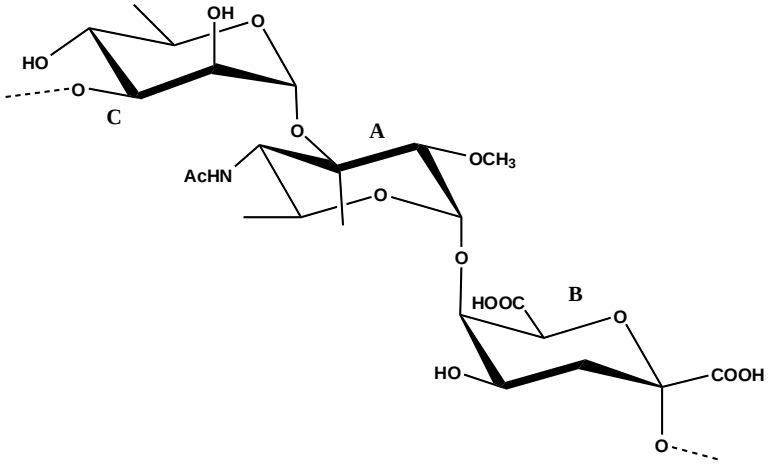

Figure 7.3.4: Structure of the O-polysaccharide from *R. palustris* BisA53.

7.4 Conformational studies of polysaccharide

In order to determine the absolute configuration of the 3-C-methyl-2-O-methyl-Qui4N (residue **A**), we have used a protocol based on NOE data and computational approach. Lipkind et al. demonstrated that main structural factors determining the preferred conformation in disaccharides, and therefore the corresponding NOEs, are the configuration of the glycosidic linkage, the nature of the sugar, the position of glycosylation and the absolute configuration of the constituent residues. Taking into account this above, and given that the absolute configuration of the other two residues **B** and **C** was known, we measured and compared the NOE-derived key inter-proton distances with those predicted for models taking in account the two possible absolute configurations of residue **A** (L and D).

The first step was the building of the potential energy surfaces for each disaccharide connected by a glycosidic linkage; Φ represents the torsion angle about H1-C1-O-CX' whereas Ψ about C1-O-CX'-H'; five distinct disaccharide entities were constructed considering the above determined repeating unit: [→3)-C-(1→3)-A-(1→5)-B-(2→]$_n$ and the two possible absolute configurations of residue A, drawn with both D and L configuration ($A_L$and A_D) and subjected to extensive calculations using MM3*force field to build the potential energy surfaces for both disaccharides whose relative orientation is defined by Φ and Ψ torsion angles around the glycosidic linkage.

The resulting adiabatic energy maps indicating global minima are reported in Fig. 7.4.1

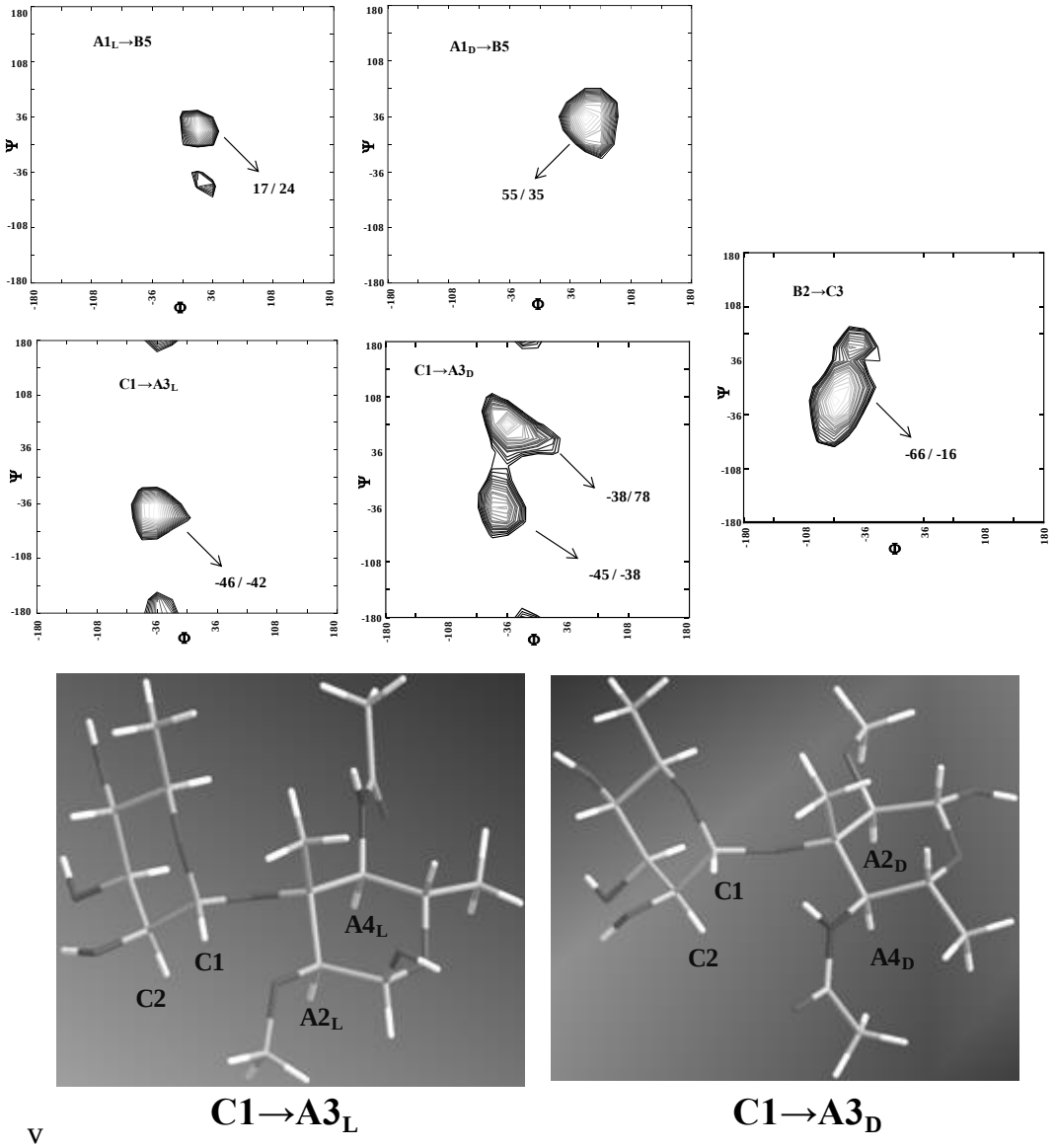

V

Figure 7.4.1: **a**) Relaxed energy maps for the disaccharide fragments composing the O-polysaccharide from *R. palustris* BisA53; the two maps for A1 → B5 linkage differ in the absolute configuration of **A** residue. The positions of global and major local minima in the maps are indicated. b) View of representative structures of **A1→B5** disaccharides differing in the absolute configuration of **A**; key protons for the definition of the absolute configuration of **A** are indicated (see text).

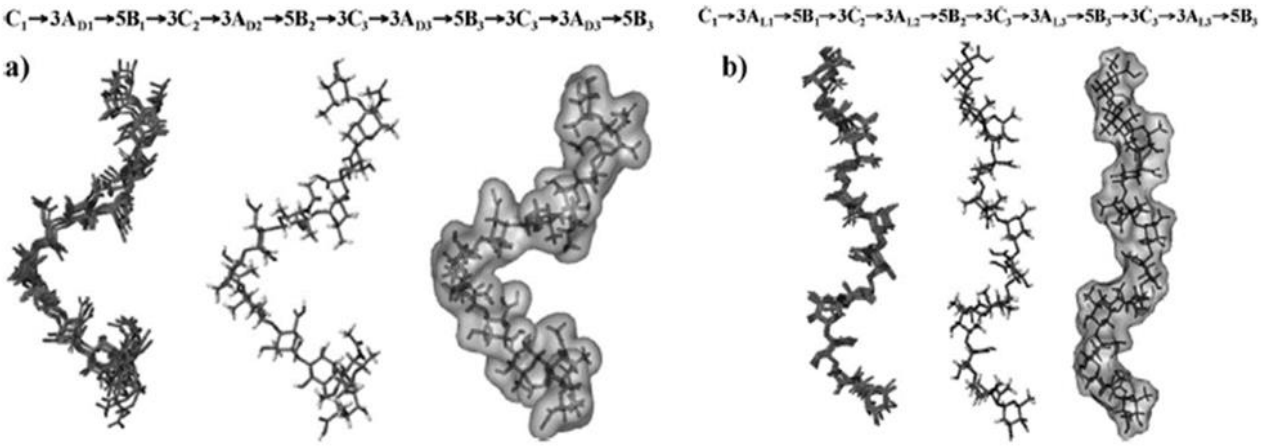

Figure 7.4.2:View of representative structures and Connelly surface of PS2 species built with four repeating units; **a**) the two dodecasaccarides [$C_1\rightarrow 3A_{D1}\rightarrow 5B_1]_4$and **b)**[$C_1\rightarrow 3A_{L1}\rightarrow 5B_1$] differ for the absolute configuration of **A** residue.

Molecular mechanic calculations furnished an estimation of the conformational regions energetically accessible and predicted the existence of slightly different minima for the glycosidic linkages involving **A** residue: the global minimum was located at Φ/Ψ 17/24for $A1_L\rightarrow$ B5, and at Φ/Ψ 55/35 for $A1_D\rightarrow$ B5 (Fig. 7.4.1); as the glycoside linkage involving **C** and **A** residues, in C1 → $A3_L$ the global minimum was located at Φ/Ψ−46/−42 while in C1 → $A3_D$ two energetically comparable minima were present, located at −38/78and −45/−38. Starting subsequently, two oligomers containing two and four repeating units and differing for the absolute configuration of A residue were built from the minima of the energy maps and the conformational behavior was studied by using molecular dynamic simulation:

$C_1\rightarrow 3A_{L1}\rightarrow 5B_1\rightarrow 3C_2\rightarrow 3A_{L2}\rightarrow 5B_2\rightarrow 3C_3\rightarrow 3A_{L3}\rightarrow 5B_3\rightarrow 3C_3\rightarrow 3A_{L3}\rightarrow 5B_3$

$C_1\rightarrow 3A_{D1}\rightarrow 5B_1\rightarrow 3C_2\rightarrow 3A_{D2}\rightarrow 5B_2\rightarrow 3C_3\rightarrow 3A_{D3}\rightarrow 5B_3\rightarrow 3C_3\rightarrow 3A_{D3}\rightarrow 5B_3$

The initial structures were extensively minimized and trajectory coordinates were sampled every ps; 5000 simulations were performed in GB/SA water solvation model as implemented in MacroModel (MMOD).

A first analysis of MD results showed that torsion angles remained in the broad low energy regions previously predicted by the MM calculation, although C → $3A_D$ torsional most selected the minimum around −45/−38 (see Fig. 7.4.1) The computational models obtained from the MD were then compared to the experimental results. Ensemble average inter-proton distances for each saccharide entity were extracted from dynamic simulations and translated into predicted NOEs by a full-matrix

relaxation approach. The corresponding average distances obtained for the simulation from (r−6) values and predicted for both the hexasaccharides built with residue **A** in D and L configuration were compared to those collected experimentally (Table7.4.1).

A comparison of the simulated and measured distances allowed us to evaluate the absolute stereochemistry of residues **A**, that resulted to be L for which case an excellent agreement was found between calculated and experimental data. In detail, the key NOEs and derived distances considered for the definition of the absolute configuration of **A** were those of H-1 **C** with H-2 **A** (strong) and of H-1 **C** withH-2 **A** (medium), only predictable with L configuration of **A** (Table 7.4.1, Figs. 7.3.2, 7.4.1), in which the H-1 and H-2of the α-rhamnose **C** point toward and H-2 **A** and far from H-4 **A**(the side of the sugar ring of **A** residue containing H-2 and far from the side containing H-4); as a further confirmation, a mild-strong NOE contact also with A2-OCH3was present in the NOESY spectrum.

In case of a D configuration, NOE effects of H-1 and H-2 **C** with H-4 **A** were expected and conversely, the NOE of H-1/H-2 **C** with H-2 **A** would have been absent (Table 7.9.1; Fig. 7.3.2).

$C_1 \rightarrow 3A_{L1} \rightarrow 5B_1 \rightarrow 3C_2 \rightarrow 3A_{L2} \rightarrow 5B_2$ and **$C_1 \rightarrow 3A_{D1} \rightarrow 5B_1 \rightarrow 3C_2 \rightarrow 3A_{D2} \rightarrow 5B_2$**

	Experimental 100 ms	Experimental 200 ms	Observed NOE	Hexasaccharide - Calculated D		Hexasaccharide- Calculated L	
A1-B5	2.79	2.85	Strong	2.85±0.29	2.80±0.27	2.74±0.26	2.75±0.27
C1-A2	2.89	2.99	Strong	4.45±0.12	4.20±0.44	3.16±0.37	3.16±0.27
C2-A2	3.40	3.35	Medium	4.49±0.25	4.60±0.35	3.57±0.41	3.53±0.28
C1-A4	-----	-------	Absent	3.43±0.24	3.64±0.49	4.26±0.44	4.37±0.15
C2-A4	-----	-------	Absent	3.79±0.25	4.00±0.30	4.31±0.31	4.35±0.24

$C_1 \rightarrow 3A_{L1} \rightarrow 5B_1 \rightarrow 3C_2 \rightarrow 3A_{L2} \rightarrow 5B_2 \rightarrow 3C_3 \rightarrow 3A_{L3} \rightarrow 5B_3 \rightarrow 3C_3 \rightarrow 3A_{L3} \rightarrow 5B_3$
$C_1 \rightarrow 3A_{D1} \rightarrow 5B_1 \rightarrow 3C_2 \rightarrow 3A_{D2} \rightarrow 5B_2 \rightarrow 3C_3 \rightarrow 3A_{D3} \rightarrow 5B_3 \rightarrow 3C_3 \rightarrow 3A_{D3} \rightarrow 5B_3$

	Dodecasaccharide - Calculated L					Dodecasaccharide - Calculated D			
A1-B5	2.75±0.27	2.75±0.26	2.75±0.26	2.75±0.25	**A1-B5**	2.84±0.27	2.83±0.27	2.84±0.27	2.82±0.27
C1-A2	3.16±0.26	3.16±0.25	3.17±0.24	3.15±0.26	**C1-A2**	4.37±0.12	4.37±0.15	4.38±0.22	4.00±0.44
C1-A4	4.37±0.14	4.37±0.14	4.37±0.13	4.3±0.13	**C1-A4**	3.38±0.25	3.37±0.28	3.38±0.25	3.76±0.44
C2-A2	3.50±0.28	3.53±0.27	3.54±0.25	3.53±0.27	**C2-A2**	4.50±0.28	4.49±0.28	4.50±0.27	4.69±0.28
C2-A4	4.32±0.24	4.35±0.22	4.36±0.22	4.35±0.23	**C2-A4**	3.84±0.22	3.81±0.24	3.83±0.27	4.00±0.35

Table 7.4.1: Experimental (from NOESY experiments) and calculated (from MD calculations) *inter*-proton distances for oligomer built with two and four repeating units

The effect of the different relative orientation of **A** and **C** rings could be in turn translated into a different three-dimensional arrangement of the two above oligomers (Figs. 7.4.2), built with four repeating units and differing for the absolute configuration of **A**. The shape of the dodecasaccharide

showed the differences in the conformational and spatial arrangement. The oligomer with **A** residue in D configuration gave rise to a more compact and pace structure while the oligomer with **A** in L configuration assumed a more extended conformation with a helicoidal disposition.

The O-chain isolated from *Rhodopseudomonas* Bis A53 consisted of a novel tri-saccharide repeating unit made up of rhamnose, non stoichiometrically acetylated at O-2, and Dha, both D configured, and of a novel monosaccharide, a derivative of 4-amino-l-quinovose, branched by a methyl group at carbon 3 and carrying a methoxy group at O-2; its absolute configuration was defined by using an NMR-based molecular mechanics approach: **[→3)-α-D-Rha-(1→3)-α-L-Sug-(1→5)-α-D-Dha-(2→]$_n$**

The combined NOE-based molecular dynamics approach allowed a satisfactory description of both 3D structures; a complete study of the O-chain highlighted a significant level of hydrophobicity since it was constituted by three deoxy-sugars variously decorated by acetyl and methyl groups, acting as shield of hydroxyl and amino groups and thus further increasing the polysaccharide hydrophobic character.

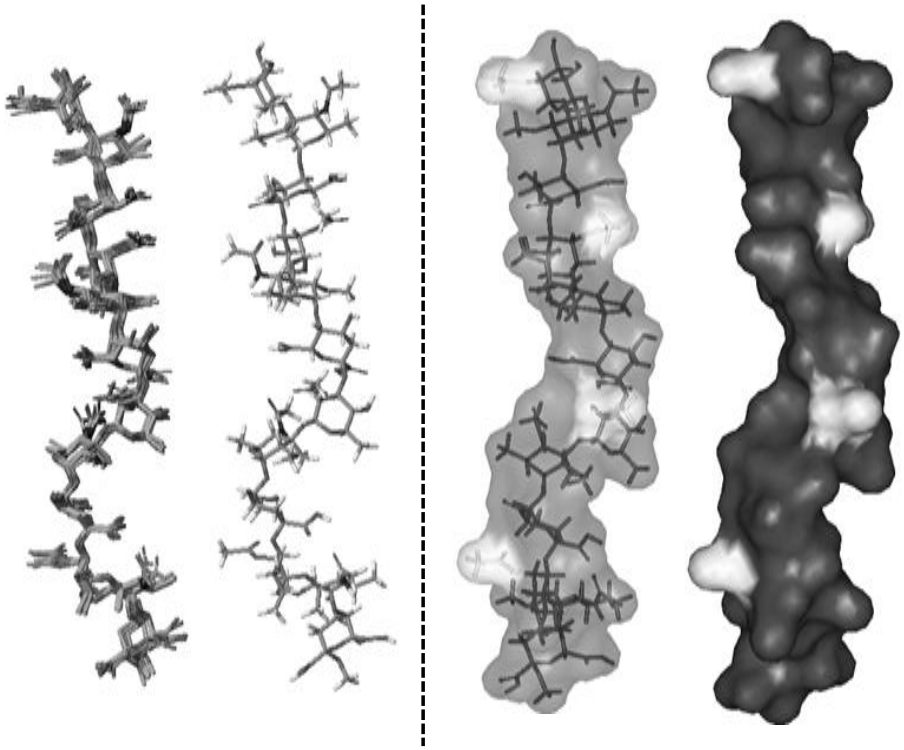

Fig. 7.4.3: View of representative structures and Connelly surface of **PS1**; the preferential disposition of the acetyl groups of the rhamnose units is highlighted (light grey).

Chapter VIII
Experimental methods

8.1 Bacterial growth

8.1.1 *Burkholderia* strains

Pure cultures of *Burkholderia* were grown in Tryptic Soy Broth supplemented with 10 g L-1glycerol (TSB) or MGY medium (M9 minimal medium supplemented with 1.25 g L-1 yeast extract and 10 g L-1 gycerol) at 30 °C. For production of biomass, 18.5 L TSB media were inoculated with1.5 L *B. gladioli* pre-culture (OD600 = 1.4) and grown for 3 days under constant stirring (300rpm) at 30 °C in a fermentor (final OD600 = 3.5). Biomass was harvested by centrifugation andwashed twice with sucrose solution (300 mM) and lyophilized.

8.1.2 *Pantoea ananatis*

P. ananatis was routinely grown at 28 °C in TSB medium. For the isolation of bacterial polysaccharides, 1 L of TSB liquid medium was inoculated with 1 mL of early stationary phase cultures of P. ananatis and incubated on an orbital shaker at 180 rpm for three days at 28 °C. After incubation, the cells were harvested by slow-speed centrifugation. Bacterial pellets were washed three times with 0.9% (w/v) NaCl, and then freeze-dried.

8.1.3 *Bradyrhizobium* strains

Bradyrhizobium sp. BTAi1 and ORS278 were grown in Arabinose-Gluconate [HM salts + 0.1% Larabinose, 0.1% gluconate and 0,1% of yeast extract] medium [AGM].

The specific composition of medium expressed in g/l is reported in the following table.

Salt	g/L
$FeCl_3$	0,004 g
$CaCl_2$	0,010 g
Na_2HPO_4	0,125 g
$MgSO_4 \cdot 7H_2O$	0,180 g
Na_2SO_4	0,250 g
NH_4Cl	0,320 g
HEPES	1.3 g
MES	1.1 g
L-Arabinose	1.0 g
Na-Gluconate	1.0 g
Yeast extract	1.0 g

The pH was adjusted to 6.6 with addition of NaOH 4M. The growth was performed in three days at 30 °C with shaking (100 rpm). The broth culture was centrifuged, the cells were washed with water, ethanol, acetone and etilic ether and finally freeze-dried.

8.2 LPS and LOS extraction

Dried cells were extracted three times with a mixture of aqueous 90% phenol/chloroform/petroleum ether (2:5:8 v/v/v, 10 ml/g dry cells).[130] After removal of the organic solvents under vacuum, the LOS fraction was precipitated from phenol with water, washed first with aqueous 80% phenol, and then three times with cold acetone, each time centrifuged, and lyophilized.

LPS extraction was subsequently performed extracting the cells with a mixture of 90%phenol/water 1:1 at 68°C (20 ml/g dry cells), according to the conventional hot phenol-water procedure.[131] The water and the diluted phenol phase were dialysed against water (14-12kDa molecular weight cut-off). After dialysis, the extract was centrifuged and lyophilized.

The extracts were digested with DNase, RNase and Proteinase K, dialysed and freeze-dried again. Sodium dodecyl sulfate polyacrylamide gel electrophoresis (SDS-PAGE) was performed as described on all the fraction obtained. LPS and LOS are screened with a 13,5%-polyacrylamide gels were stained with silver nitrate according to the described procedure.[132]

8.3 Isolation of lipid A and oligo(OS)/polysaccharide(PO) fraction

8.3.1 Isolation of PO from *Burkholderia gladioli*

LPS was treated with anhydrous hydrazine (1 mL), stirred at 37 °C for 90 min, cooled, poured into ice-cold acetone (20 mL) to allow its precipitation. Precipitated was centrifuged (3000 g, 30 min), washed with ice-cold acetone, dried, dissolved in water, and lyophilized.

Other aliquots of LPSs were hydrolyzed in 1% acetic acid (100°C, 3h) in order to obtain the lipid A fraction. It was purified according to Que and co-workers procedure.[133]

8.3.2 Isolation of PO from *Burkholderia fungorum*

The O-polysaccharide chain from *B. fungorum* LPS was obtained by acetic acid hydrolysis 1% (100°C, 3 h). Lipid A fraction was precipitated from aqueous solution centrifuging at 4 °C, 8500 g, 1 h. As for LPS, the supernatant (6 mg) was purified by gel-permeation chromatography on a Biogel P-10 column (flow: 12 mL h-1)(Bio-Rad, Hercules, CA), using water as eluent.

8.3.3 Isolation of polysaccharide from *Pantoea ananatis*

Afterward the hydrolysis under mild acidic conditions of LPS released the O-antigen and lipid A sediment. The latter was removed by centrifugation and the supernatant was loaded onto a size exclusion chromatography on TSK50 column (Toyopearl HW-50), using ammonium bicarbonate 50mM as eluent.

---

[130] Galanos C., Lüderitz O., Westphal O., *Eur. J. Biochem.,* **1969**,**9**, 245-249.
[131] Westphal O., Jann K., *Meth. Carbohydr. Chem*., **1965**,*5*, 83–91.
[132] Kittelberger R., Hilbink F., *J. Biochem. Biophys. Meth.,***1993**, *26*, 81-86.
[133] Que N.L.S., Lin S., Cotter R.J., Raetz C.R.H.,*J. Biol. Chem*., **2000**, *275*, 28006-28016.

8.3.4 Isolation of polysaccharide and lipid A fractions from *Bradyrhizobium* species

In order to obtain polysaccharide fraction, (10 mg) of LPSs were hydrolyzed in 1% acetic acid (100°C, 5h) in order to obtain the lipid A fraction. So, adequate amounts of chloroform and methanol were added to the hydrolysate to obtain chloroform/methanol/hydrolysate2:2:1.8 (v/v/v), and the mixture was vigorously shaken, then centrifuged. The chloroform phase, containing the lipid A, was collected and washed twice with the water phase from a freshly prepared two-phase Bligh/Dyer mixture [chloroform/methanol/water, 2:2:1.8 (v/v/v)]. The organic phases were collected and dried.

8.4 Chemical analysis

Around 500 μg of LPS, were generally utilized for sugar and fatty acid analysis.

Monosaccharide analyses were realized by means of GC-MS of acetylated *O*-methyl glycosides derivatives, obtained after methanolysis (2M HCl/MeOH, 85°C, 18 h) and acetylation with acetic anhydride in pyridine (85°C, 30 min).The absolute configuration of the monosaccharides was obtained according to the published method.[134]

The ring size and the attachment points were determinated by a methyilation analysis.

The sample was firstly methylated with CH3I/NaOH in DMSO. After this treatment a chloroform/water extraction was performed, the organic phase was evaporated and hydrolysed with 4 M trifluoroacetic acid (100°C, 3h), carbonyl reduced with NaBD4, acetylated with acetic anhydride: pyridine (1:1, v/v) and analysed by GC-MS.

Fatty Acids were revealed as their Methyl Esters derivatives. Total fatty acids content was determined after strong hydrolysis of Lipid A, first with 4 M HCl (100°C, 4 h) and subsequently with 5 M NaOH (100°C, 30 min). Fatty acids were then extracted with chloroform, methylated with diazomethane and analysed by GC-MS.

8.5 Mass spectrometry

8.5.1 *Burkholderia* strains

MALDI mass spectra of native LOSs samples were performed in linear-mode on a Perspective (Framingham, MA, USA) Voyager STR instrument, equipped with delayed extraction technology. Ions formed by a pulsed laser beam (nitrogen laser, λ 337 nm) were accelerated by 24 kV and detected in negative-ion (LOSs) and in positive-ion polarity (Lipid A moieties).

Sample preparation: the native LOSs required specific preparations as described in details.[135]

[134] Leontein K., Lönngren J.,*Meth. Carbohydr. Chem*., **1978**,*62*, 359- 362.

[135] Sturiale L., Garozzo D., Silipo A., Lanzetta R., Parrilli M., Molinaro A. *Rapid. Commun. MassSpectrom.,* **2005**, *19*, 1829-1834.

Briefly, a few aliquot of sample was first desalted with cation exchange beads (Dowex 50WX8, Sigma-Aldrich) in the ammonium form, prior to crystallization on the MALDI plate. A thin film composed of 2,4,6-trihydroxyacetophenone (THAP) and nitrocellulose (trans-blot membrane, BioRad) was used as matrix. MS analyses of Lipid A species were performed by dissolving the samples obtained after acetate buffer hydrolysis in CH3Cl/CH3OH (50:50). Such samples were finally mixed in a 1:1 (v/v)ratio with the matrix solution [THAP, 75 mg mL-1 inCH3OH/trifluoroacetic acid/CH3CN (7:2:1)],deposited onto the MALDI plate and left to crystallize at room temperature.

8.5.2 *Bradyrhizobium* species

Mass spectrometry of the native, was performed on a 4800 Proteomics analyzer MALDI time-of-flight/time-of-flight mass spectrometer (Applied Biosystems, Framingham, MA) in reflector mode, in positive polarity. Compounds were dissolved in CHCl3/CH3OH (50:50, v/v) at a concentration of 1mg/ml. Matrix solution was prepared by dissolving trihydroxyacetophenone (THAP) in CH3OH/ 0.1% trifluoroacetic acid/CH3CN (7:2:1, by volume) at a concentration of 75 mg/ml. One microliter of the sample/matrix solution (1:1, v/v) was deposited onto a Opti- TOF*i*384 well plate and allowed to dry at room temperature. Mass spectra, resulting from the sum of 1250 laser shots, were obtained with a resolution higher than 10,000 (as the ratio between the mass of the peak and its full width at half maximum intensity) and with mass accuracy below 100 ppm.

8.6 NMR analysis

All NMR spectra were carried out using a Bruker DRX-600 equipped with a cryogenic probe. 1Dand 2D 1H-NMR spectra on oligo-/polysaccharides were recorded in D2O. ROESY and NOESY spectra were measured using data sets (t1xt2) of 4096x512 points with mixing times between 100 ms and 400 ms. Double quantum filtered phase sensitive COSY experiments were performed using data sets of 4096x800 points; total correlation spectroscopy experiments (TOCSY) were performed with a spinlock time of 100 ms, using data sets (t1xt2) of 4096x512 points. In all homonuclear experiments the data matrix was zero-filled in the F1 dimension to give a matrix of 4096x2048 points and was resolution enhanced in both dimensions by a cosine-bell function before Fourier transformation. Coupling constants were determined on a first-order basis from 2D phase sensitive double quantum filtered correlation spectroscopy (DQF-COSY).[136,137] Heteronuclear single quantum coherence(HSQC) and heteronuclear multiple bond correlation (HMBC) experiments were measured in the1H-detected mode via single quantum coherence with proton decoupling in the 13C domain,

[136] Piantini U., Sørensen O.W., Ernst R.R., *J. Am. Chem. Soc.*, **1982**, *104*, 6800-6801.
[137] States D.J., Haberkorn R.A., Ruben D.J., *J. Magn. Res.*,**1982**, *48*, 286-292.

using data sets of 2048x256 points. Experiments were carried out in the phase-sensitive mode according to the described method. [138]

A 60 ms delay was used for the evolution of long-range connectivity in the HMBC experiment. In all heteronuclear experiments the data matrix was extended to 2048x1024 points using forward linear prediction extrapolation.[139]

8.7 Conformational analysis and MD simulations on *B. gladioli* O-chain

Molecular mechanics calculations were carried out using the MM3* force field as included in MacroModel8.0. A dielectric constant of 80 was used. For each disaccharide structure, both ϕ and ψ were varied incrementally using a grid step of 18°. Each (ϕ,ψ) point of the map was optimized using 2000 P-R (Polak-Ribiere) conjugate gradients. The molecular dynamic simulations were run using the MM3* force field; bulk-water solvation was simulated using the MacroModel generalized Born GB/SA continuum solvent model. All simulations were run at 300 K. Structures were initially subjected to an equilibration time of 300 ps, then a10000 ps molecular dynamic simulation was performed with a dynamic time-step of 1.5 fs, and a bath constant *t* of 0.2 ps, with the SHAKE protocol for the hydrogen bonds. Trajectory coordinates were sampled every 2 ps, and a total of 5000 structures were collected for every simulation.[140,141]

Ensemble average interproton distances were calculated using the NOEPROM program,[142] using the isolated spin-pair approximation as described.[143]

Coordinate extractions were carried out with the program SuperMap, supplied with the NOEPROM package, and data were visualized with ORIGIN software.

Solvent-accessible surfaces were calculated with the Surface utility of Macromodel, and with the Molecular Surface displays of the Chem3D package.

[138] de Beer R., van Ormondt D., *NMRBasic Princ. Prog*., **1992**, *26*, 201-248.
[139] Hoch J.C., Stern A.S. In Hoch J.C. and Stern, A.S. (Eds.) *NMR data processing.* Wiley Inc. New York, **1996**, 77-101.
[140] Mari S., Sanchez-Medina I., Jimenez-Barbero J., Bernardi A., *Carbohydr.Res.,* **2007**, *342*, 1859-1868.
[141] Bernardi A. et al.,*Chem. Eur. J.,* **2002**, *8*, 4598-4612.
[142] Asensio J.L., Jimenez-Barbero J., *Biopolymers,* **1995**, *35*, 55-75.
[143] Corzana F. et al.,*J. Am. Chem. Soc.,* **2007**, *129*, 2849-2865.

8.8 Biological assay

8.8.1 Construction of the BTAi1Δshc mutant and complementation.

Our collaborators to create theBTAi1Δshc mutant, the complete shc gene was deleted and replaced by the kanamycin resistance (KnR) gene by double crossover recombination as described below. The KnR gene was under the control of its own promoter and no termination sequence was introduced downstream this gene. A 2,331-bp shc gene fragment including 99-bp upstream and 177-bp downstream regions was amplified using the primers SHCFW (5'-CGCTACGGCCAGTTGATTGGATTT-3') and SHCRV (5'-TGCATCCGAAGCTCAGGACAATGA-3' and cloned into pGEM-Teasy vector (Promega Corp., Madison, WI, USA). The resulting plasmid was named pGEM-T::shc. The Not I fragment sized ca. 2.4 kb digested from pGEMT::shc was ligated with NotI-digested pJQ200SK58 that is not replicable in Rhizobium species, and which contains a counter selectable sacB marker, resulting in pJQ::shc. This pJQ::shc was introduced into DH5α (pKD78), which has λ Red recombinase gene controlled by araBAD promoter, by electroporation. The kanamycin-resistance gene was amplified from pKD4 [144] using the primersPS1 (5'-GTGTAGGCTGGAGCTGCTTC-3') and PS2 (5'-CATATGAATATCCTCCTTAG-3'). Using the PCR product as a template, the kanamycin-resistance genewas re-amplified with two 60-bp primers PSHC1 and PSHC2, which have 40-bplinkers homologous to both bordering regions of the shc gene at 5' ends of PS1 andPS2.

The sequences of PSHC1 and PSHC2 are 5'-GCCCTGCAATCGACGGTGCGCGCGGCGGCGGATTGGCTGAGTGTAGGCTGGAGCTGCTTC-3'

and5'GTACATGCCGTAGCGGAGCATGAAGGCGCGGGACAATTCCCATATGAATATCCTCCTTAG-3', respectively. The consequent PCR product was introduced into DH5a (pKD78/pJQ::shc) and the λ Red recombinase was induced.

The resulting plasmid named pShc::Km was transferred into BTAi1 by triparental mating[145] and the shc gene replacement in sucrose-resistant clones was confirmed using PCR.

For complementation of the mutant, the complete shc gene was cloned down stream of the nptII promoter into the pMG103-npt2-GFP plasmid[146]harbouringa streptomycin/spectinomycin-resistance gene. For this, the streptomycin/spectinomycin-resistance gene was first liberated from pHRP315[147] byBamHI digestion and cloned into the corresponding site of pMG103-npt2-GFP; the shc gene

[144] Datsenko K. A. &Wanner B. L., *Proc. Natl Acad. Sci. USA*, **2000**, *97*,6640‑6645.
[145] Lee H. I., Lee J. H., Park K. H., Sangurdekar D. & Chang W. S., *Appl. Environ. Microbiol*., **2012**,*78*, 2896‑2903.
[146] Bonaldi K. et al.,Mol. *Plant Microbe Interact*.,**2010**,*23,* 1537‑1544.
[147] Parales R.E., Harwood C.S.,*Gene*, **1993**,*133*,23‑30.

amplified using the primers SHC-BTAi1-F (5'-GGCGGAGATCTTCCCTATAGGGCGGGGTGAATTC-3') and SHC-BTAi1-R (5'-CCGTCACTAGTCGCGCGACGGGATGGCTCGCAATG-3') was then cloned into the BglII/SpeI sites located downstream of the nptII promoter.

8.8.2 Plant cultivations and symbiotic analysis.

A. evenia seeds were surface-sterilized by immersion in sulphuric acid under shaking during 40min. Seeds were abundantly washed with sterile distilled water and incubated overnight in sterile water. Seeds were then transferred for 1 day at 37 °C in darkness on 0.8% agar plate for germination. Plantlets were then transferred on the top of test tubes covered by aluminium paper for hydroponic culture in BNM. Plants were grown in closed mini green house in a 28 °C growth chamber with a 16-h light and 8-h dark regime and 70% humidity. Seven days after transfer, each seedling was inoculated withn1ml of cell suspension resulting from a 5-day-old bacterial culture washed in BNM and adjusted to reach an optical density of one at 600 nm. For nodulation and nitrogen fixation kinetics at different times post inoculation (6, 8, 10, 12 and19 days), five plants were taken to count the number of nodules on the roots and to analyse the nitrogenase activity by ARA. For this, each plant was placed into125-ml glass vials sealed with rubber septa. Air (12.5 ml) was removed from each vial, to which 12.5 ml of acetylene was then injected. Gas samples (1 ml) were with drawn after 3 h of incubation at 25 °C and the ethylene produced was measured using gas chromatography.

8.8.3 Transmission electron microscopy

Microscopic observations were performed on three to five nodules originating from different plants per condition. For this, the nodules were fixed in a 4% glutaraldehyde, 0.1M cacodylate buffer (pH 7.2), post fixed in 1% osmium tetroxide, dehydrated using a series of acetone washes and embedded in TAAB 812 epon resin. Ultrathin sections (60 nm) were mounted oncollodion carbon-coated copper grids, contrasted using uranyl acetate and lead citrate and examined at 80 kV with a TEM (Jeol 100CX II).

Conclusions

The natural ecosystem is based on coexistence of plants, animals, and humans. This cohabitation results in countless interactions between beneficial and pathogenic organisms; very close relationships have evolved in host-specific symbioses, which are usually beneficial for both partners. In most cases, symbiosis derives from metabolic complementation between the host and microbe, in which one partner provides missing nutrients to the other. Moreover, microbes can contribute in many ways to host development by synthesizing hormone-like compounds and affecting host immunity. On the contrary, some microorganisms, as pathogens, are able to trigger immune response in the host cell creating lesions on tissues and eventually lead to death of the host.

Within this frame, my PhD project in these three years was focused on studying the role of bacterial glyco-conjugates in the activation or suppression of immune response in plant cells.
Glyco-conjugates represent a very heterogeneous group of biomolecules, which includes lipopolysaccharides (LPS), peptidoglycan (PGN), glycolipids and glycoproteins. LPSs, in particular, are pivotal in mediating many processes within host-bacteria interaction like adhesion, recognition, pathogenesis, symbiosis. Therefore, to understand the molecular basis of bacterium–host interaction, it was important to elucidate the structure of LPS and to identify how bacterium modifies the LPS in response to different environments. It has been already demonstrated that a correct structure of LPS is required to establish a disease (pathogens) or to produce a beneficial outcome (symbiont) in host-microbe interaction.
A part of this PhD thesis was focused on isolation, purification and characterization of LPS from plant pathogen bacteria while a second, considerable part of the project thesis was center on the study of bacteria LPS and in particular of the lipid A, involved in *Aeschynomene* legume symbiotic process.

As for plant pathogen bacteria, the LPS from two plant pathogens, namely *Burkholderia fungorum* and *Burkholderia gladioli pv. cocovenenas* was isolated, purified and characterized. The isolated O-chains were characterized with a combination of chemical, spectrometric and spectroscopic approaches, which allowed to define new O-polysaccharide structures, which had a novel structural features.
In case of *B. gladioli*, a distinctive feature of the O-chain is the presence of methylated sugar residues contributing to create a hydrophobic shield, as also confirmed by conformational studies showing three-dimensional shapes with a different packing and extension. Such chemical features determine the physico-chemical properties of the bacterial envelope and might contribute to the ability to adapt the membrane surface to the host. Even for *Burkholderia fungorum* the O-antigen is formed by a

rhamnose chain non stochiometrically substituted by xylose. It conserved both the right hydrophobicity to interact with cell host and with the production of diverse polysaccharides, substituted and non- substituted by xylose, bacteria mask themselves from attack of immune system of the host cell.

A consistent portion of PhD project has been devoted to the study of lipid A from several *Bradyrhizobium* strains, conducted throughout the entire PhD project with aim of understanding the biosynthetic pathway of lipid A constituents and of hopanoid moeities covalently attached to *Bradyrhizobia* lipid A, that seems crucial for the bacterial life.

Almost all *Bradyrhizobium* strains ,displayed a very unusual lipid A, containing two very long chain fatty acids to which a hopanoid moiety is covalently linked and also a peculiar sugar backbone including two diammino glucose residues.

The typical acylation pattern of *Bradyrhizobium* lipids A seems to be a strategy for bacteria to strictly control fluidity and rigidity of outer membrane depending on environmental changes.

The presence of a hopanoid molecule covalently attached to lipid A (we named HoLA, standing for Hopanoid-Lipid A) had never been described in any LPS including those from non-photosynthetic *Bradyrhizobium* strains. For these reasons, via MALDI mass spectrometry the full architecture of lipid A from mutants for the hopanoids and/or very long chain fatty acids biosynthesis was studied

Moreover, the O-antigen region isolated from several *Bradyrhizobium* strains have revealed also an important role in the suppression of innate immunity.

Previous studies have demonstrated that *Bradyrhizobium* strain Btai1 and also ORS 285 biosynthesizes a LPS with a peculiar homopolymeric O-specific chain constituted by an unusual 1,7-linked sugar, named Bradyrhizose. Despite *Bradyrhizobium* strains display a very heterogeneous and peculiar composition of O-antigen portion, previous studies demonstrated that the O-specific side chain was not pivotal in establishment of early stage of symbiotic process, because the LPS mutants lacking the O-chain and with a progressive truncation until core region had the minimal structure requested to trigger immune responses as LIR (localized induced resistance).Thus, we proceed in analysis of the structure of the core oligosaccharide, which disclose a very unusual structure never found before from LPS of several mutants lacking the O-chain, with the final aim to explain their role throughout the symbiotic process.

I also isolated and characterised the O-polysaccharide structure from the phylogenetically close bacterium *Rhodopseudomonas palustris* strain BisA53, which displayed a novel saccharide structure formed by a repeating unit of **[→3)-α-D-Rha-(1→3)-α-Sug-(1→5)-α-D-Dha-(2→]$_n$**